ROLE OF SODIUM-CALCIUM EXCHANGE IN CARDIAC PHYSIOLOGY AND PATHOPHYSIOLOGY

BY

CECILIA HURTADO

A Thesis
Submitted to the Faculty of Graduate Studies
in Partial Fulfillment of the Requirements
for the Degree of

DOCTOR OF PHILOSOPHY

Department of Physiology
Faculty of Medicine
University of Manitoba
and the Division of Stroke and Vascular Disease
St. Boniface General Hospital Research Centre
Winnipeg, Manitoba

THE UNIVERSITY OF MANITOBA

FACULTY OF GRADUATE STUDIES

*****

COPYRIGHT PERMISSION PAGE

Role of Sodium-Calcium Exchange in Cardiac Physiology and Pathophysiology

BY

Cecilia Hurtado

A Thesis/Practicum submitted to the Faculty of Graduate Studies of The University of Manitoba in partial fulfillment of the requirements of the degree of

DOCTOR OF PHILOSOPHY

To my parents

TABLE OF CONTENTS

ABSTRACT

The sodium-calcium exchanger (NCX) is thought to be a critical protein in excitation-contraction coupling in the heart through its regulation of intracellular [Ca^{2+}]. The exchanger removes Ca^{2+} from the cell in exchange for extracellular Na^{+} in the "forward mode" to induce cardiac relaxation. Although still controversial, NCX may also participate in cardiomyocyte contractile activity in a *reverse mode* by bringing Ca^{2+} into the cell in exchange for intracellular Na^{+}. In addition to its important physiological role, the NCX has been associated with the pathology of ischemia-reperfusion injury, glycoside toxicity, cardiac hypertrophy and heart failure. Therefore, it be a valuable therapeutic target in the treatment of heart disease.

A limitation in the study of the exchanger has been the dearth of pharmacological blockers that specifically inhibit the NCX. I found that blockaged of the Na^{+}-H^{+} exchanger, an upstream component of the NCX in the ischemia-reperfusion pathway, solely during early reperfusion can provide cardioprotection in isolated cardiomyocytes. We have also described the development of RNA interference, a new genetic tool, to down-regulate the expression of the NCX and characterized the effect of NCX depletion. We showed that neonatal cardiomyocytes with nominally depleted NCX through adenovirally delivered short hairpin RNA (shRNA) can still contract. When this new tool was compared to alternative approaches it was found to be highly efficient. The data support an important but not a critical role for NCX in excitation-contraction coupling in the heart. We also studied the function of the cardiac (NCX1.1) and renal (NCX1.3) isoforms of the exchanger, expressed in neonatal cardiomyocytes and HEK-293 cells, and

found that the cardiac isoform causes more severe Ca^{2+} overload during ischemia-reperfusion injury and glycoside toxicity. In summary, our results demonstrate that the NCX is important in defining contractile activity in the normal heart but it is not essential. It is also important in defining contractile dysfunction during ischemic and drug-induced challenges. Overall, these results identify NCX as an important molecule to target to develop new strategies to influence heart function and dysfunction.

ACKNOWLEDGMENTS

I would like to express my strongest gratitude to my supervisor, Dr. Grant N. Pierce. I thank him for being supportive and encouraging and for giving me freedom to work and grow in the lab. I would also like to thank Dr. Pierce for helping me achieve my goals and helping me reach all those last minute deadlines. I thank Grant and Gail for being so friendly to me and my family. I wish to express my gratitude to the members of my PhD committee, Dr. Nasrin Mesaeli, Dr Ian Dixon and Dr Larry Hryshko, for many years of guidance. I am specially grateful to Nasrin, the doors of her lab and office have been always open for me. She taught me many things and answered uncountable questions. I would like also to thank the other Professors of the Division that have provided valuable guidance, Drs Jeff Wigle and James Gilchrist. Also to Dr Hamid Messaeli, who was my tutor during the first years in the lab. I extend my gratitude to Janet Labarre and Gail McIndless for their secretarial assistance. A special thanks to Michele Prociuk, Annette Kostenuk, Thane Maddafford and Dr Elena Dibrov for their help with experiments. I would also like to extend my gratitude to ALL the members of the Pierce lab and the Division of Stroke and Vascular Disease. I thank Radoy, for being fun to be with, for keeping my eyes open in life and for standing for my 'collections' of papers. I thank Paula and Martin for their love and friendship. And finally, I thank my dear parents, for being so close to me even if I am far away; for being models of integrity and dedication and providing me, my brother and sister with absolutely everything they have.

LIST OF FIGURES

LIST OF TABLES

LIST OF DEFINITIONS

Ad-NCX1.1: adenovirus coding for canine NCX1.1.

Ad-NCX1.3: adenovirus coding for canine NCX1.3.

Ad-NCX1.1-EGFP: adenovirus coding for canine NCX1.1 fusion protein to EGFP.

Ad-NCX1.3-EGFP: adenovirus coding for canine NCX1.3 fusion protein to EGFP.

Ad-AS-NCX1.1: adenovirus coding antisense rat NCX1.1.

Ad-RNAi: adenovirus coding for shRNA against the NCX.

Ad-XIP: adenovirus coding for XIP.

AP: action potential.

CICR: calcium induced calcium release.

DMA: 5-(N,N-dimethyl)-amiloride.

DMEM: Dulbecco's Modified Eagle Medium.

DMSO: dimethylsulfoxide.

E-C coupling: excitation-contraction coupling.

EGFP: enhanced green fluorescent protein. Brighter form of the green fluorescent protein (GFP).

HEK-293: human embryonic kidney cells.

HEK-293-NCX1.1: HEK-293 cells expressing NCX1.1 (stable transfected).

HEK-293-NCX1.3: HEK-293 cells expressing NCX1.3 (stable transfected).

KB-R7943: pharmacological inhibitor of the NCX.

MOI: multiplicity of infection. Number of virus per cell used for infection.

NCX: sodium-calcium exchanger.

PBS: phosphate buffer solution.

PCR: polymerase chain reaction.

PMCA: plasmalemmal calcium pump.

RISC: **R**NAi **i**nduced **s**ilencing **c**omplex. Ribonuclease complex that uses siRNA sequence to target homologous mRNA for degradation.

RNAi: RNA interference. Mechanism of gene silencing initiated by double stranded RNA.

SERCA: sarcoplasmic-endoplasmic reticulum calcium pump.

shRNA: short-hairping RNA, hairpin of RNA that is processed within the cells into siRNA.

siRNA: small interfering RNA. 21-25 nucleotides long RNA duplex recognized by nuclease RISC.

SR: sarcoplasmic reticulum.

XIP: e**x**changer **i**nhibitory **p**eptide. 20 nt long peptide that blocks NCX activity.

INTRODUCTION

Calcium is used within cells as an intracellular messenger. Local and temporal changes in Ca^{2+} concentration activate a wide variety of cellular functions. Intracellular Ca^{2+} concentration, therefore, needs to be tightly regulated. A number of channels and transporters maintain calcium homeostasis. The sodium-calcium exchanger (NCX) is one of the transporters that is particularly important in the heart because of its involvement in the mechanism of excitation-contraction coupling (Barry and Bridge, 1993).

In addition to its important physiological role, the NCX has been associated with the pathology of ischemia-reperfusion injury (Tani and Neely, 1989), glycoside toxicity (Satoh *et al*, 2000), cardiac hypertrophy (Kent *et al*, 1993; Menick *et al*, 1996) and heart failure (Hasenfuss, 1998; Hasenfuss *et al*, 1999; Pogwizd *et al*, 1999) Therefore, it has the potential of being a valuable therapeutic target in the treatment of heart disease. The study of the NCX would be of great value not only to advance our understanding of the function of the heart during normal conditions but also to devise strategies to improve cardiac performance under pathological challenge as well.

A limitation in the study of the exchanger has been the dearth of pharmacological blockers that specifically inhibit the NCX (Blaustein and Lederer, 1999). In this thesis, we analyzed the protective effect of a blocker of the Na^{+}-H^{+} exchanger, an upstream component of the NCX in the ischemia-reperfusion pathway. We have also described the development of a new genetic tool to down-regulate the expression of the NCX and characterized the effect of NCX depletion in neonatal cardiomyocytes during conditions that are expected to stimulate NCX activity. We also studied the function of the cardiac

and renal isoforms of the exchanger, expressed in neonatal cardiomyocytes and HEK-293 cells, to determine the involvement of the exchanger and the relative contributions of each isoform during ischemia-reperfusion injury and glycoside toxicity.

REVIEW OF THE LITERATURE

The sodium-calcium exchanger (NCX)

The NCX is a plasmalemmal protein. It is found in almost all cell types and is abundant in excitable tissues, like the brain and the heart (Blaustein and Lederer, 1999). It transports Ca^{2+} in exchange for Na^{+} and is able to remove Ca^{2+} from the cell or transport it into the cell. The direction of this movement depends on the concentration gradient across the membrane for Ca^{2+} and Na^{+}, and also on the membrane potential. Generally, in the heart, the NCX plays an important role in Ca^{2+} removal from the cell during relaxation (Bridge *et al*, 1988; Crespo *et al*, 1990) and may also contribute to Ca^{2+} influx during the peak of an action potential (Bers, 2001). These two aspects will be discussed further in the following passages.

Structure

The 938 amino acids that form the mature cardiac NCX protein are arranged in 9 transmembrane segments (Figure 1) (Nicoll *et al*, 1999). Five transmembrane segments are present in the amino part of the protein and are separated from the other 4 by a large intracellular loop. A leader peptide, corresponding to the first amino acids of the protein, is removed during processing of the protein (Durkin *et al*, 1991). Once the leader peptide is removed, the resulting amino end is extracellular and glycosylated (Hryshko *et al*, 1993). Two regions with homologous sequences are found within the protein: α-1 is

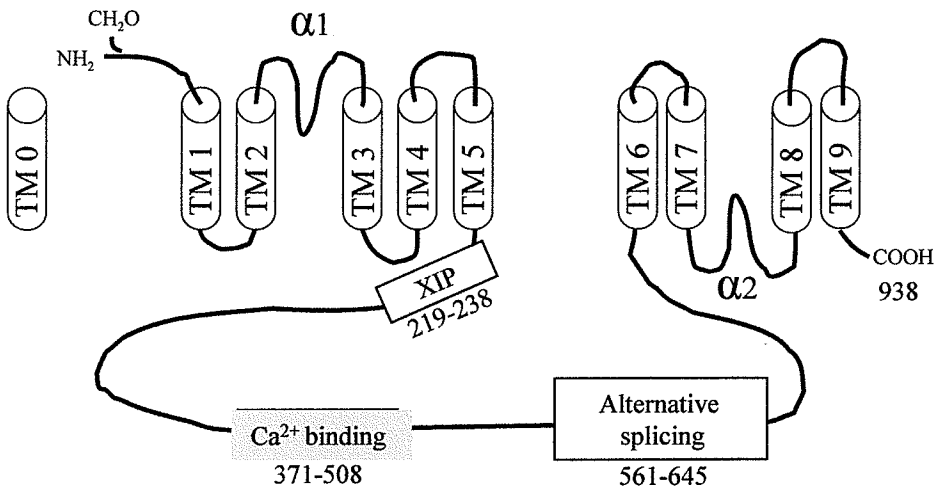

Figure 1. Topological model of the cardiac NCX. Regulatory regions of the intracellular loop are indicated with boxes. Numbers indicate the amino acids positions. TM, transmembrane segments; α1 and α2, regions of intramolecular homology; XIP, exchanger inhibitory peptide region. From Philipson and Nicoll. *Annu. Rev. Physiol*, 2000;62:111-33. With modifications.

located between transmembrane segments 2 and 3, and α-2, between transmembrane segments 7 and 8. The α-1 and α-2 sequences form reentrant loops that are involved in ion translocation (Doering *et al*, 1998; Iwamoto *et al*, 2000; Nicoll *et al*, 1996a). These regions of homology are believed to have originated by gene duplication and can be found in other proteins of the NCX superfamily (Philipson *et al*, 2002). The large intracellular loop is involved in regulation of NCX activity. It contains the XIP (e**X**changer **I**nhibitory **P**eptide) region, the regulatory Ca^{2+} binding site and the region of alternative splicing. The region of alternative splicing will be discussed in the NCX isoforms section. The intracellular loop also contains 2 regions of internal homology named β-1 and β-2 repeats. The role of these repeats is not clear yet (Philipson *et al*, 2002). The C-terminus of the protein is found on the cytoplasmic side.

The topology of the NCX that is currently accepted was determined by studying the ability of cysteine residues at different locations to form disulfide bonds (Iwamoto *et al*, 2000; Nicoll *et al*, 1999). These studies indicated that α repeats are located on opposite sides of the membrane and close to each other in the folded protein. A previous model, based on hydropathy analysis of the cloned NCX, had established that the exchanger was composed of 12 transmembrane segments (Nicoll *et al*, 1990).

The XIP region corresponds to amino acids 219 to 238, and is located close to the N-terminus of the intracellular loop. The sequence of this region was found to be similar to a calmodulin binding site (Li *et al*, 1991). It is rich in hydrophobic and basic amino acids (Figure 43, Results section). To test its regulatory properties, a peptide containing the sequence of this region was synthesized (XIP) and was found to inhibit the exchanger

(see NCX inhibitors). Mutational analysis of the endogenous XIP region indicated that it is involved in Na^+_i regulation of the exchanger (Matsuoka *et al*, 1997).

Regulatory Ca^{2+} (see NCX regulation) binds to the region of the intracellular loop that spans amino acids 371 – 508 of the cardiac NCX (Levitsky *et al*, 1994). Mutations within this region affect the calcium regulatory properties of the exchanger (Matsuoka *et al*, 1995). Binding of Ca^{2+} to this region causes conformational changes in the protein that are thought to activate the protein.

The variable region of the gene *NCX1* corresponds in the cardiac exchanger protein to amino acids 561 to 681, located towards the C-terminus of the intracellular loop. This region of the gene undergoes alternative splicing.

Localization

In cardiomyocytes, NCX is found on the cell surface, t-tubules and intercalated discs (Kieval *et al*, 1992). Thomas *et al* using confocal laser scanning microscopy, showed NCX staining in adult cardiomyocytes in the vertical t-tubules, but not in the longitudinal t-tubules (Thomas *et al*, 2003). NCX was co-localized with the ryanodine receptor (Thomas *et al*, 2003). A previous study using the same technique had failed to show any co-localization of NCX with either the Na^+ channel or ryanodine receptors but did show co-localization of ryanodine receptors with L-type Ca^{2+} channels (Frank *et al*, 1992). Thomas *et al* (Thomas *et al*, 2003), looking for further resolution, used electron microscopy differential gold labeling and measured the distance that exists between the different transporters. They found that the distance separating the NCX from ryanodine

receptors or L-type Ca^{2+} channels was the same as the distance between these latter two transporters (which were previously found to co-localize). It would be important to resolve this discrepancy in the future because the activity of the NCX in the Ca^{2+} entry mode would require physical proximity between these transporters to become physiologically important in excitation-contraction coupling.

Function

The NCX is thought to be a critical protein in excitation-contraction (E-C) coupling in the heart through its regulation of intracellular [Ca^{2+}] (Barry and Bridge, 1993; Bers, 2000; Blaustein and Lederer, 1999). The exchanger removes Ca^{2+} from the cell in exchange for extracellular Na^+ in the *forward mode* to induce cardiac relaxation (Barry and Bridge, 1993; Blaustein and Lederer, 1999; Bridge *et al*, 1988; Crespo *et al*, 1990). Although still controversial, NCX may also participate in cardiomyocyte contractile activity in a *reverse mode* by bringing Ca^{2+} into the cell in exchange for intracellular Na^+ (Bers *et al*, 1988; Leblanc and Hume, 1990; Levesque *et al*, 1994). The quantity of Ca^{2+} that enters the cell is insufficient to support contraction on its own, but Ca^{2+} entry through the exchanger induces the sarcoplasmic reticulum (SR) to release larger quantities of Ca^{2+} to fully support cardiomyocyte contraction (Levesque *et al*, 1994; Litwin *et al*, 1998). However other studies do not support NCX contribution to SR Ca^{2+} release (Bouchard *et al*, 1993; Sipido *et al*, 1997). Ca^{2+} influx through the exchanger is favored when $[Na^+]_i$ is high and at depolarized membranes potentials (Bers, 2002). These conditions occur at the peak of the action potential during each beat. The role of

the exchanger in E-C coupling becomes even more significant in the fetal and neonatal myocardium where the SR is not yet fully mature (Artman, 1992; Bassani and Bassani, 2002; Boerth *et al*, 1994).

The NCX has also been implicated in a variety of pathophysiological processes in the heart. For example, Na^+-Ca^{2+} exchange has been implicated in ischemic/reperfusion injury to the heart (Tani and Neely, 1989). An acidic environment induced by ischemia is thought to stimulate the Na^+-H^+ exchanger to bring Na^+ into the cardiomyocyte, which subsequently reverses the NCX to move Ca^{2+} into the cell in such quantities that it causes cell damage and necrosis (Hurtado and Pierce, 2000; Pierce and Czubryt, 1995). Changes in Na^+-Ca^{2+} exchange in other pathological conditions like cardiomyopathies (Makino *et al*, 1985; Wagner *et al*, 1989), post-infarction (Litwin and Bridge, 1997), heart failure (Flesch *et al*, 1996; Studer *et al*, 1994) and in cardiac hypertrophy (Gomez *et al*, 2002; Heyliger *et al*, 1985) have been identified as well.

Stoichiometry

The NCX transports 3 Na^+ in exchange for 1 Ca^{2+}. Therefore, NCX is electrogenic: it transports 1 positive charge in the direction Na^+ is transported. Two important aspects of NCX electrogenicity are first (a practical one), it allows measurements of NCX activity using electrophysiological techniques, and second, NCX activity will contribute to the electrical properties of the cell. The 3:1 electrogenic stoichiometry was re-evaluated through a study by Fujioka *et al* (Fujioka *et al*, 2000b) that suggested a 4:1 stoichiometry. The most recent work on this topic, from Donald

Hilgemann's laboratory, has indicated a stoichiometry of 3.2:1 (Kang and Hilgemann, 2004). The authors proposed a model whereby the exchanger, besides simply transporting 3 Na^+:1 Ca^{2+}, has one transport mode that imports 3 Na^+:1 Ca^{2+} and another mode that imports 1 Na^+ (these last two modes work at a slower rate). It remains unclear what the precise stoichiometry of the NCX is but it is generally considered by most to be a simple 3:1 ratio.

Thermodynamics

The equilibrium or reversal potential for the NCX (E_{NCX}) is the membrane potential (E_m) at which the driving force caused by the concentration gradient of Ca^{2+} and Na^+ equals the driving force created by the electrical potential difference across the membrane. At this potential no ions will flow through the exchanger. At an E_m larger than E_{NCX}, the exchanger will produce an outward current (Ca^{2+} influx), and at an E_m smaller than E_{NCX}, it will produce an inward current (Ca^{2+} efflux). The driving force for the exchanger is

$Vm - E_{NCX}$

The equilibrium potential for the exchanger (considering a 3 Na^+ : 1 Ca^{2+} stoichiometry) is:

$E_{NCX} = 3 * E_{Na+} - 2 * E_{Ca2+}$

E_{Na+} is the Nernst equation or equilibrium potential for Na^+ and E_{Ca2+}, for Ca^{2+}. {$Ex=RT/nZ * \ln[x]_o/[x]_i$; or $60/n * \log [x]_o/[x]_i$; where R is the general gas constant, T is the absolute temperature; n is the charge number and Z is Faraday's constant}.

Then,

$E_{NCX} = 3 * 60 \log [Na^+]_o/[Na^+]_i - 2 * 30 \log [Ca^{2+}]_o/ [Ca^{2+}]_i$.

Changes in $[Ca^{2+}]$, $[Na^+]$, and membrane potential will affect E_{NCX}, and consequently, the direction and magnitude of transport. For example, for a rat cardiomyocyte at rest, we can assume the ionic concentrations to be: $[Na^+]_o$= 140 mM, $[Na^+]_i$= 16 mM [49], $[Ca^{2+}]_o$= 1.4 mM and $[Ca^{2+}]_i$= 100 nM. Then E_{NCX} would be – 78 mV, a value close to the resting potential. If we assume an E_m= - 82 mV there will be a very small inward current (Ca^{2+} efflux) through the exchanger. During phase 0 of the AP, the E_m is more positive than E_{NCX}, so the exchanger reverses and generates Ca^{2+} influx (outward current). During the peak of the Ca^{2+} transient (due to activation of L-type Ca^{2+} channels and Ca^{2+} release from the SR), $[Ca^{2+}]_i$ increases, and this results in an increase in E_{NCX}. When E_{NCX} becomes more positive than the E_m, NCX extrudes Ca^{2+} from the cytoplasm and contributes to the plateau of the AP with inward current.

Intracellular Na^+ concentration is thought to be a prime effector for the reversal of the NCX (Bers *et al*, 2003; Leblanc and Hume, 1990). A 5 mM increase in $[Na^+]_i$ would modify E_{NCX} from – 78 mV to – 100 mV. When the E_m is – 82 mV and the E_{NCX} is – 100 mV, the exchanger would function in the Ca^{2+} entry mode.

Models of over-expression and down-regulation

Over-expression of NCX

To clarify the role played by the NCX in the regulation of Ca^{2+} homeostasis in the heart and to observe the changes in its expression in disease states, alternative approaches

have been used to modify its expression level. NCX expression has been up-regulated by the use of transgenic mice and adenoviral vectors and has been down-regulated in knock-out mice and through the use of antisense technology.

Adachi-Akahane *et al* developed a transgenic mouse for cardiac specific expression of the exchanger. The canine NCX1.1 gene was expressed under the α-myosin heavy chain promoter in this model (Adachi-Akahane *et al*, 1997). In heterozygous mice, 1.5 - 3 fold higher NCX activity was measured using isotope uptake and electrophysiological methods, respectively. No changes in intracellular Na^+ concentration, resting Ca^{2+}, Ca^{2+} transient amplitude or adaptations in other Ca^{2+} regulatory proteins were observed (Terracciano *et al*, 1998; Yao *et al*, 1998). Increased NCX activity, however, accelerated relaxation and the decay of the caffeine-released Ca^{2+} transients (in intact cells and under voltage clamp). These observations support the role of the exchanger in Ca^{2+} efflux. One study showed higher SR Ca^{2+}content in NCX over-expressing cells (Terracciano *et al*, 1998). To sustain an increase in Ca^{2+} efflux via the exchanger without a depletion of $Ca^{2+}{}_i$ (since no changes in Ca^{2+} current were observed), an increase in Ca^{2+} entry through the same exchanger has been proposed (Terracciano *et al*, 1998). The importance of the reverse mode exchanger was shown in experiments where depolarization of the membrane to positive potentials caused SR Ca^{2+} release in cells with high NCX expression. It was also shown that Ca^{2+} entering the cell through NCX can be buffered by the SR. Work by Yao *et al* revealed that myocytes from heterozygous animals could maintain Ca^{2+} transients at a low frequency of stimulation after blockade of the L-type Ca^{2+} channel, showing that increased levels of NCX (working in reverse mode) can contribute to Ca^{2+}-induced Ca^{2+} release from the SR (Yao

et al, 1998). In this last situation, SR function was required indicating that NCX can induce Ca^{2+} release from the SR but can not contribute enough Ca^{2+} to support contraction on its own.

Heterozygous NCX transgenic mice did not show a cardiac disease phenotype. On the contrary, homozygous NCX over-expressors were found to exhibit mild hypertrophy by 3.5 months of age (22 % increase in heart weight to tibia length ratio) (Reuter *et al*, 2004). Homozygous postpartum females and mice from both sexes showed more severe hypertrophy under stress conditions that resulted in heart failure (Reuter *et al*, 2004). Characterization of excitation-contraction coupling in ventricular myocytes from homozygous mice showed a decrease in gain. In other words, an increased L-type Ca^{2+} channel current activated a smaller Ca^{2+} transient without changes in SR Ca^{2+} content. The mechanism for increased and slower inactivation of the L-type Ca^{2+} channel current could not be completely explained by the authors, because no changes were observed in channel density and, in addition, NCX was shown to have no direct effect on channel activity (when NCX activity was transiently blocked, an enhanced L-type current was maintained).

NCX transgenic mice were shown to be more susceptible to ischemia-reperfusion injury (Cross *et al*, 1998). The effect was observed only in males, probably due to the protective effect of estrogen in females. Estrogen prevented the rise of $[Na^+]_i$ that drives NCX in males (Sugishita *et al*, 2001). The mechanism responsible for the gender difference in Na^+_i is not known. In this last study, after 30 minutes of ischemia, $[Ca^{2+}]_i$ in myocytes from transgenic mice was 1.5 fold higher than in cells from wild type mice. However, another study using the same transgenic mice showed that increased NCX

expression had a protective effect. Transgenic hearts showed preserved Ca^{2+} transients during ischemia and hypoxia (Hampton *et al*, 2000).

The other approach to induce increased expression of the exchanger has been to use NCX adenoviral transfection vectors. The effects observed varied depending on the species from which myocytes were obtained. Adenoviral-driven overexpression of the exchanger in rabbit ventricular myocytes provided evidence to indicate that Ca^{2+} efflux through the exchanger was dominant in this species. The changes observed included a depletion of SR Ca^{2+}content and a reduction of the amplitude of the Ca^{2+} transient (Ranu *et al*, 2002). In this case, relaxation and decay of the Ca^{2+} transient were prolonged. Conversely, in adult rat ventricular myocytes, the effect of increasing the NCX expression depended upon the extracellular Ca^{2+} concentration. SR Ca^{2+} content and Ca^{2+} transients decreased at low $[Ca^{2+}]_o$ and increased at high $[Ca^{2+}]_o$ (Zhang *et al*, 2001).

Down-regulation of NCX

The first approach that was used to decrease the expression of the NCX was to employ antisense oligodeoxynucleotides (ODN). ODNs are synthetic DNA molecules with a complementary nucleotide sequence to a specific mRNA. RNA-DNA duplexes, formed by base-pairing between the mRNA and the ODN, activate cleavage of the corresponding mRNA by RNAse H (Fiset and Soussi Gounni, 2001). ODNs may also interfere with the ability of the mRNA to access the ribosomes for translation. A limitation for this methodology is the low efficiency of transfection that can be achieved

in cardiomyocytes. ODNs when modified eg, as phosphorothioated ODN, are relatively stable molecules.

For the study of the effects of ODNs on NCX expression, 19 nucleotide long phosphorothioate ODNs targeting the 3' untranslated region of the RNA were initially used at a concentration of 3 μM in neonatal cardiomyocytes (Lipp *et al*, 1995). In this first study, ODNs nearly abolished NCX activity within 48 hours. Another group used 0.5 μM of a pair of ODN sequences targeting the region around the start codon for the NCX (Slodzinski *et al*, 1995). These ODNs exhibited a significant effect after 4 days of treatment. NCX half-life was measured as 33 hours (Slodzinski and Blaustein, 1998). This would indicate that when effects were observed just 24-48 hours after treatment and using high concentrations of ODNs, these effects were probably due to a non-specific action of the ODNs (Lipp *et al*, 1995; Takahashi *et al*, 1999). The most recent study used 2 μM ODN to target one specific sequence near the NCX start site. This technique was used to demonstrate that decreased expression of NCX prevents Ca^{2+} overload in adult cardiomyocytes upon reoxygenation after anoxia (Eigel and Hadley, 2001).

To complement the data examining the effects of down regulation of NCX expression using the ODN approach, NCX1 knock-out mice have also been generated. Ablation of the NCX1 gene was performed independently by four laboratories (Cho *et al*, 2000; Koushik *et al*, 2001; Reuter *et al*, 2002b; Wakimoto *et al*, 2000). Even though some differences were observed between the four knock-out mice models, all of the mouse lines resulted in embryonic lethality.

The most significant characteristics of the knock-outs were as follows. Homozygous NCX-/- mice died at 9.5 -10 dpc (Cho *et al*, 2000; Reuter *et al*, 2002b;

Wakimoto *et al*, 2000) or 11.5 dpc (Koushik *et al*, 2001). Prior to death, the embryos were found to be smaller, with signs of necrosis in tissues other than the heart. The heart itself was also smaller in size, with an increased number of apoptotic cells (Cho *et al*, 2000; Wakimoto *et al*, 2000). In one case, however, the incidence of apoptosis was normal and the heart was normal (Koushik *et al*, 2001). Spontaneous contractions of the heart and Ca^{2+} transients could be observed only in 30 % of the embryos and at significantly lower frequency (Cho *et al*, 2000), or in one study they were not observed at all (Koushik *et al*, 2001). The heart tubes, however, responded to electrical stimulation, and surprisingly, Ca^{2+} transients and contractions were very similar to control responses (Reuter *et al*, 2003). The cardiomyocytes, therefore, appeared to be able to remove Ca^{2+} in the absence of NCX. However diastolic Ca^{2+} was significantly elevated when the stimulation frequency was increased (Reuter *et al*, 2003). The cardiomyocytes also showed myofibrillar disorganization (Reuter *et al*, 2003; Wakimoto *et al*, 2000). Reuter *et al* observed almost complete depletion of SERCA protein without changes in PMCA in the homozygous null mouse (Reuter *et al*, 2003). The ability of the cells to extrude Ca^{2+} in the absence of NCX and without upregulation of PMCA expression (the other Ca^{2+} extrusion mechanism) would suggest that the activity or efficiency of the PMCA might be able to increase. Despite the decrease in SERCA protein, SR Ca^{2+} content was not altered (Reuter *et al*, 2003). The NCX1 -/+ heterozygous mice showed no cardiac defects. NCX protein expression in the heart and other tissues was 50 % of wild type (Reuter *et al*, 2003; Wakimoto *et al*, 2000), or was the same as in control (Koushik *et al*, 2001).

NCX1 expression was restricted in only the heart before and at the time of lethality (Koushik *et al*, 1999). Consequently, lethality must have been due to the lack of

NCX1 in the heart. The lack of heart contractile function would limit the perfusion of nutrients in the developing embryo to maintain growth. It is not clear what causes the lack of spontaneous contractions. It could be either a consequence of the myofibril disorganization, or an effect of the absence of NCX on the pacemaker activity of the heart. Re-introduction of cardiac expression of the NCX1 did not rescue the NCX knock-out mouse (Cho *et al*, 2003).

Henderson *et al* recently developed a cardiac-specific knock-out of NCX1 using the Cre-lox system (Henderson *et al*, 2004). Cre recombinase activity is under the MLCv2 (myosin light chain 2) promoter. Therefore, ablation of the gene occurs in ventricular cardiomyocytes during development. The MLCv2 promoter activates at 8 dpc (days post-coitum) in mouse (O'Brien *et al*, 1993). As opposed to the global knock-out, the cardiac specific NCX1 knock-out survived to adulthood. Cardiac function was depressed 20 – 30 % despite the NCX expression being inhibited by ~ 90 %. However, the animals are unable to survive physiological stress (breeding). Animals also died at a younger age, probably due to heart failure. Approximately 90 % of the cardiomyocytes in the knock-out animal showed no NCX1 expression, whereas the remaining cells expressed normal levels of NCX1. No compensatory changes were observed in the other Ca^{2+} regulatory proteins. SR Ca^{2+} content was not affected and interestingly, no differences in the shape and magnitude of the Ca^{2+} transients were observed. The L-type Ca^{2+} current, however, was significantly decreased. Therefore, the authors hypothesized that the hearts were able to maintain Ca^{2+} fluxes by a combination of up-regulating the activity of the PMCA and decreasing the amount of Ca^{2+} that enters the cell through the

Ca^{2+} channels. However, PMCA expression was not altered and PMCA activity was not measured.

Isoforms

Variability in NCX isoforms and their degree of expression and tissue distribution is, in mammals, under three levels of regulation: the existence of different genes, the use of alternative promoters and, finally, alternative splicing of the RNA transcript.

a. NCX genes. Three genes code for the NCX in mammals: *NCX1* (Nicoll *et al*, 1990), *NCX2* (Li *et al*, 1994) and *NCX3* (Nicoll *et al*, 1996b). Whereas *NCX1* is expressed in several tissues, *NCX2* and *NCX3* are both expressed mainly in brain and skeletal muscle (Quednau *et al*, 1997).

b. Alternative promoters. The NCX1 gene contains three alternative promoters (Barnes *et al*, 1997; Lee *et al*, 1994; Scheller *et al*, 1998). Depending on the promoter, 3' alternative exons 1 could be incorporated, creating transcripts that are: cardiac specific, kidney specific and, one that is ubiquitous. This third transcript has highest expression in brain. The alternative exon 1 is spliced to a common exon 2. Exon 2 starts at position -31 from the translational start codon (upstream). Because exon 1 is present in the 5' UTR (untranslated terminal repeat), its sequence will not affect protein sequence. The functional importance of the different promoters is, therefore, related to the level of expression of the protein (either constitutive or regulated by tissue specific factors (Nicholas and Philipson, 1999)).

c. Alternative splicing. Variations in the structure of the protein are generated by alternative splicing of the mRNA. *NCX1* and *NCX3* undergo alternative splicing of the primary transcript. The region that undergoes splicing corresponds to the carboxyl terminus of the intracellular loop of the protein. In NCX1, the part of the gene that codes for this region is composed of six exons (A, B, C, D, E and F, corresponding to exons number 3-8 of the 12 exons that compose NCX1) (Kofuji *et al*, 1994). NCX3 codes for exons A, B and D. Exons A and B are mutually exclusive (only one of them has to be present). Inclusion of both A and B would produce a shift in the reading frame of the message. Exons A or B are followed by a combination of the other 4 cassette exons. Combinations of the different exons could lead to 32 isoforms. Up to now, 12 different isoforms of NCX1 have been identified. The isoforms are expressed in a tissue-specific manner (Lee *et al*, 1994; Quednau *et al*, 1997). In general, excitable tissues contain isoforms with exon A, and all other tissues contain isoforms with exon B. The isoforms that relate to this study are NCX1.1 (ACDEF) and NCX1.3 (BD) (Figure 2). The former is the only isoform found in the heart and is also present in skeletal muscle. Reilly and Lattanzi also described NCX1.8 in the heart (Reilly and Lattanzi, 1996). However, this finding could not be detected by others (Quednau *et al*, 1997). NCX1.3 is found in several non-excitable tissues and is the most abundant isoform in the kidney (White *et al*, 1996).

The origin of the different genes and splice variants was discussed by Quednau *et al* (Quednau *et al*, 1997). Both *NCX1* and *NCX3* genes contain mutually exclusive exons A and B. These 2 exons have a certain degree of homology and they probably originated by gene duplication. Since it is unlikely that intragenic events creating the exons occurred

Genomic organization of NCX1

NCX1.1 (heart)

NCX1.3 (kidney)

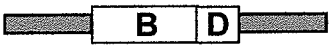

NCX1.4 (brain)

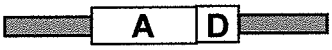

Figure 2. NCX1 genomic organization and exon composition of NCX1.1, NCX1.3 and NCX1.4 isoforms

independently in the different NCX genes, it is probable that first, the alternative exons were originated, and then, the new genes, also by gene duplication. Furthermore, closer homology exists between exon A in NCX1 compared to exon A in NCX3, than exon A with B in either gene.

The sequence corresponding to the splicing variants is located in the region corresponding to amino acids 561-645, overlapping with part of the exchanger known to be important for regulation (a region of the intracellular loop involved in regulation was determined by deletion mutants to be between amino acids 562-685) (Matsuoka *et al*, 1993). These observations lead to the idea that the diversity of splice isoforms is related to regulation of exchanger activity.

The activities of the different isoforms are regulated by different factors as well. For example, significant differences between the NCX1.1, NCX1.3 and NCX1.4 isoforms regarding ionic regulation were detected in excised giant patch studies on exchanger protein expressed in Xenopus oocytes (Dyck *et al*, 1999; Matsuoka *et al*, 1995). These differences are described in the following section of this thesis on "Ionic Regulation ". In addition, Ruknudin *et al* showed differences in the ability of cAMP-dependent protein kinase A (PKA) to phosphorylate and activate the exchanger isoforms. NCX1.1, but not NCX1.3, was affected by PKA phosphorylation (Ruknudin *et al*, 2000).

Ionic regulation

Na^+_i and Ca^{2+}_i, besides being the substrates for the exchanger, are also its allosteric modulators. Na^+ acts at the intracellular loop of the protein to produce Na^+

dependent inactivation (I_1) (Hilgemann *et al*, 1992b). Ca^{2+}_i removes I_2 inactivation (Hilgemann *et al*, 1992a). Deletion mutants of the intracellular loop, or treatment of the cytoplasmic side of the protein with proteases result in an exchanger that does not respond to regulation (remains fully active) (Hilgemann, 1990; Matsuoka *et al*, 1993). An example of I_1 and I_2 in an outward current is shown in Figure 3.

Na^+_i dependent inactivation is observed in NCX outward current measurements as a decay from a peak to a steady state current level, and is due to the entry of the fully Na^+ loaded form of the exchanger into an inactive state (Hilgemann *et al*, 1992b). Once the exchanger has bound 3 Na^+, it can either cycle or enter the inactive state I_1. A rise in Na^+_i increases peak current and also the degree of inactivation (increases the population of exchangers that enter the inactive state) (Figure 4). Mutations in the XIP region alter the rate and degree of I_1 indicating that this region is involved in the process (Matsuoka *et al*, 1997).

In the absence of Ca^{2+}_i, the exchanger enters an inactive state called I_2. Ca^{2+} binding to a high affinity site on the large intracellular loop removes this inactivation (Levitsky *et al*, 1994; Matsuoka *et al*, 1995). Further increases in Ca^{2+}_i cause an increase in outward current. The site for regulatory Ca^{2+} binding is different from the site for transport Ca^{2+} binding.

I_1 and I_2 have been extensively studied using the giant patch clamp technique (Hilgemann, 1989) in membrane patches from ventricular cells (Fujioka *et al*, 2000a) and from Xenopus oocytes expressing NCX1 (Dunn *et al*, 2002; Dyck *et al*, 1999). There is also evidence for I_2 in intact cells (Maxwell *et al*, 1999; Weber *et al*, 2001). I_1

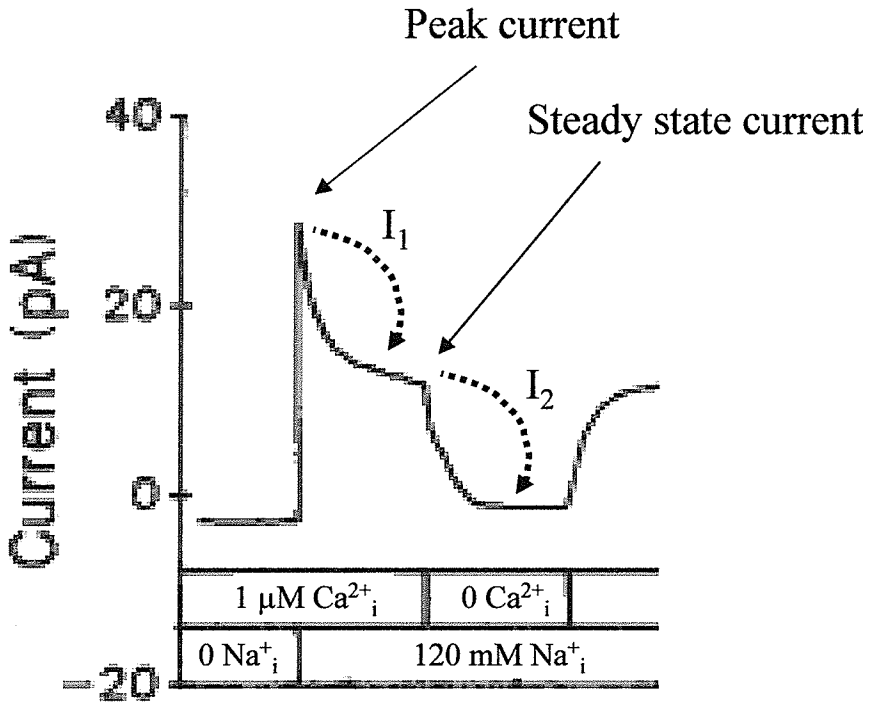

Figure 3. Ionic regulation of the cardiac NCX. Example of outward current measurement using giant membrane patches from *Xenopus* oocytes expressing NCX1.1. Application of 120 mM Na^+_i in the presence of 1 μM Ca^{2+}_i and 8 mM transported [Ca^{2+}] in the pipette, activates an outward current. Peak outward current decays to a steady state due to I_1 (sodium dependent inactivation). Removal of Ca^{2+}_i causes the exchanger to enter another inactive state: I_2. From Hilgemann *et al. Nature*, 1990; 344 (6263):242-245. Modified.

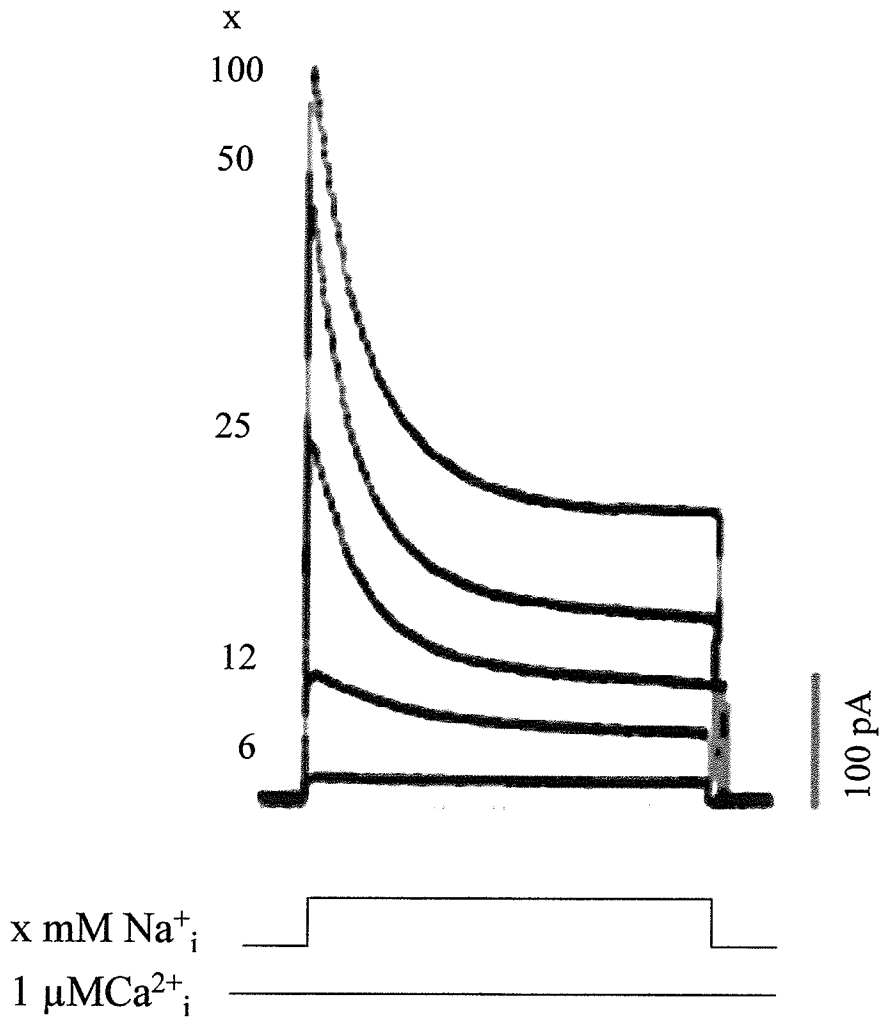

Figure 4. Sodium dependent inactivation. Example of outward currents activated by different $[Na^+]_i$ in the presence of 1 μM regulatory Ca^{2+}_i. Peak outward current, steady state current and the extent of inactivation increase as $[Na^+]_i$ increases. From Matsuoka *et al. J Gen Physiol*, 1995; *l* 105 (3):403-420.

and I_2 are also interrelated. An increase in regulatory Ca^{2+}_i can alleviate I_1 (Figure 5). In addition, mutations that affect I_1 have also an effect on I_2 (Matsuoka *et al*, 1995).

Hyrshko and co-workers analyzed the properties of ionic regulation of the NCX1.3 (kidney) and NCX1.4 (brain) splice variants (Dyck *et al*, 1999). As was mentioned earlier, NCX1.3 contains exons BD, and isoform NCX1.4 contains exons AD. Therefore, the differences observed are attributed to the protein sequence coded by A/B. The regulatory properties of the cardiac NCX1.1 were analyzed in another study by Matzuoka *et al* (Matsuoka *et al*, 1995). NCX1.4 behaves in a similar way to the cardiac NCX1.1 (both contain exon A). Inactivation of the outward current (Ca^{2+} entry mode) is significantly more pronounced in NCX1.3. Furthermore, an increase in Ca^{2+}_i can reduce Na^+ dependent inactivation in the 1.1 and in the 1.4 isoforms but not in the 1.3 isoform (Figure 6). A subsequent study used chimeras and mutants to identify the amino acids responsible for the differences between exon A or B containing exchangers (Dunn *et al*, 2002). The study showed that the 10^{th} and 17^{th} amino acids in exon A, an aspartic acid and a lysine, respectively, are critical molecular determinants of the Ca^{2+} regulatory properties.

The affinity of the regulatory site for Ca^{2+}_i in the cardiac exchanger was shown to be 0.3 to 3 μM (Levitsky *et al*, 1994) or 44 nM (Fang *et al*, 1998), depending on the methods used for its determination. Because resting $[Ca^{2+}]_i$ is ~ 100 nM, the second value would indicate that within cells, the exchanger is always fully activated and that Ca^{2+}_i would, therefore, not play any physiological role . The results from Maxwell *et al* (Maxwell *et al*, 1999), Weber *et al* (Weber *et al*, 2001) and from a recent publication by

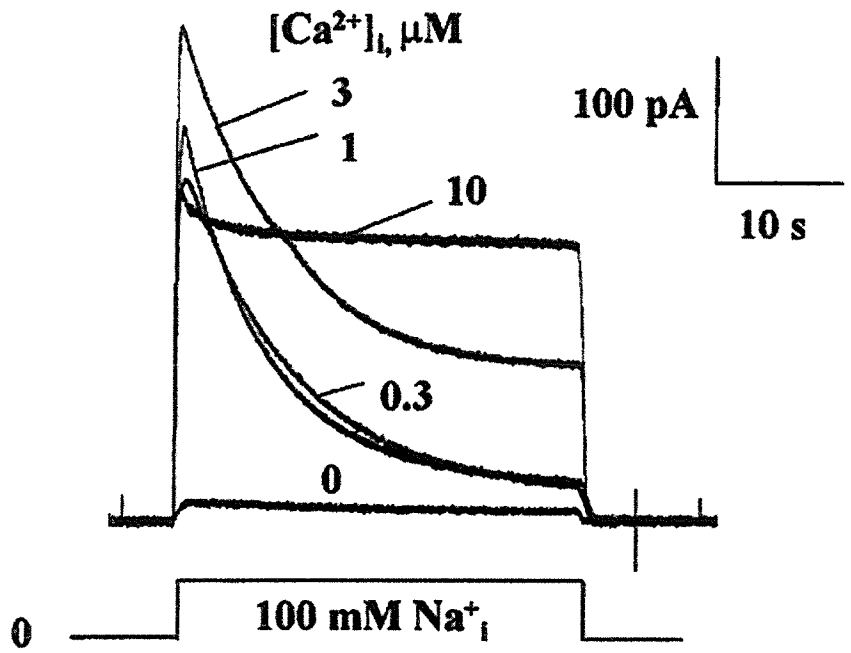

Figure 5. Calcium dependent regulation. $[Ca^{2+}]_i$ dependence of I_2 and interrelation between I_1 and I_2. Higher $[Ca^{2+}]_i$ can limit the degree of I_1 (from Hryshko. *Ann NY Acad Sci.* 976: 166-175 (2002)).

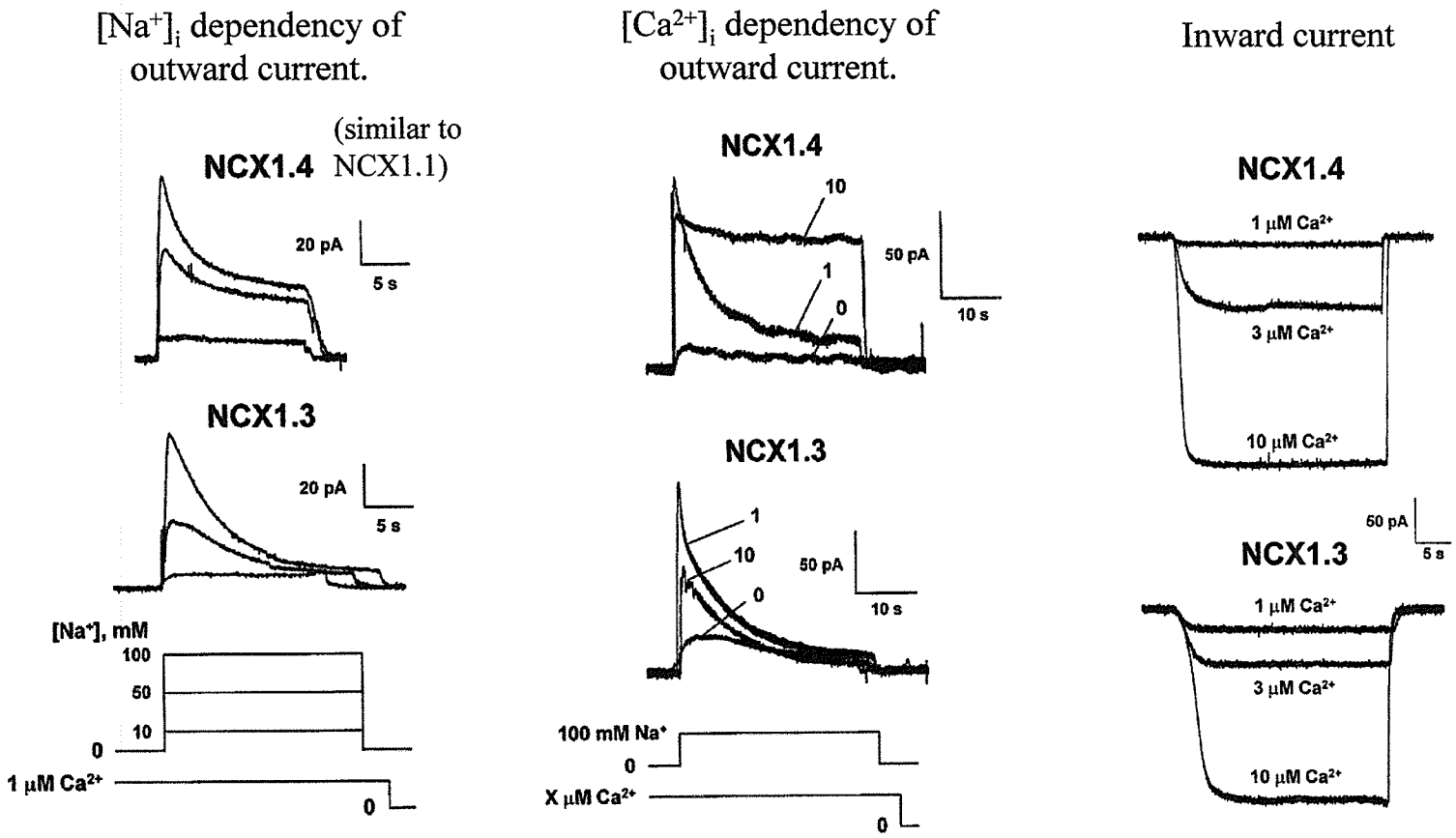

Figure 6. Ionic regulation of NCX1 isoforms (From Dyck *et al. J Gen Physiol,* 1999; 114 (5):701-711).

Ottolia *et al.* (Ottolia *et al*, 2004), however, support a role for ionic regulation in intact cells.

Inhibitors

A limited number of selective inhibitors exist for the NCX. A variety of compounds, however, with different degrees of affinity and selectivity have been used as NCX blockers. For example, divalent cations have been used to block to NCX. Ni^{2+} is commonly used at a concentration ~ 5 mM to block the exchanger in electrophysiological studies (Ehara *et al*, 1989; Kimura *et al*, 1987). Ni^{2+} has not been considered to be transported by the exchanger, however, some reports show the contrary (Egger *et al*, 1999; Hoya and Venosa, 1995). The potency of Ni^{2+} as a blocker of NCX with respect to other cations was determined to be: $La^{3+} > Cd^{2+} > Ni^{2+} > Co^{2+} > Mn^{2+} > Mg^{2+}$ (Iwamoto and Shigekawa, 1998). Alternatively, Ba^{2+}can inhibit NCX activity by essentially replacing Ca^{2+} (NCX transports Ba^{2+} in exchange for Na^{+}).

Derivatives of amiloride were also used as NCX blockers. Benzamil, DBM (N^5-(2,4-dimethylbenzyl-amiloride) and DCM (3,4-dichlorobenzamil) have IC_{50} values of 100 μM, 10 μM and 17 μM, respectively (Karwatowska-Prokopczuk *et al*, 1998; Siegl *et al*, 1984). The use of these drugs has been limited because they have a relatively poor selectivity (they can also block the Na^{+}/H^{+} exchanger and voltage-activated Ca^{2+} channels). DCM was also shown to induce a stronger inhibition of the Ca^{2+} efflux mode of the NCX (Watano *et al*, 1996). Amiodarone and other antiarrhythmic agents also block the exchanger with low selectivity (Watanabe and Kimura, 2000). CGP-37157 is a strong

inhibitor of the mitochondrial sodium-calcium exchanger (IC_{50}= 0.36 uM). CGP was shown to inhibit the plasmalemmal NCX, however, with lower affinity (IC_{50}= 7 uM) (Omelchenko *et al*, 2003).

A peptide that is 20 amino acids long containing the same sequence as part of the intracellular loop of the NCX protein, works as an inhibitor of the exchanger when applied on the cytoplasmic side of the membrane (Li *et al*, 1991). Its sequence is shown in Figure 44 (Results section). It has been named XIP (eXchanger Inhibitory Peptide). It can be used in excised patches or, alternatively, it can be injected into the cells. XIP has an IC_{50} of 0.15 – 1.5 μM. A limitation for its use is that XIP was shown to have inhibitory effect on PMCA (IC_{50}= 2.5 μM) and SERCA (IC_{50}= 1 μM(Enyedi and Penniston, 1993)). Because its sequence is similar to a calmodulin binding site, it may also interfere with calmodulin signaling.

KB-R7943 was first described in 1996 (Watano *et al*, 1996). It blocks preferentially the reverse mode of the exchanger (Ca^{2+} entry). The IC_{50} for this mode in intact cells is 1.2 to 2.4 μM whereas for the Ca^{2+} exit mode is ~ 30 μM. (Iwamoto *et al*, 1996). In patch clamp studies, the IC_{50} was 0.3- 0.9 μM and 17 μM for the outward and inward currents, respectively (Watano *et al*, 1996). This drug is water soluble (up to 100 μM) and its inhibitory effect is reversible. It works from the extracellular side of the protein through an interaction with the α2 internal repeat of the protein (Iwamoto *et al*, 2001). It has antiarrhythmic effecs (Amran *et al*, 2004; Elias *et al*, 2001), prevents Ca^{2+} overload (Satoh *et al*, 2000) and protects against ischemia-reperfusion injury (Kuro *et al*, 1999; Ladilov *et al*, 1999).

SEA0400 (SEA) is the most potent NCX blocker currently available (Matsuda *et al*, 2001). It is approximately 10 times more potent than KB-R7943. In cultured cardiomyocytes, it had an IC_{50} value of 92 nM (Takahashi *et al*, 2003). Similar to KB-R7943, SEA preferentially inhibits the reverse mode of NCX. Exchanger mutants with an altered XIP region showed a different sensitivity to SEA (Iwamoto *et al*, 2004) and, in a recent study on the mechanism of action of SEA, the drug was shown to promote a Na^+_i-dependent inactive state. It can either stabilize or modulate the transition of NCX1.1 exchangers into I_1 (Bouchard *et al*, 2004). Only a few laboratories currently have access to this compound. These laboratories have shown that SEA is protective against myocardial ischemia-reperfusion injury (Yoshiyama *et al*, 2004), hypoxia in the kidney (Iwamoto *et al*, 2004) and during brain ischemia (Matsuda *et al*, 2001). These exciting positive results have been tempered by recent findings that have dampened the enthusiasm slightly for the clinical development of these compounds. Both KB-R and SEA may not be selective inhibitors for the exchanger. Reuter et al showed that application of 5 μM KB-R or 100 nM SEA to heart tubes from NCX1 knock-out mice can significantly depress Ca^{2+} transients (Reuter *et al*, 2002a). This would suggest that the drugs are affecting other significant Ca^{2+} transport pathways besides NCX during the E-C coupling process.

NCX in the kidney

In the kidney, normally 99 % of the filtered Ca^{2+} is reabsorbed by the nephron. Reabsorption occurs at the proximal tubule, the thick ascending limb of Henle's loop and

at the distal convoluted tubule. Part of Ca^{2+} reabsorption occurs through a transcellular pathway. This is an active process that involves first the diffusion of Ca^{2+} across the apical membrane into the cell down its electrochemical gradient, likely via Ca^{2+} channels. Ca^{2+} then leaves the cell across the basolateral membrane against its electrochemical gradient via the NCX and the plasmalemmal calcium pump (Berne and Levy, 1998). The renal NCX is predominantly expressed in the kidney cortex particularly in the distal convoluted tubule (Yu *et al*, 1992), and is located at the basolateral surface of the cells (Bourdeau *et al*, 1993; Reilly *et al*, 1993).

Excitation contraction coupling

The mechanism of E-C coupling is initiated by an action potential that depolarizes the membrane (Figure 7). Opening of voltage-operated Ca^{2+} channels allows Ca^{2+} to flow from the extracellular space into the cytoplasm, driven by a large concentration gradient. Ca^{2+} that enters the cell then induces the opening of Ryanodine receptors allowing further Ca^{2+} release from the sarcoplasmic reticulum, a process called "Ca^{2+} induced Ca^{2+} release" (CICR) (Fabiato, 1985). Upon the increase in $[Ca^{2+}]_i$, Ca^{2+} binds to the contractile filaments to activate contraction. For relaxation to take place Ca^{2+} has to be removed from the cytoplasm. Part, is transported back into the SR through the sarcoplasmic endoplasmic reticulum calcium pump (SERCA), a small amount is transported into mitochondria through the Ca^{2+} uniporter and, the rest is removed from the cells. The main Ca^{2+} extrusion mechanism in the heart is the NCX and a minor

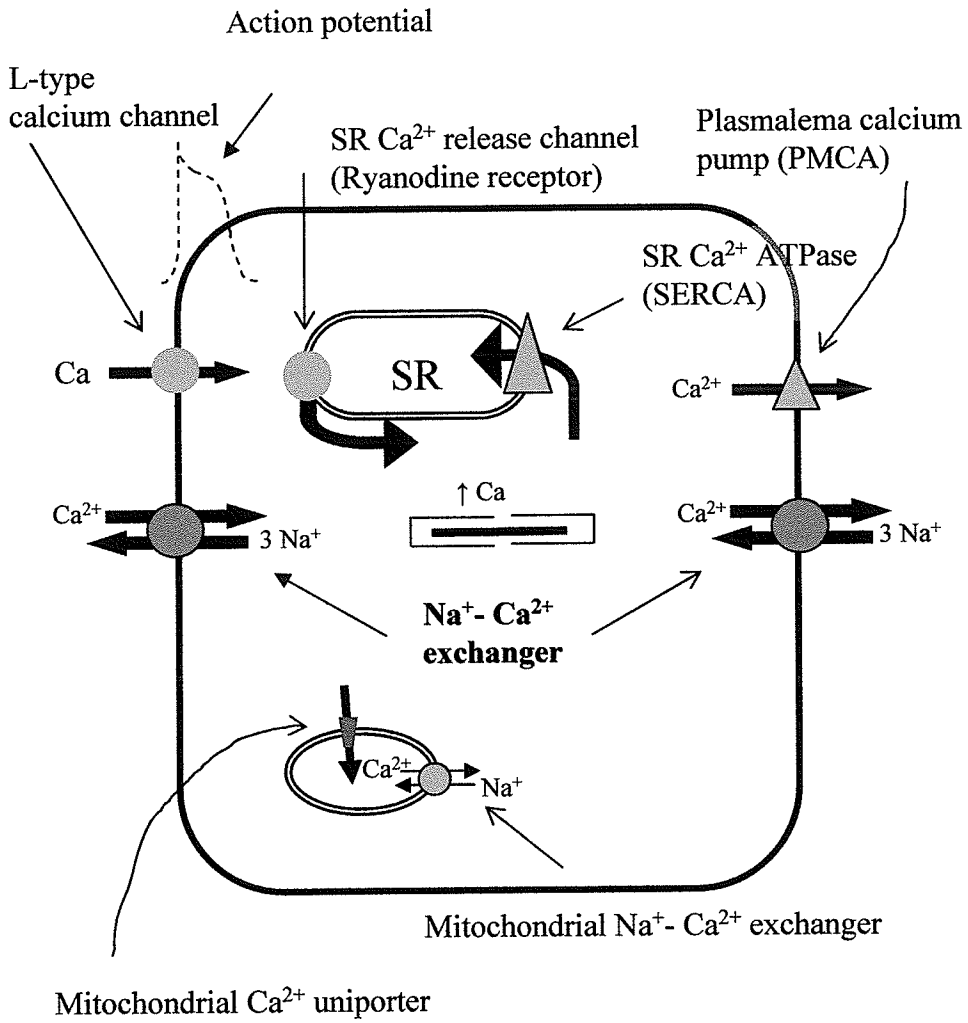

Figure 7. Excitation contraction coupling in the heart. Calcium channels, pumps and exchangers involved in the mechanism of excitation contraction coupling and calcium homeostasis in the heart. In adult cardiomyocytes, most of EC coupling occurs at the t-tubules-junctional SR interface.

contributor is the plasmalemmal calcium pump (PMCA) (Bers, 1991; Crespo *et al*, 1990; Wier, 1990). The relative contribution of each transporter to the removal of cytoplasmic Ca^{2+} varies between species, and also depends on the developmental stage of the animal (Bers, 2001).

Changes during development

CICR is less important early in development. Mature CICR is reached 3-4 weeks after birth in the rat (Fabiato, 1982; Vornanen, 1984), before that time, the heart is more dependent on transarcolemmal Ca^{2+} fluxes to induce contraction. The SR is not well developed at the time of birth. SERCA expression starts in the rat embryo at day 9 of development (Moorman *et al*, 1995) and increases after birth (Lompre *et al*, 1991). Ryanodine receptor density is also relatively low at the end of gestation. Some authors found that ryanodine (compound that blocks SR Ca^{2+} release) had no effect in neonatal cardiomyocytes (Nakanishi *et al*, 1988; Tanaka and Shigenobu, 1989), others found a minor effect (Agata *et al*, 1993; Escobar *et al*, 2004) and others a more significant effect (Seki *et al*, 2003; Wibo *et al*, 1991).

Ca^{2+} influx in the neonate is mediated by L-type Ca^{2+} channels (major source) (Cohen and Lederer, 1988; Vornanen, 1996), T-type Ca^{2+} channels (Xu and Best, 1992) and NCX (Artman, 1992; Nabauer and Morad, 1992). The changes in NCX expression during development oppose those of SERCA (Reed *et al*, 2000). NCX mRNA and protein levels peak at birth and then decline (Artman, 1992; Boerth *et al*, 1994; Vetter *et*

al, 1995). Relaxation in newborn myocytes may occur predominantly through Ca^{2+} extrusion through NCX as opposed to Ca^{2+} uptake by the SR.

Another difference in E-C coupling between adults and neonates is that T-tubules are absent at birth. They develop around 10 days after birth in the rat. Previous to that time the smaller volume/surface relation is enough to provide Ca^{2+} to the myofilaments for contraction.

Action potential

Cardiomyocytes, like other excitable cells, are able to produce action potentials (AP). When the membrane potential reaches the threshold potential, an AP fires, and propagates along the cell membrane and to neighboring cells. The AP is produced by acute changes in the permeability of the membrane to Na^+, K^+, Ca^{2+} and Cl^- ions. During the AP, ion channels open that allow ions to flow down their electrochemical gradient, driving the E_m close to the equilibrium potential for the specific ion. Figure 8 shows the shape of one action potential and the changes in conductance of the different ion channels that are involved in the AP (1991). The AP can be divided in 4 phases:

- Phase 0 is caused by the fast and self-regenerative activation of Na^+ channels. Na^+ channels activate around -70 mV. The Na^+ current causes the upstroke of the AP. Inactivation of the Na^+ channels is voltage and time dependent.
- Phase 1 is due to fast repolarization, caused by K^+ exit from the cell (It_{o1}, Ca^{2+} independent K^+ channel current) and entry of Cl^- (It_{o2}, chloride current). It_{o2} is

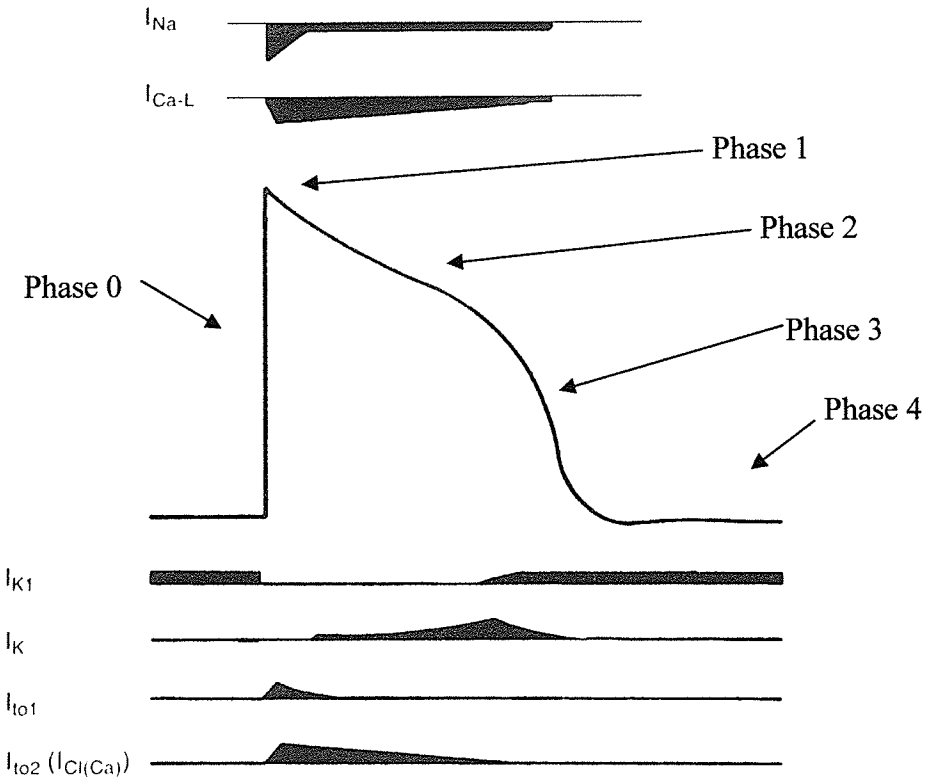

Figure 8. The cardiac action potential. Representative action potential from ventricular tissue. Phases 0 – 4 are indicated with arrows. Ionic currents that are involved at each time point are shown on top (inward currents) or below (outward currents). From *Circulation*, 1991, 84 (4): 1831-51.

Ca^{2+} dependent and therefore more important during the first part of the AP plateau.

- Phase 2. This prolonged plateau phase is characteristic of the cardiac AP. During this phase the membrane potential is maintained relatively constant due to the balance of depolarizing and repolarizing currents. The depolarizing current is caused by the Ca^{2+} current that is due mainly to L-type Ca^{2+} channel activation. This channel has a slow voltage dependent inactivation process. The repolarizing currents are Ito_2 that is initiated at the beginning of the plateau and IK that is active at the end of the plateau.
- Phase 3 is a repolarization phase due to the slow activation of the K channels: IK_r and IK_s. During this phase the Ca^{2+} channels are already closed.
- Phase 4 is maintained by the K channel inward rectifier IK_1 that transports current at potentials close to the E_m (because it inactivates at more positive potentials). This phase is unstable in cells that show automaticity.

In the rat, there is a significant change in the shape of the AP from the newborn to the adult. The duration of the ventricular AP progressively decreases with advancing age until the plateau phase nearly disappears in the adult and it resembles a spike (Langer *et al*, 1975).

The AP in neonatal cardiomyocytes is inherently unstable. This instability leads to spontaneous electrical activity (Jongsma *et al*, 1983). The mechanism responsible for the spontaneous contractions is unclear but two hypotheses have been proposed to explain this event. The I_f (funny current) has been identified in neonatal cardiomyocytes and has

been proposed to be responsible for the unstable phase 4 of the AP (Er *et al*, 2003). Alternatively, spontaneous SR Ca^{2+} release from the SR would induce Ca^{2+} efflux through NCX, that would contribute with depolarizing current (Yang *et al*, 2002). Either mechanism is possible or a combination of both may also participate in the spontaneous electrical activity exhibited by the neonatal cardiomyocytes. This spontaneous activity disappears as the animal ages. Adult cardiomyocytes do not exhibit any spontaneous electrical activity unless they are in a damaged state.

The NCX is involved in determining the shape of the AP (Grantham and Cannell, 1996). It contributes to the shape of the AP because NCX is electrogenic. When the NCX removes Ca^{2+}, it carries an inward current, and when it brings Ca^{2+} into the cell, it produces an outward current. In rabbit adult and rat neonatal cardiomyocytes (because of the prolonged AP), Ca^{2+} extrusion occurs late during the AP. In rat adult ventricular myocytes that have a short AP, NCX contributes with an inward current earlier during the Ca^{2+} transient (Bers, 2002).

Myocardial ischemia

Ischemic heart disease is a major cause of mortality (Antman and Braunwald, 1997). Ischemia is defined as an imbalance between the oxygen supply and the demand of a tissue (Opie). Myocardial ischemia can be caused by complete or partial obstruction of a coronary artery, most commonly due to the development of an atherosclerotic plaque or a vasospasm. It can generate arrhythmias and, if prolonged, it can affect survival of the myocardium. A severe myocardial infarction will impair cardiac function.

The normal ionic homeostasis of the heart is altered during ischemia. Anaerobic glucose metabolism, ATP breakdown and accumulation of CO_2 and lactate result in intracellular acidosis. Low intracellular pH activates the Na^+-H^+ exchanger to extrude intracellular H^+ in exchange for extracellular Na^+ (Lazdunski *et al*, 1985). Influx of Na^+ through the Na^+-H^+ exchanger and via Na^+ channels (Eng *et al*, 1998) together with decreased efflux through the Na^+-K^+ ATPase causes intracellular Na^+ accumulation. The elevation of Na^+_i decreases Ca^{2+} efflux through the NCX and can activate Ca^{2+} entry through the reverse mode of this exchanger (Hearse and Bolli, 1992), causing Ca^{2+} overload (Tani and Neely, 1989). In addition, at reperfusion, the rapid washout of extracellular H^+ generates a larger pH gradient between the inside and outside of the cell that causes further activation of the Na^+-H^+ exchanger and NCX (Hurtado and Pierce, 2000).

A significant increase in Ca^{2+}_i results in cell injury through induction of hyper-contracture (Piper *et al*, 2003) and activation of proteases that act on contractile myofibrils and other cellular proteins (Goll *et al*, 2003; Papp *et al*, 2000; Perez *et al*, 1999; Tsuji *et al*, 2001; Yoshida *et al*, 1995). Therefore, procedures that prevent the increase in Ca^{2+}_i are cardioprotective.

Reperfusion and Na^+-H^+ exchange inhibition

Early reperfusion of an ischemic tissue is an absolute requirement for survival. However, reperfusion can also have deleterious effects (Braunwald and Kloner, 1985; Forman *et al*, 1990; Hearse and Bolli, 1992; Marban *et al*, 1989). Strong research support

exists for the use of Na^+-H^+ exchange blockers to protect the myocardium during ischemia-reperfusion (Docherty *et al*, 1997; Karmazyn, 1988; Meng *et al*, 1993; Meng and Pierce, 1990). Nevertheless, there is still controversy regarding the most effective time for drug delivery.

Numerous studies have demonstrated that Na^+-H^+ exchange inhibitors present prior to and during the ischemic insult can provide significant cardioprotection. They can decrease cell contracture, infarct size, the incidence of arrhythmias, improve myocardial function and decrease mortality (Avkiran, 1999; Scholz *et al*, 1995). There would appear to be no conflict in results on this issue. However, studies that initiate drug treatment at the time of reperfusion have given conflicting results. Some studies show protection when the inhibitors are present immediately before reperfusion or at reperfusion (Docherty *et al*, 1997; duToit and Poie, 1993; Gumina and Gross, 1999; Linz *et al*, 1998; Rohmann *et al*, 1995; Xiao and Allen, 2000). Other studies have shown no protection at all when drugs are introduced during reperfusion (Karmazyn, 1988; Khandoudi *et al*, 1997; Klein *et al*, 2000; Miura *et al*, 1997; Murphy *et al*, 1991). The possibility that the introduction of the drug during late reperfusion inhibits the effects of late ischemia was directly addressed and discounted (Maddaford and Pierce, 1997). However, it is clear that the majority of studies that have compared the cardioprotective effects of drug delivery before reperfusion to those when the drug is delivered solely at reperfusion have shown superior protection in the former intervention as opposed to the latter.

Resolving the factors responsible for this controversy is critical in directing the characteristics of clinical trials in the future. Two basic possibilities exist:

1. The drug *must* be present during ischemia to achieve cardioprotection;

2. The drug does not need to be present during ischemia to induce cardioprotection but several factors hinder its actions when administered solely during reperfusion. For example, drug diffusion across the vascular wall may be limited and one cause of conflicting findings (Maddaford and Pierce, 1997).

RNA interference (RNAi)

RNAi is the process of sequence specific post-transcriptional gene silencing initiated by double stranded RNA that is homologous in sequence to the silenced gene. This phenomenon was first observed in *C. elegans* by Fire and co-workers (Fire *et al*, 1998). They surprisingly discovered that a mixture of sense and antisense RNA, the control for their antisense mediated down-regulation experiments, was ten-fold more efficient than the antisense RNA itself. RNAi was found to be similar to the phenomenon of co-suppression previously described in plants (Jorgensen, 1990). RNAi was later also observed to occur in diverse organisms (Fire *et al*, 1991; Lohmann *et al*, 1999; Ngo *et al*, 1998; Pal-Bhadra *et al*, 1997; Romano and Macino, 1992). It serves as a natural mechanism of defense against viral infections, transposon elements and probably, may contribute to the regulation of gene expression (Denli and Hannon, 2003; Hannon, 2002). RNAi is now being used as a powerful tool to study gene function.

Double stranded RNA is processed within the cell by the ribonuclease III Dicer into 21-22 nucleotides long RNA duplexes (siRNA or small interfering RNAs). siRNAs contain a phosphate group on the 5' end, and 2 nucleotides overhang on the 3' end. These characteristics are necessary for siRNA to be recognized by the next component of the

RNAi pathway: the multinuclease complex RISC (**R**NAi **I**nduced **S**ilencing **C**omplex). RISC unwinds the short duplex RNA and uses it to find mRNAs of homologous sequence (through base-pairing of the antisense sequence of the duplex with the mRNA). RISC then proceeds to cleave the mRNA (at the midpoint of the homologous sequence), preventing its translation (Figure 9).

Double stranded RNAs introduced into invertebrate cells (and also in mammalian embryonic cells) are processed by DICER to induce the RNAi pathway. In all other mammalian cells, however, long dsRNA activate a non-specific mechanism that leads to apoptosis. Double stranded RNA of more than 30 nucleotides long trigger the synthesis of interferon. Interferon activates protein kinase R (PKR) and 2'-5' oligoadenylate synthase that halts all protein synthesis and induces the degradation of all mRNAs in the cell, respectively.

Elbashir *et al.* showed for the first time that RNAi can indeed be achieved in mammalian cell lines (Elbashir *et al*, 2001). They were able to by-pass the interferon response by transfecting the cells with synthetic siRNAs. An alternative approach to transfection of naked siRNA (that is labile to degradation and difficult to transfect) was described by Paddison *et al* (Paddison *et al*, 2002). This approach consisted of the transfection of mammalian cells with DNA expression plasmids that code for RNA duplexes of 30 or less nucleotides long. The RNA duplexes synthesized within the cell are also processed by DICER to form siRNA that induces gene silencing. The method could be achieved by placing the sense and antisense sequences under separate promoters (either on the same or on two separate plasmids), or by using a sequence that codes for a

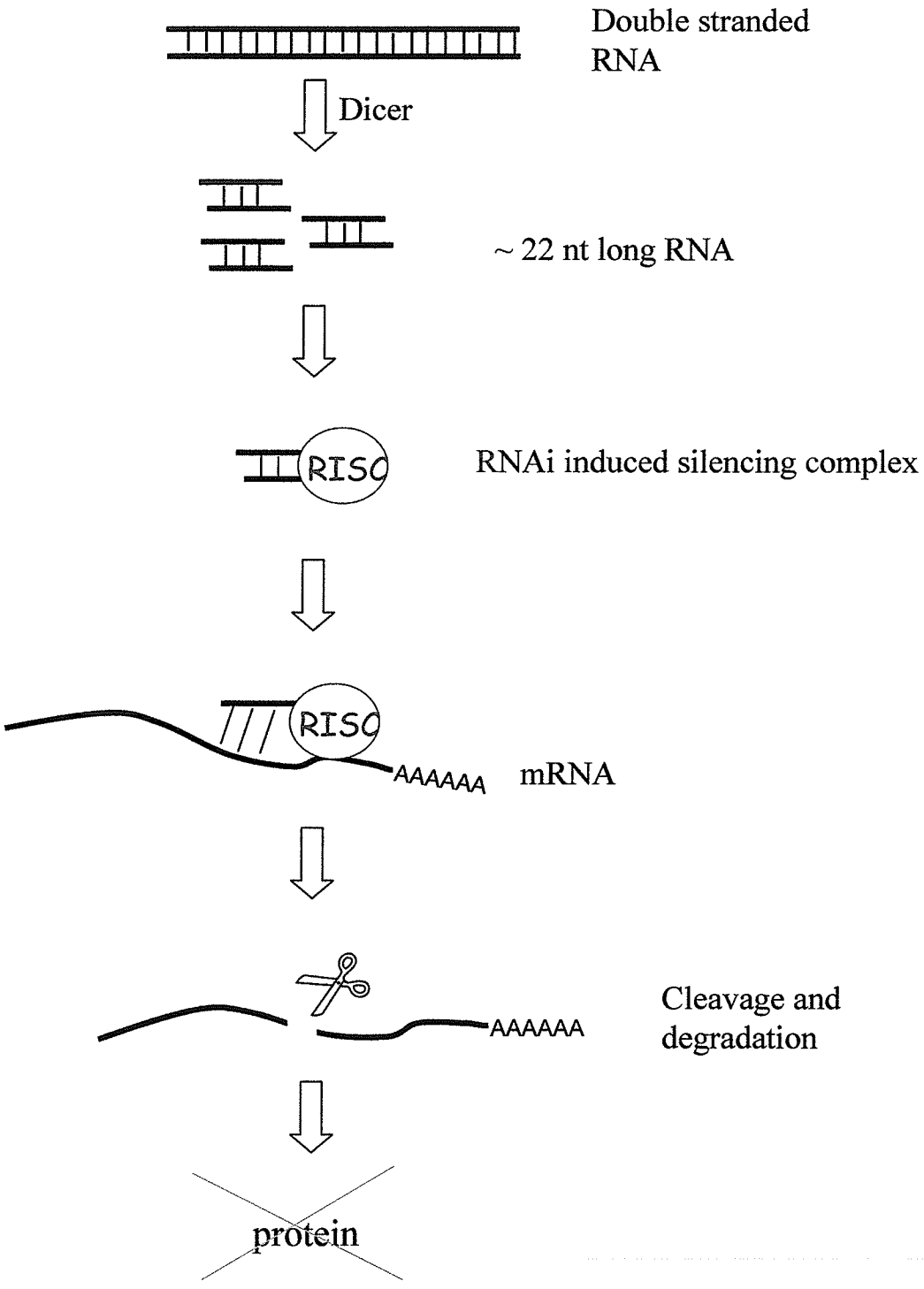

Figure 9. Mechanism of RNA interference

self-complementary short RNA hairpin (shRNA), where the sense and antisense sequences are separated by a loop of nucleotides (Figure 10). For the present study the shRNA approach was used, and to achieve high efficiency of transfection in cardiomyocytes, the shRNA construct was introduced into a replication deficient recombinant adenovirus vector.

Adenovirus vectors are the vectors of choice for high efficiency of transfection in-vitro for non-dividing cells. The advantage of adenoviral transfection vectors is that because they remain episomal, they do not cause insertion mutations that could disrupt or alter the expression of important genes. However, this characteristic limits the use of adenovirus vectors to non dividing cell types (the transgene can not be transmitted to both daughter cells as the cells divide).

1. Chemically synthesized siRNA (naked siRNA)

2. DNA expression vectors

a. Separate plasmids coding for sense and antisense strands of siRNA

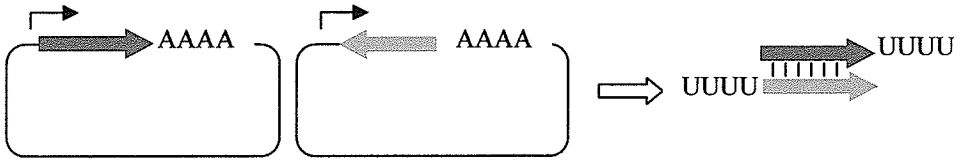

b. One plasmid coding for sense and antisense sequences under separate promoters

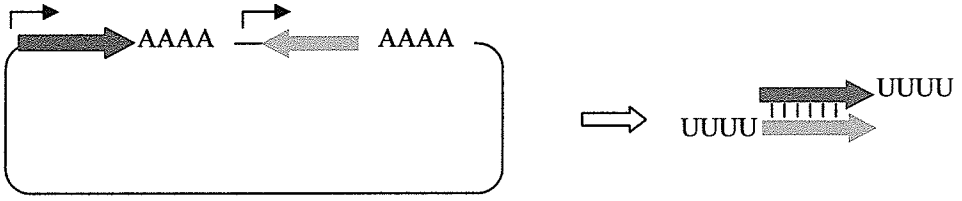

c. One plasmid coding for a shRNA with sense and antisense sequences and RNA linker

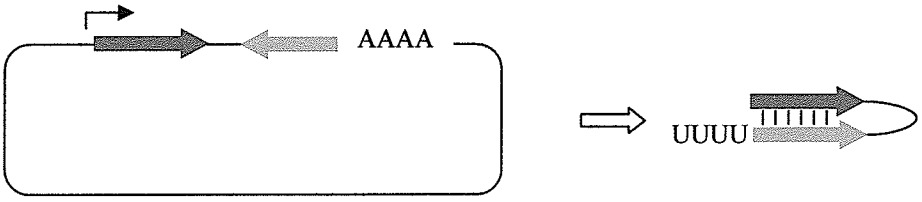

Figure 10. Approaches to induce RNAi. Chemically synthesized siRNA can be introduced by lipid based transfecting reagents (LR) or by electroporation. DNA expression vectors can also be transfected by LR or can be efficiently transduced using viral vectors.

METHODS

Isolation of neonatal cardiomyocytes

Neonatal cardiomyocytes were isolated from the ventricles of 0-24 hours old Sprague-Dawley rats as described by Doble *et al* (Doble *et al*, 1996). Thirty-six hearts were used per cell preparation. The hearts were removed from the animals, washed and minced into small pieces. The pieces of tissue underwent 6 rounds of enzymatic digestion for 10 minutes in a spinner flask at 37°C and under continuous agitation. For each digestion 10 ml of phosphate buffer saline w/ glucose (PBS-G) containing 740 units of collagenase II, 370 units of trypsin I and 2,880 units of DNAse I were used. After each round of digestion isolated cells were collected into a flask containing fetal bovine serum (FBS) to stop the enzymatic reaction. Cells were filtered through 100 μm mesh, spun at 2,000 rpm for 5 minutes and were then run through a Percoll gradient to separate cardiomyocytes from other cell types (fibroblasts, smooth muscle and endothelial cells). The densities of the bottom and top layers of the gradient were 1.076 and 1.053 g/ml, respectively. The cells were added on top of the gradient and centrifuged at 3,500 rpm for half an hour. Cardiomyoctes were then washed with F10 media and resuspended in F10 media containing 10 % Hyclone serum, 10 % horse serum and 100 units/ml penicillin and 100 ug/ml streptomycin. Cardiomyocytes were seeded at a density of 0.8×10^6 cells per 35-mm culture dish. The following day, the cells were switched to DMEM medium containing 0.5 % FBS, 20 nmol/L selenium, 10 μg/mL insulin, 10 μg/mL transferrin, 2 mg/mL BSA, and 20 μg/mL ascorbic acid. The medium was replaced every 48 hours or

daily if required. For the action potential measurement experiments, and when the cells were electrically stimulated, 2 days before use, the cells were dissociated using collagenase and trypsin and re-plated on collagen coated coverslips at lower density.

Isolation of adult cardiomyocytes

Ventricular cardiomyocytes were isolated from adult male Sprague-Dawley rats. The rats were anesthetized, hearts were removed and attached to an aortic cannula in a Langendorf perfusion apparatus. The hearts were perfused for 10 minutes with calcium free IB1/MEM Jocklic solution at a rate of 10 ml/min and at 37°C. Atria were removed. The solution was changed to an IB3/MEM Jocklic solution containing 216 units/mg of collagenase type 2 and 0.6 mg/ml hyaluronidase for 15 minutes. After digestion the heart was removed from the cannula and scissor minced in IB3 in a Petri dish. The pieces of tissue were disgregated by pipetting very gently. The preparation was filtered through 2 layers of gauze into a sterile centrifuge tube. The cell suspension was spun at low speed and cells were resuspended in 20 ml of IB3. $CaCl_2$ was added every 5 min to increase the calcium concentration in the solution to 1.25 mM. Cells were then transferred to M199 media and seeded on laminin pre-coated coverslips and kept in an incubator overnight.

Culture of HEK-293 cells

Human embryonic kidney-293 (HEK-293) cells were obtained from Quantum. The cells were grown in DMEM 5 % FBS. For generation of stocks cells were grown in 10 %

FBS and frozen in 40 % FBS-DMEM and 10 % DMSO and kept at - 80°C. Culture passages were kept below 30 and cell confluency below 70 %. Passaging of the cells was performed every 2-3 days by washing the plate with PBS and then incubating with trypsin for 2 minutes at room temperature. Cells were spun down at 600 rpm for 5 minutes.

Stable transfection of HEK-293 cells

HEK-293 cells expressing the NCX1.3 isoform were generated by co-transfection of the cells with the pShuttle-NCX1.3 and pCDNA3Hygro using Lipofectamin. HEK-293 cells expressing the NCX1.1 isoform were generated by transfecting 293 cells with the plasmid pCDNA3Hygro-NCX1.1. 200 ug/ml hygronomicin was used to select stable transfected clones. NCX expression was verified by Western blot. Several clones of each isoform had to been screened to find colonies that express similar levels of either NCX1.1 or NCX1.3.

Plasmids

Original plasmids

- Bluescript II SK (+) containing the dog cardiac cDNA NCX1.1 inserted at Bam HI – Hind III was obtained from Dr. Hryshko (University of Manitoba)

- Bluescript II SK (+) containing the dog cardiac cDNA NCX1.3 inserted at Bam HI – Hind III was obtained from Dr. Hryshko (University of Manitoba)
- pShuttle-CMV (7,465 bp, Quantum)
- pShuttle (6,621 bp, Quantum)
- pAdEasy-1 (33,441 bp, Quantum)
- pIRES2-EGFP (Clontech)
- pEGFP-N1 (Clontech)
- pEGFP-1 (Clontech)
- pCDNA3-Hygro (Invitrogen)
- pCDNA3-rat NCX1.1 provided by Dr. Lytton (University of Calgary)
- pGEM 1 U6 provided by Dr. Hannon (Cold Spring Harbor Laboratories)

Recombinant plasmids generated for the study

- pShuttle-CMV-NCX1.1. The BamH I – Hind III insert (3189 bp) from Bluescript II SK (+) dog NCX1.1 was inserted into the pShuttle-CMV in Bgl II – Hind III (7431bp)
- pShuttle-CMV-NCX1.3. The Xho I- Kpn I fragment form Bluescript II SK (+) dog NCX1.3 (737 bp) containing a Ssp I site replaced the Xho I- Kpn I fragment in pShuttle-CMV-NCX1.1 (850 bp)
- NCX(end)-EGFP fusion protein. The stop codon of NCX1.1 was removed by perfoming PCR with a forward primer that includes the KpnI site (position 2460)

and a reverse primer that contains a BamH I and is in reading frame with EGFP in pEGFP1. Forward primer: NCXEXF:

5'TTAGAATTCATGGTACCAGACACATTTGC3' (GAATTC = EcoR I; ATG= start codon; GGTACC= Kpn I; underlined sequence: complementary to NCX), annealing temperature: 54.

Reversed primer: NCXBR:

5'ATATGGATCCGGGAAGCCTTTTATGTGGCAG3' (GGATCC= BamH I; underlined sequence: complementary to the end of NCX1, nucleotides before stop codon), anealing temperature: 56 C.

Template used: pShuttle-NCX1.1

The conditions used for the PCR reaction were: 3 min at 94 °C, 25 cycles of 45 sec denaturing at 94 °C, 30 sec annealing at 54 °C and 45 seconds extension at 72 °C, followed by 3 min at 72 °C. The PCR reaction mix consisted of (final concentration): 250 uM dNTPs (A, C, G, T), 1 uM primers (forward and reversed), 5 mM $MgCl_2$, 1 X PCR buffer, 2 units Taq DNA Polimeraze (5u/ul) and 100-200 ng of template DNA . The PCR fragment was digested with EcoR I/ BamH I and was introduced into EcoR I- BamH I digested pEGFP-N1 to form pEGFPN1-NCX1.1. This plasmid contained the end of NCX1 fused to EGFP and contained a start codon upstream of the NCX1 sequence. The functionality of the fusion protein was verified by transient transfection of the plasmid into HEK-293.

- pShuttle-CMV-NCX1.1-EGFP. The 1.14 Kb Xba I-Kpn I insert from pEGFN1-NCX1.1 was inserted in the pShuttle-NCX1.1 digested with Xba I – KpnI. (approximately 10 Kb).

- pShuttled-NCX1.3-EGFP. The XhoI- KpnI insert form Bluescript II SK (+)dNCX1.3 (737 bp) containing an sspI site replaces the XhoI- KpnI fragment from pShuttleCMV-NCX1.1EGFP.
- pShuttle-CMV-EGFP. The Not I (blunted)/ Bgl II insert (791bp) from pEGFP-1 was inserted into pShuttle-CMV digested with Xho I (blunted)/ Bgl II insert.
- pCDNA3Hygro-NCX1.1. The BamH I/ Hind III insert from Bluescript II SK (+) dog NCX1.1 was inserted into pShuttle-CMV digested with BamH I/ Hind III.
- pShuttle-NCX1.1 dog antisense. The Bgl II (blunted)/ Xba I insert from Bluescript II SK (+) dog NCX1.1 was inserted in the 3' – 5' orientation in the pShuttle-CMV digested with Hind III (blunted) and SpeI.
- pShuttle-NCX1.1 rat antisense. The BamH I / Hind III insert from pCDNA3-rat NCX1.1 was inserted in the 3' – 5' orientation in the pShuttle-CMV/ Bgl II/ Hind III.
- pShuttle-XIP-ires-EGFP. An insert containing the kozak sequence (GCCACCATG), start codon (ATG), nucleotide sequence for XIP (AGGAGGCTGCTGTTTTACAAGTATGTCTACAAGAGGTATCGGGCCGG CAAGCAGAGGGGA), and stop codon (TAA), flanked by restriction sites, EcoR I (5', GAATTC) and BamH I (3',GGATCC) was generated by PCR. The primers used were: XipRev (5'TATGGATCCTTATCCCCTCTGCTTGCCG3') and XIP-2Forw (5' ATGAATTCGCCACCATGAGGAGGCTGCTGTTTTAC 3'). The conditions used for the PCR reaction were:3 min 94°C; 0.45 min 94°C; 0.30 min 54°C; 0.30 min 72°C; 30 cycles: 3 min 72°C, using pShuttle-NCX1.1 as template. The insert was introduced into pIRES2-EGFP. From where XIP-ires-EGFP was

removed to be introduced into the multiple cloning site of pShutlle-CMV vector. This construct codes for one polycistronic mRNA that is translated within the cells into 2 proteins: the 21 aa peptide (20 + start codon methionine) and EGFP.

- pShuttle-XIP-ires-XIP. Through a series of subcloning steps we replaced the EGFP in the previous construct by another XIP sequence (with kozak sequence, start and stop codon). The polycystronic mRNA synthesized from this construct is translated into 2 XIP peptides.

pShuttle plasmids for RNAi

Three sequences were chosen from the NCX cDNA sequence to construct the RNAi vectors (Figure 11). For control, we generated one construct containing the scrambled sequence of one of the sequences previously mentioned.

The DNA insert introduced into the promoter-less p-Shuttle plasmid for generation of adenoviruses consisted of the human U6sn RNA promoter followed by the nucleotide sequence coding for an RNA hairpin and flanked by restriction enzymes sites. The inserts were generated by PCR using the pGEM 1 U6 plasmid as the template, the forward primer and one of the reverse primers (Figures 12 and 13). We followed protocols described in www.cshl.org/public/science/hannon.html with some modifications. All the primers were purchased from Sigma Genosys. The forward primer corresponds to the SP6 sequence upstream of the U6 (italics) promoter and contained the Kpn I restriction site (underlined) in the 5' end (5' gcc<u>ggtacc</u>*agaatacaagcttggctgcagg* 3'). The reverse primers contained (in the 5'- 3' orientation with respect to the transcript) a region

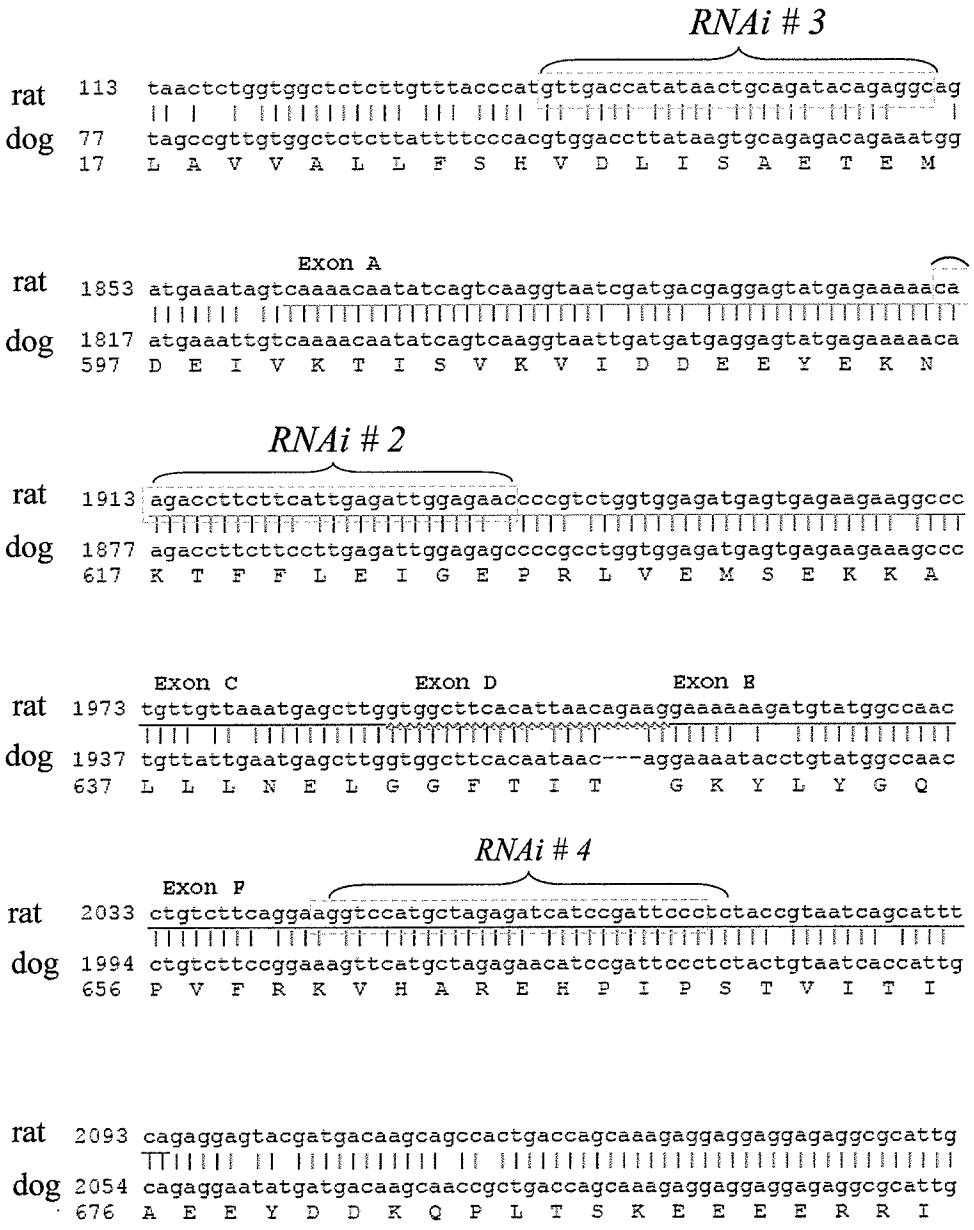

Figure 11. RNAi sequences designed to target NCX1.1. Segment of the rat and dog NCX1.1 cDNA sequence, showing the nucleotides targeted by the Ad-RNAi constructs (light blue dashed boxes). Underlined in different colors are the exons A, C, D, E and F.

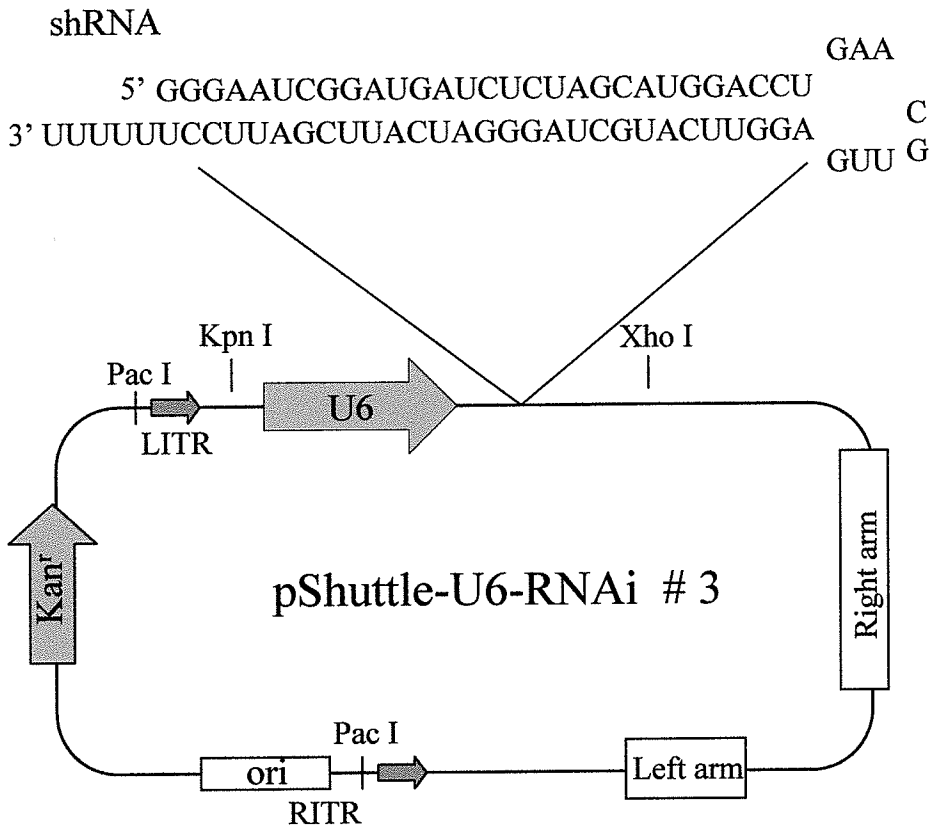

Figure 12. Example of RNAi construct and hairpin. Diagram of pShuttle-U6-RNAi #3 used to generate one of the adenoviruses for RNAi against NCX. Sequence of the shRNA coded by this vector is shown on top of the figure. RNAi #3 targets nucleotides 142 to 171of the NCX1. U6, U6 promoter; Kan^r, kanamycin resistance; ori, origin of replication; Right and left arms for recombination with AdEasy-1; LITR and RITR left and right internal terminal repeats.

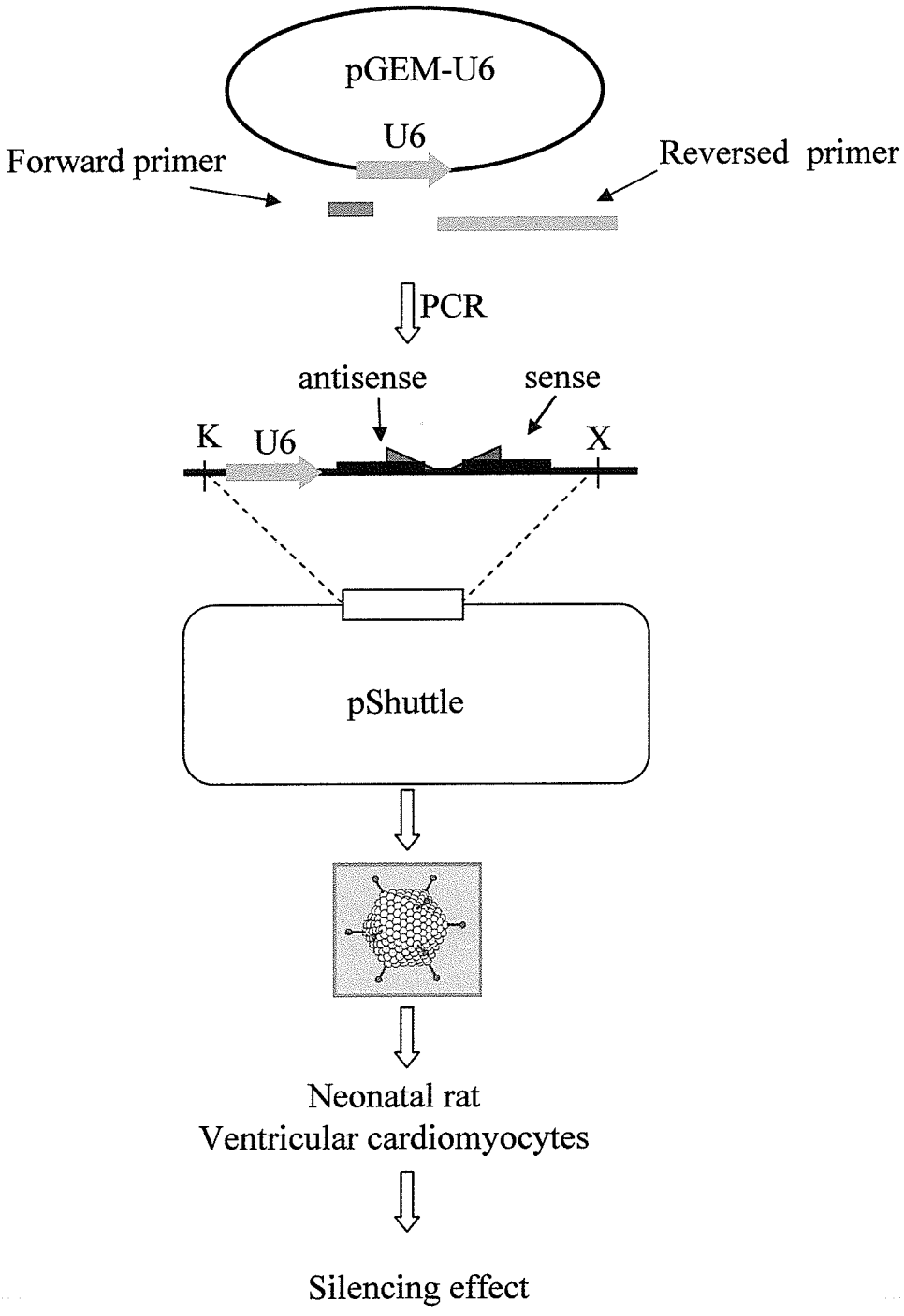

Figure 13. Procedure for generating adenovirus for RNAi

complementary to the end of the U6 promoter (italics), an anti-sense sequence (all caps), an 8 nucleotide spacer loop (bold), a sense sequence (which ends with a C), and 6 Ts to signal pol III termination (6 As in the primer, underlined) and one Xho I restriction site (ctcgag). The sense and antisense sequences form a 29 nucleotides long stem. Some of the A nucleotides in the **sense** sequence were changed to G and some C were changed to T to form G-U pairing that provided stability to the hairpins during propagation in bacteria.

Reverse primers:

- RNAiNC11-142 rev or RNAi # 3 (targets 29 nucleotides starting 142 nucleotides from translation start site)

  5'gcgctcgagaaaaaaggaatcgaatgatccctagcatgaacct**caagcttc**AGGTCCATGCTAGA GATCATCCGATTCCC*ggtgtttcgtcctttccacaa* 3').
- RNAiNC11-1910 rev or RNAi # 2 (targets exon A of NCX1.1)

  (5'gcgctcgagaaaaaagttctccaacctcaacgaagaaggcctcg**caagcttc**CAAGACCTTCTTC ATTGAGATTGGAGAAC*ggtgtttcgtcctttccacaa* 3').
- RNAi NC11-2040 rev or RNAi # 4 (targets exon F of NCX1.1)

  5'gcgctcgagaaaaaagcccctgtacctgcaattatacggtcaac**caagcttc**GTTGACCATATAAC TGCAGATACAGAGGC*ggtgtttcgtcctttccacaa* 3').
- RNAiNC scrambled (the sense sequence was generated by randomly reorganizing the sense sequence of RNAiNC11-142rev)

(5'gcgctcgagaaaaaagtccaccaccagtatcctagccctattac**caagcttc**GTAACAGAGCTAG GATACTAGTGGTAGAC*ggtgtttcgtcctttccacaa* 3').

All of the sense sequences were blasted against rat sequence databases to verify that the RNAi would not alter the expression of other endogenous genes. The PCR conditions were: 95 °C for 3 min; 30 cycles of 95 °C for 30 seconds, 58 °C for 30 seconds and 72 °C for 1 minute followed by one cycle of 72 °C for 10 minutes. 4 % DMSO and 50 pmol of each primer were used for the PCR reaction. After purification, the PCR product was digested with the enzymes Xho I and Kpn I, and ligated into the p-Shuttle digested with the same enzymes. Following PCR reaction and enzyme digestion, the DNA was gel purified using Perfectprep gel clean up kit (Eppendorf). All the p-Shuttle-RNAi recombinant plasmids were sequenced to verify the accuracy of the PCR reaction.

Construction of recombinant replication deficient adenoviruses

The first step was to generate the recombinant pShuttle vector containing the sequence of interest under the CMV or another mammalian promoter. The recombinant pShuttle vector was linearized with the restriction enzyme Pme I. 1 ug of this plasmid was co-transformed with 0.1 ug of the Ad-easy plasmid into recombination efficient BJ5183 electrocompetent cells. As a control, we performed a transformation with only the linearized recombinant pShuttle vector. The transformed cells were plated on LB-Kanamycin agar plates and grown for 24 hours at 37°C. The smaller size colonies (not present in the control) were selected and grown in liquid LB-Kanamycin media for 12

hours in a shaker at 37°C. Plasmid DNA was prepared by regular miniprep and digested with the enzyme Pac I to distinguish the recombinant plasmids. These plasmids were further characterized using other restriction enzymes. The chosen recombinant plasmid was transformed into DH10 competent *E. coli*, amplified and purified by Quiaprep spin Qiagen Kit. The plasmid was then linearized with Pac I and cleaned through a Qiagen plasmid mini column. $1x10^6$ 293-HEK cells of low passage number were transfected with 5 ug of the linearized DNA plasmid and 20 ul of Lipofectamin (Invitrogen). After the cells showed complete CPE (cytopathic effect), usually 3 to 7 days, cells were collected and then frozen and thawed 3 times to release the virus particles from the cells. Presence of the transgene in the adenovirus construct was verified by performing PCR on the virus lysate using primers within the insert. Two rounds of virus amplification were then performed. Titration of the virus was performed using the Tissue Culture Infectious Dose 50 ($TCID_{50}$). This first viral production generated was used for preliminary characterization of the virus. For further virus production, single plaques of the virus were purified. A monolayer of HEK-293 cells was infected with diluted virus stock and then overlayed with DMEM 1.25 % Low Melting Point Agarose. After 15-20 days, isolated single plaques could be observed. Several single plaques were collected amplified and transgene expression measured. The chosen plaque was then amplified to obtain homogenous populations of viruses. The procedure used to generate adenoviruses is summarized in Figure 14.

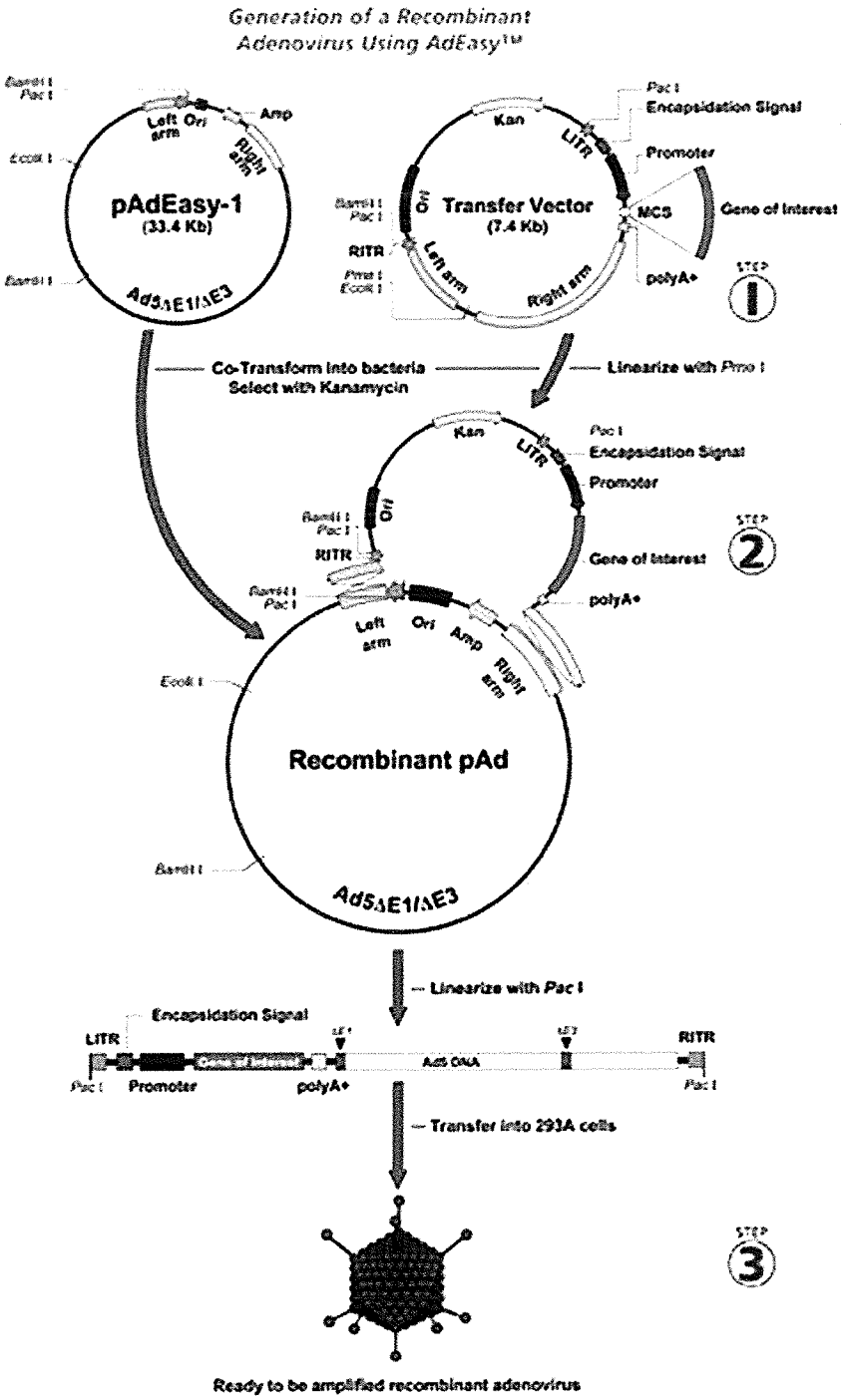

Figure 14. Procedure for generation of adenoviral vectors. Plasmids and recombination mechanism used for the generation of replication deficient recombinant adenovirus vectors (obtained from Quantum).

Recombinant adenoviruses generated for the study

- Ad-NCX1.1
- Ad-NCX1.3
- Ad-NCX1.1-EGFP (fusion protein)
- Ad-NCX1.3-EGFP (fusion protein)
- Ad-EGFP
- Ad-QBI+ (expresses β-galactosidase, was obtained from Quantum)
- Ad-NCX1.1rat antisense
- Ad-NCX1.1dog antisense
- Ad-RNAi (3 sequences)
- Ad-RNAi scramble
- Ad-XIP ires EGFP
- Ad-XIP ires XIP

Immunocytochemistry

Cells on coverslips were fixed for 12 minutes in 4 % paraformaldehyde PBS, permeabilized with 0.1 % Triton X-100 and blocked with 2 % milk 0.1 % Triton X-100 PBS. R3F1 primary antibody was used in 1:150 dilutions, followed by Alexa conjugated goat anti-mouse secondary antibody (1:700 dilutions). Nuclei were stained with Hoechst 33342. Cells were mounted on glass slides using FluorSave (Calbiochem). All cells were imaged in a Zeiss fluorescent microscope.

Western blots

Samples were washed 2 times with cold PBS, lysed with RIPA buffer (50 mM Tris , 150 mM NaCl, 1 % Triton X 100, 0.5 % sodium deoxycholate, 1 mM EDTA, 1 mM EGTA, pH 7.5 with the addition of 1 mM PMSF, 1mM benzamidine and a protease inhibitor cocktail), scraped with a rubber policeman and collected into an eppendorf tube. The samples were kept on ice for approximately 30 min, vortexed 5 seconds every 10-15 minutes and spun at 14,000 rpm in a tabletop microcentrifuge at 4° C for 12 min. The supernatant was transferred to a new eppendorf tube, frozen in liquid N_2 and stored at -80° C until used. Total protein concentration was measured with the DC BioRad Protein Assay Kit. Fifty ug of total protein in Laemmli sample buffer were loaded per gel lane. Sodium dodecyl sulfate-polyacrylamide gel electrophoresis (SDS-PAGE): 4-16 % Tris-HCl acrylamide gradient gel from BioRad or 7.5 % continuous gels were used. We transferred proteins onto nitrocellulose membrane in a wet transfer apparatus overnight at 4°C at 35 V for NCX, myosin and PMCA. For SERCA2, transfer was performed overnight at 300 mA constant current. The membrane was blocked for 1 h at room temperature with 5 % skim milk in TBS and then incubated with the primary antibody in 1 % skim milk.

The primary antibodies used were: anti NCX (R3F1 monoclonal, dilution 1:1,000, Swant), anti PMCA (MA3-914, dilution 1:1,000, Affinity BioReagents), anti SERCA2 (MA3-919, dilution 1: 500, Affinity BioReagents), Anti actin A2066 (1:2,000, Sigma), anti myosin (MF 20 M α L- meromyocin, dilution 1: 200, Developmental Studies Hybridoma Bank), anti NaK ATPase α1 subunit (dilution 1:300, Developmental Studies

Hybridoma Bank), anti XIP (dilution 1:1000) and XIP control peptide (Alpha Diagnostic). The membrane was incubated with the appropriate horseradish conjugated secondary antibody and signal was developed using West Fento (PMCA and Serca2) or West Pico chemiluminescence substrate from Pierce. Signal was collected in a BioRad detection system and quantified by densitometry analysis using Quantity One software (BioRad).

Western blot protocol for XIP peptide. We used the Tricine-SDS-PAGE system (Schagger and von Jagow, 1987). This method is used to separate small proteins and peptides (1- 30 kDa). Samples were prepared in 4 % SDS, 12 % glycerol (w/v), 50 mM Tris, 2 % mercaptoethanol (v/v), HCl to pH 6.8. A 16.5 % separating gel, with a 10 % spacer gel overlaid by a 4 % stacking gel was used. Ultralow color MW markers (from Sigma) were used. The gel was run for 1 hour at 30V and then 90 V at 4°C. Transfer onto PVDF membranes (for sequencing) was performed using a semi-dry transfer apparatus (200 mA for 45 minutes). 20 % methanol was included in the anode buffer. 600 μg of total protein lysate from HEK-293 cells and 0.5 μg of XIP peptide were used.

Biotinylation of surface membrane proteins

Biotinylation of surface membrane proteins was performed on neonatal cardiomyocytes attached to the culture plate using the biotinylating reagent EZ-Link-Sulfo-NHS-Biotin from Pierce, as recommended by the manufacturer.

NCX immunoprecipitation

After biotinylation, neonatal cardiomyocytes were lysed with RIPA buffer containing protease inhibitors. NCX protein was immunoprecipitated using the R3F1 monoclonal antibody following standard protocols. Biotinylated NCX was recognized by PAGE-Wb using anti-biotin primary antibody.

Measurement of NCX activity

^{45}Ca uptake assay: NCX activity was measured as Na^+_i dependent ^{45}Ca uptake. The protocol described by Vemuri *et al* was followed (Vemuri *et al*, 1989). Cells were plated on 35 mm Petri dishes. Cells were washed twice with a Na^+ loading solution (140 mM NaCl, 2 mM $MgCl_2$ and 10 mM 3-(N-morpholino) propanesulfonic acid (MOPS), pH 7.4), and incubated at 4° C for 10 minutes with the same Na^+ loading solution with the addition 5 mM ouabain. The purpose of this step was to increase intracellular $[Na^+]$. The solution was then replaced by 2 ml of uptake medium containing 25 μM $CaCl_2$, 0.3 μCi/ml $^{45}Ca^{2+}$, 10 mM MOPS (pH7.4), 5mM ouabain and either 140 mM KCl or 140 mM NaCl at room temperature. After 2 minutes, 3 fast washes were performed with 3 ml of an ice-cold solution containing 140 mM KCl and 1 mM EGTA, pH 7.4 to stop the uptake reaction. The cells were then collected with 500 μl of 0.5 N NaOH. A 20 μl aliquot of the lysate was used for the measurement of protein concentration and 100 μl for radioactive counting in a Beckman scintillation counter. Measurements were performed in duplicate. NCX activity was calculated from the difference between the

uptake in the KCl solution minus the uptake in the NaCl solution (blank) and was expressed as ^{45}Ca counts/mg protein/2 minutes of uptake reaction.

In another series of experiments, NCX activity was measured by replacing extracellular sodium chloride in the perfusion buffer by lithium chloride.

Spectrofluorometric measurements of Ca^{2+}_i and pH_i

Intracellular Ca^{2+} and pH were studied using the fluorescent indicators Fura-2 and BCECF respectively. The cells were loaded with the ester (AM) form of the dye. Measurements were carried out using a dual excitation, single emission spectrometer from Photon Technology International. Individual cells were studied on coverslips using a Nikon Diaphot epifluorescent microscope with a 40X oil immersion objective lens. Alternatively, populations of cells on coverslips were studied using a cuvette system. The excitation wavelengths used were 340 and 380 nm for the Ca^{2+} bound and Ca^{2+} unbound forms of Fura-2. Emission was recorded at 505. Signal was collected at 25 Hz. Intracellular Ca^{2+} levels were represented as the 340/380 fluorescence ratio of the Fura-2 emission. For BCECF, the excitation wavelength were 440 and 500 nm and emission was detected at 525 nm at 10 Hz. Calibration of the BCECF signal was carried out following the protocol described by Massaeli *et al* (Massaeli and Pierce, 1997).

Loading conditions for Fura-2 were: 1μM for 30 minutes for adult cardiomyocytes, 2 μM (with 0.04 % Pluronic Acid) for 20 minutes for neonatal cardiomyocytes and 4 μM (with 0.08 % Pluronic Acid) for 20 minutes for HEK-293 cells. A 2 uM BCECF and 15 minute loading condition was used for all cell types for the

measurement of pH_i. Following loading, the cells were allowed 20-30 minutes for dye de-esterification.

Video Edge detection

Passive and active cell shortening of adult cardiomyocytes was determined by a video edge detection system (Crescent Electronics, Sandy, UT) coupled to a Pulnix monochrome CCD camera, which captures data at a rate of 60 Hz. Video Edge detection was also used to measure the frequency of spontaneous contractions in neonatal cardiomyocytes.

Action potential recordings

A glass cover slip seeded with 3-6 day transfected neonatal rat cardiac myocytes was placed in a bath mounted on an inverted microscope (Nikon, Tokyo, Japan) and perfused with Tyrode's solution containing (mM) NaCl 132.0, HEPES (sodium salt) 20.0, $MgSO_4$ 1.2, glucose 11.1, KCl 4.0 and $CaCl_2$ 2.0 adjusted to pH 7.4. Action potentials were recorded in current clamp mode using the perforated patch clamp technique. Borosilicate glass pipettes (World Precision Instruments, Inc., Sarasota, FL, USA) were pulled on a P-87 micropipette puller (Sutter Instrument Co., Novato, CA, USA) to a resistance of 2-5 MΩ. Immediately prior to use, pipette tips were filled with antibiotic-free solution containing (mM) L-aspartic acid (monopotassium salt) 130.0, KCl 15.0, HEPES (free acid) 5.0, NaCl 10.0, $CaCl_2$ 0.5, and $MgCl_2$ 1.0 (pH 7.3). The rest of

the pipette was back-filled with pipette solution containing Amphotericin B (Sigma Chemical Co., St. Louis, MO, USA), which had been prepared as a stock of 30 mg/ml in dimethyl sulfoxide and diluted to 120 μg/ml.

Pipettes were connected to the headstage of an Axopatch-1D amplifier (Axon Instruments, Foster City, CA, USA) and grounded via a Ag-AgCl wire inserted through an agar bridge seated in the bath. Upon gigaseal formation, Amphotericin B was allowed to perforate the cell membrane and membrane potential was recorded in current clamp mode. No holding potential was applied to the cells. Cells were stimulated by injection of 3 ms depolarizing pulses at 2000 ms cycle length using a Pulsar 6i stimulator (FHC, Brunswick, ME, USA). All experiments were performed at room temperature of 21 ± 2 ^{o}C. Action potentials were recorded and analyzed using PClamp 7.0 software (Axon Instruments). Action potential durations were calculated for 50 % (APD_{50}) and 90 % (APD_{90}) repolarization.

Composition of perfusion solutions

- Adult cardiomyocytes:

Hepes control buffer: 140 mM NaCl, 6 mM KCl, 1 mM $MgCl_2$, 1.25 mM $CaCl_2$, 6 mM HEPES (pH 7.4), 10 mM dextrose and 0.02 % BSA. This buffer was extensively bubbled with O_2.

Ischemia-mimetic buffer: 140 mM NaCl, 8 mM KCl, 1 mM $MgCl_2$, 1.25 mM $CaCl_2$, 6 mM HEPES (pH 6.0), 0.02 % BSA and made hypoxic by bubbling it with N_2 for at least 45 min.

- Neonatal cardiomyocytes

Hepes control buffer: 140 mM NaCl, 6 mM KCl, 1 mM $MgCl_2$, 1.8 mM $CaCl_2$, 6 mM HEPES (pH 7.4), 10 mM dextrose. This buffer was extensively bubbled with air.

Ischemia-mimetic buffer was: 140 mM NaCl, 8 mM KCl, 1 mM $MgCl_2$, 1.8 mM $CaCl_2$, 6 mM HEPES (pH 6.0), 2.5 mM sodium cyanide and 10 mM sodium lactate.

- HEK-293 cells

Hepes control buffer: 140 mM NaCl, 6 mM KCl, 1 mM $MgCl_2$, 1.8 mM $CaCl_2$, 6 mM HEPES (pH 7.4), 10 mM dextrose and 0.02 % BSA. This buffer was extensively bubbled with O_2.

Ischemia-mimetic buffer: 120 mM NaCl, 8 mM KCl, 1 mM $MgCl_2$, 1.8 mM $CaCl_2$, 20 mM sodium lactate, 6 mM HEPES (pH 6.0), 0.02 % BSA and made hypoxic by bubbling it with N_2 for at least 45 min.

Ischemia reperfusion protocol

For adult and neonatal cardiomyocytes, we used a protocol that consisted of 90 minutes of simulated ischemia followed of 30 minutes of reperfusion. The cells were continuously perfused at a rate of 1 ml/min. The experiments using adult cells were performed on the microscope and the cells were electrically stimulated throughout the experiment at 0.5 Hz with 200 milliseconds duration pulses. The experiments using neonatal cells were performed in the cuvette system (measurement from a population of cells) and without stimulation.

Experimental design for the adult cardiomyocyte study: Twenty μM DMA was administered in the perfusate during the first 3 minutes of reperfusion or during the entire 90 minutes of ischemia plus the first 3 minutes of reperfusion. A third group (control) received no DMA in the perfusate (Figure 15).

Cell viability

The viability of adult cardiomyocytes was assessed by visualizing the cell morphology. Cardiomyocytes were considered healthy if they had a normal rectangular rod shape, whereas damaged cells were subjectively determined by the presence of surface blebbing, rounded cell edges or complete balling up of the cell. This subjective measure has been closely correlated with more objective measures of cell viability (Maddaford *et al*, 1999). Thus, we can reliably estimate cell damage with this technique. Healthy cardiomyocytes were counted on the full microscopic field with a 10 x lens before the beginning of ischemia and at the end of reperfusion.

Statistical Analysis

The data were analyzed for statistical significance with a one-way analysis of variance (ANOVA) followed by a Student-Newman-Keuls test when three groups were compared, and by t-test when two groups were compared. Values were expressed as mean ± SE. Statistical significance was achieved at a P value < 0.05.

RESULTS

PART I: Inhibition of Na^+-H^+ exchange at the beginning of reperfusion is cardioprotective in isolated, beating adult cardiomyocytes (indirect evidence for NCX involvement in ischemia-reperfusion injury).

Objective: To analyze the protective effect of a Na^+-H^+ exchange blocker administered either during ischemia and reperfusion or, solely at reperfusion.

Hypothesis: Inhibition of Na^+-H^+ exchange during early reperfusion is sufficient to provide cardioprotection.

Conflicting results regarding the cardioprotective effects provided by NHE blockers administered solely at reperfusion could be due to limited diffusion of the drugs through the vascular wall. To avoid this limitation, and to allow access of the drugs to the cells precisely at the time of reperfusion, a model of isolated ventricular cardiomyocytes was used. This model was previously developed and tested in Dr. Pierce's laboratory [194]. Rat ventricular cardiomyocytes, attached to a coverslip were perfused with a Hepes buffer solution. To simulate ischemia the buffer was modified: $[K^+]$ was increased, glucose was removed, pH was decreased to a value of 6 and O_2 content was decreased by extensive bubbling with N_2. Additionally, the cells were paced during the whole protocol to increase their metabolic demand. The cells were treated with the ischemia mimetic solution and the Na^+-H^+ exchanger blocker 5-(N,N-dimethyl)-amiloride (DMA)

following the protocol described in Figure 15. We analyzed cell viability, changes in intracellular pH and [Ca^{2+}] and active and passive shortening as a function of treatment.

The survival of the cells after ischemia-reperfusion was measured as a function of exposure to DMA during ischemia and reperfusion or just during reperfusion. Exposure of the cells to 90 min of ischemia and 30 min of reperfusion resulted in a loss of ~ 40 % of rod shaped cells (60 ± 1 % survival) (Figure 16). The use of DMA at the beginning of reperfusion increased the survival of morphologically healthy cells to 81 ± 1 % ($p < 0.05$). However, the additional presence of DMA throughout the ischemic period did not significantly protect the cells further (63 ± 3 % cell survival).

Changes in active and passive cell shortening during the ischemia-reperfusion insult were studied by edge detection as measurements of the functional integrity of the cells. The results of the changes in resting cell length are shown in Figure 17. They represent the mean values obtained from a number of cells from each experimental group. The values represent the difference between the resting cell length at each time point and the resting cell length before ischemia. There was a small increase in resting cell length (elongation) during ischemia that was similar amongst the three groups. During reperfusion, the cells began to shorten. This is shown as a decrease in resting cell length. The cells that were not treated with DMA at any time began to shorten earlier in reperfusion and had the largest decrease in cell length. The shortening was delayed and reduced by the administration of DMA either during ischemia and early reperfusion, or only at early reperfusion.

The changes in active cell shortening during ischemia-reperfusion are represented in Figure 18. The results are expressed as a percentage of the pre-ischemic active cell

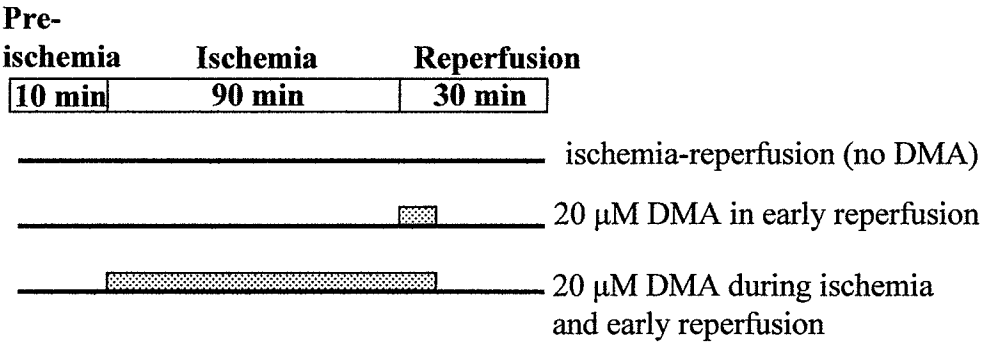

Figure 15. Experimental protocol for simulated ischemia in adult cardiomyocytes. All the cells were perfused with control buffer for 10 min, followed by 90 min perfusion with the ischemia-mimetic solution and 30 min of reperfusion with control perfusate. The dotted bars indicate the time during which DMA was administered in the perfusate (first 3min of reperfusion or 90 min of ischemia and first 3 min of reperfusion). The control cells were not treated with the drug.

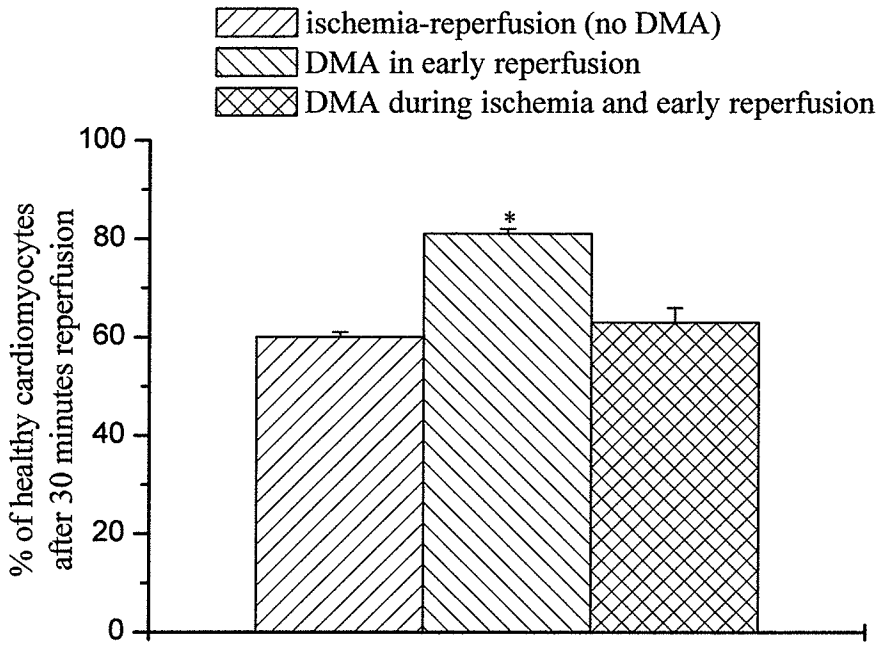

Figure 16. Cell viability as a function of DMA treatment. DMA was present during ischemia and reperfusion or just during reperfusion. Healthy, rod shaped cells were counted before ischemia and recounted at the end of reperfusion. Values are means ± SEM. for 19–30 Experiments (650–1000 cells). * $p < 0.05$ *vs* control (no DMA).

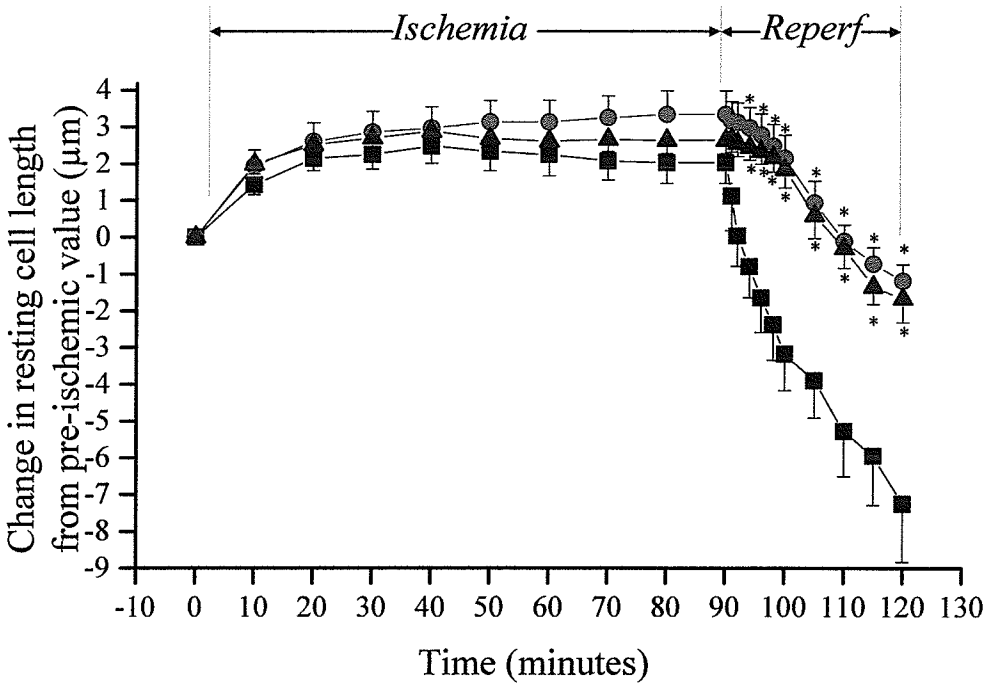

Figure 17. Resting cell lenghth as a function of DMA treatment. Change in resting cell length during ischemia and reperfusion ± drug treatment. Cells were not treated (■), or were treated with 20 µM DMA only during the first 3min of reperfusion (●) or during ischemia and the first 3minof reperfusion (▲). Each data point represents the mean value of 7–12 separate cellular experiments. * $p < 0.05$ *vs* control (no DMA).

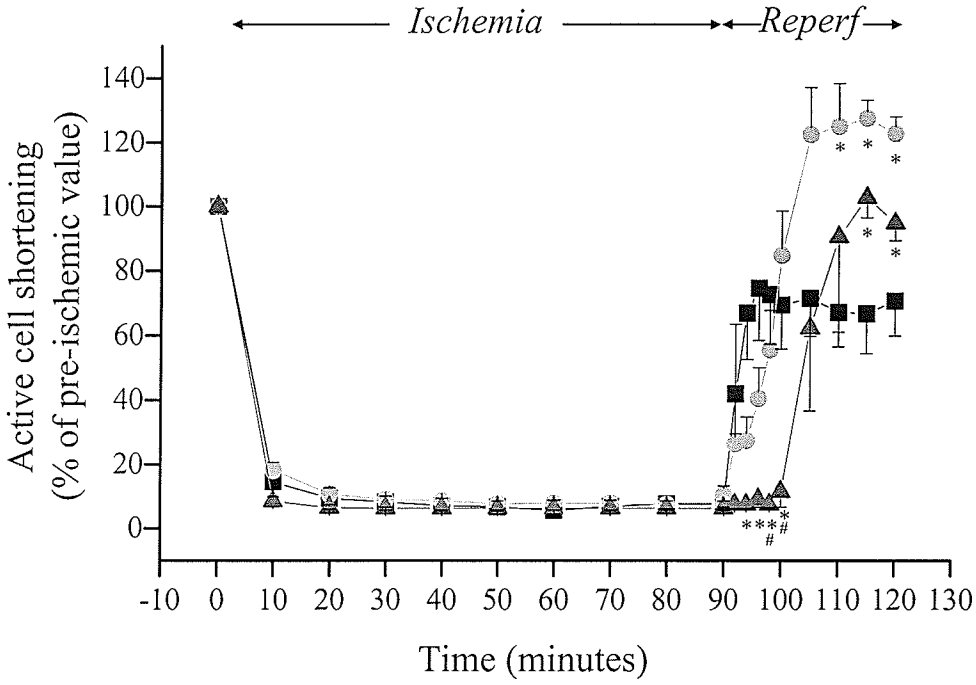

Figure 18. Active cell shortening as a function of DMA treatment. Change in active cell shortening during ischemia and reperfusion ± drug treatment. Active cell shortening before ischemia was considered 100%. Cells were not treated (■), treated with 20 μM DMA during the first 3 min of reperfusion (●) or treated with DMA during ischemia and the first 3 min of reperfusion (▲). Each data point represents the mean value of 7–12 separate cellular experiments. * $p < 0.05$ *vs* control (no DMA). # $p < 0.05$ *vs* DMA in early reperfusion.

shortening. The cells demonstrated a rapid loss of contractile function after the onset of perfusion with the ischemic solution. The recovery of contractile activity at reperfusion was earlier in the absence of DMA but it only reached 71 ± 10 % of the pre-ischemic values. When DMA was used during the first 3 minutes of reperfusion, contractile function recovered significantly better than the control values (122 ± 5 %, $p < 0.05$). Contractile function also recovered to a level that was even higher than before the ischemic perfusion was initiated. When DMA was present in the perfusion buffer during ischemia and beginning of reperfusion, the recovery of contractile function was significantly delayed by 10 minutes compared with the other two groups and the percentage of recovery was intermediate (94 ± 5 %; $p < 0.05$ *vs* control; $p < 0.05$ *vs* DMA in early reperfusion).

Intracellular pH was measured during ischemia-reperfusion using the fluorescent indicator dye BCECF. Representative recordings of intracellular pH before, during and after ischemia in one cell from each group are shown in Figure 19. The fluorescence ratio decreased slightly during the first 5 min of ischemia in all of the cells studied. The rate of decrease in fluorescence ratio during ischemia was greater when DMA was present during ischemia. During the last 30 minutes of ischemia the fluorescence was lower in the drug-treated cell when compared to the other two cells. The fluorescence ratio started to recover very rapidly after reperfusion of the control cell and it neared the pre-ischemic value by 5 min of reperfusion. In the cell that was treated with DMA only at reperfusion, the fluorescence ratio increased slowly during the first 5 min of reperfusion, recovered faster the next 25 min, but did not return to pre-ischemic values. In the cell that was treated with DMA during ischemia and reperfusion, the fluorescence ratio remained low

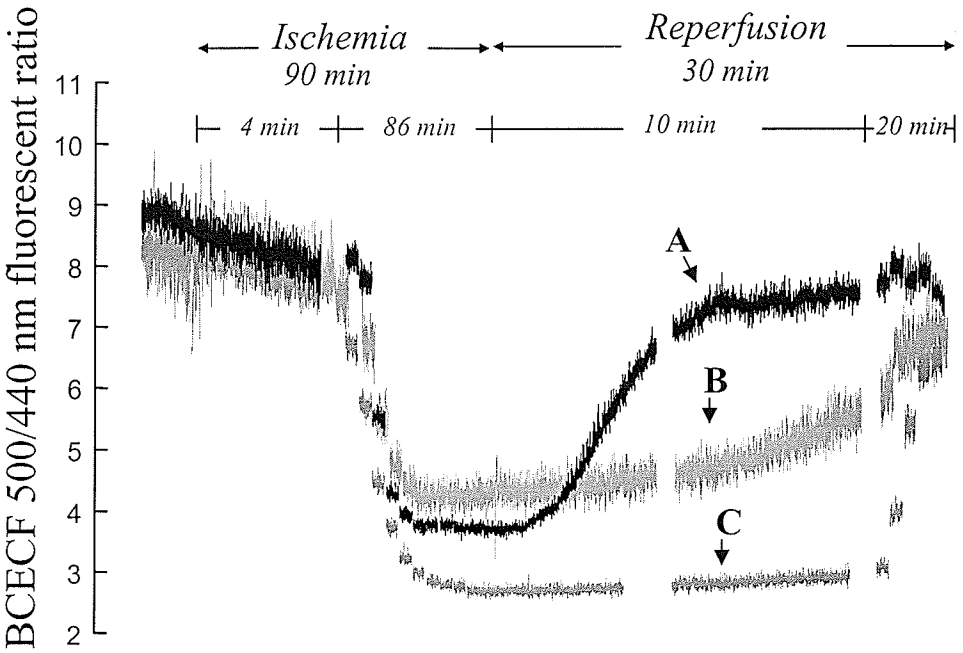

Figure 19. Representative traces of pH_i measurements during ischemia-reperfusion. Representative recordings of the BCECF fluorescence ratio in an untreated cell (A), a cell treated with 20 μM DMA during the first 3 min of reperfusion (B) and another cell treated with 20 μM DMA throughout ischemia and the first 3 min of reperfusion (C). The recording was interrupted at different time points to prevent photobleaching of the dye.

during the first 10 min of reperfusion, increased during the next 20 minutes but remained lower than in the other two cells by the end of the experiment.

These representative results are confirmed by results from a number of cells in many independent experiments (Figure 20). Qualitatively, they are similar to those shown in Figure 19. Pre-ischemic intracellular pH was ~ 7.2. Five minutes after the beginning of ischemia, intracellular pH in drug untreated cells started to decrease and reached a low value of 6.4 by 40 minutes. When DMA was present during ischemia, intracellular pH was significantly lower from 60 minutes until the end of ischemia. Upon reperfusion, pH_i recovered very rapidly in the absence of DMA. The recovery of pH_i was slower when DMA was present only for the first 3 minutes of reperfusion and even slower when DMA was administered during ischemia and at the beginning of reperfusion.

Changes in intracellular $[Ca^{2+}]$ during ischemia-reperfusion were studied in the absence of DMA and with 20 μM DMA present during the first 3 minutes of reperfusion. Because of the great amount of time needed to complete these experiments, we focused only on these two groups. The 340/380 fura-2 fluorescence ratio from a number of cells from each group is presented in Figure 21. Diastolic Ca^{2+} increased during ischemia and at the beginning of reperfusion in both groups. During the last 20 minutes of reperfusion, diastolic Ca^{2+} decreased and was lower when DMA was used. At 30 minutes of reperfusion, the difference in diastolic Ca^{2+} between the two groups reached statistical significance. Ca^{2+} transients were reduced in both groups to a similar extent during the ischemic period. However, they recovered to a different degree if DMA was present at the beginning of reperfusion. To present a comparison of these results more clearly, the Ca^{2+} transients were plotted against time and expressed as the percentage of the Ca^{2+}

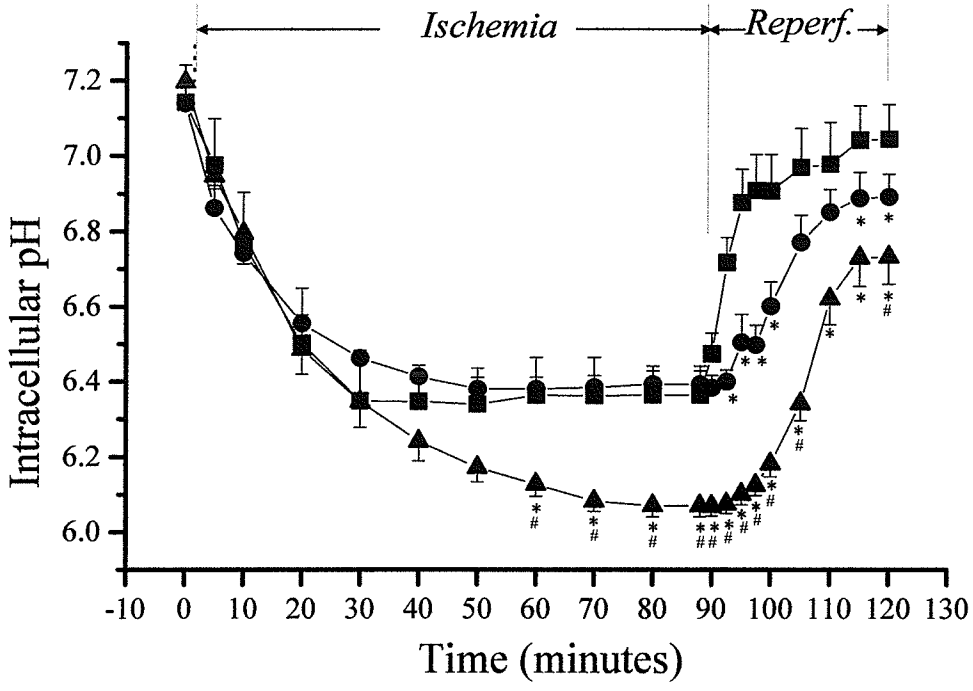

Figure 20. Changes in pH_i during ischemia-reperfusion as a function of DMA treatment. Cells were not drug-treated (■), or treated with 20 μM DMA during the first 3 min of reperfusion (●) or during ischemia and the first 3 min of reperfusion (▲). Values are means ± SE. for 8 - 10 individual cells. * $p < 0.05$ *vs* no DMA. # $p < 0.05$ *vs* DMA in early reperfusion.

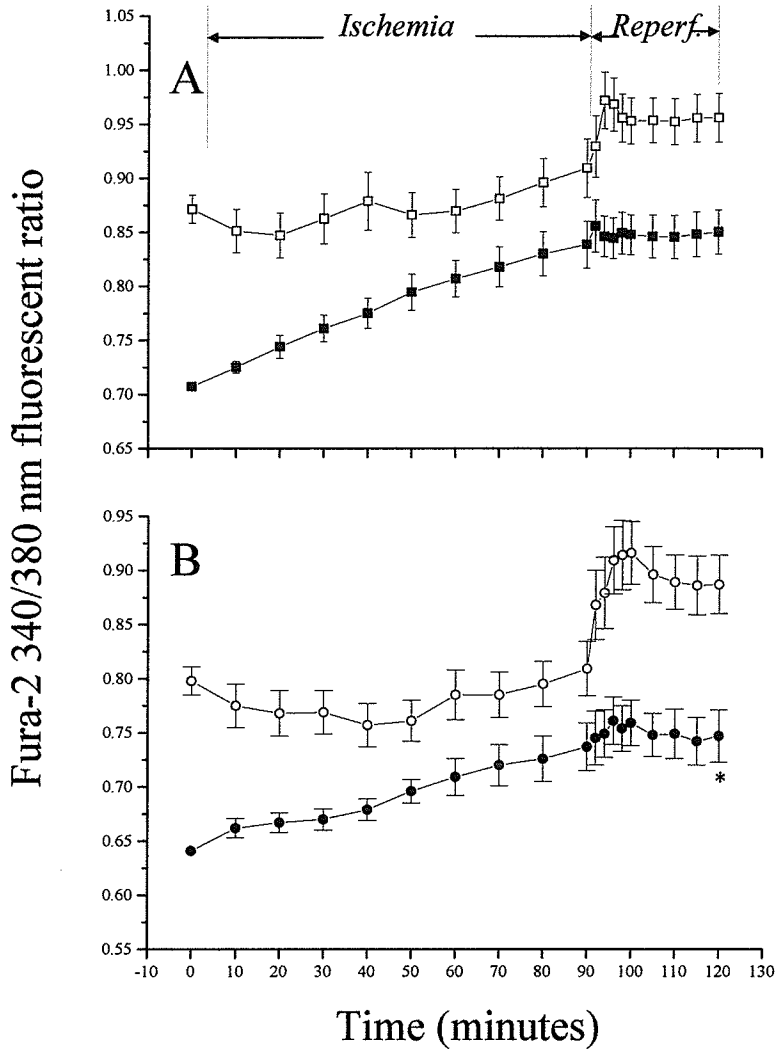

Figure 21. Changes in Ca^{2+}_i during ischemia-reperfusion as a function of DMA treatment . Changes in intracellular [Ca^{2+}] as reflected by the 340/380 fura-2 fluorescence ratio during ischemia and reperfusion in cardiomyocytes that received no treatment (□■) or cardiomyocytes that were treated with 20 μM DMA during the first 3 min of reperfusion (○●). Open symbols represent systolic calcium and closed symbols represent diastolic calcium. Ischemia started at 0 min and ended at 90 min. Values are means ± SEM. of 16 - 20 experiments. * $p < 0.05$ *vs* control (no DMA) for diastolic Ca^{2+}.

transient before ischemia (Figure 22). The Ca^{2+} transients were not significantly different between the two groups during ischemia. During the first 5 minutes of reperfusion, Ca^{2+} transients reached a maximum of 74 % in the absence of DMA treatment but declined slightly thereafter. When DMA was present at the beginning of reperfusion, the Ca^{2+} transients were significantly greater from 10-30 minutes into reperfusion than those observed in the absence of DMA. The stable Ca^{2+} transient at the end of reperfusion was 110 % of the pre-ischemic Ca^{2+} transient.

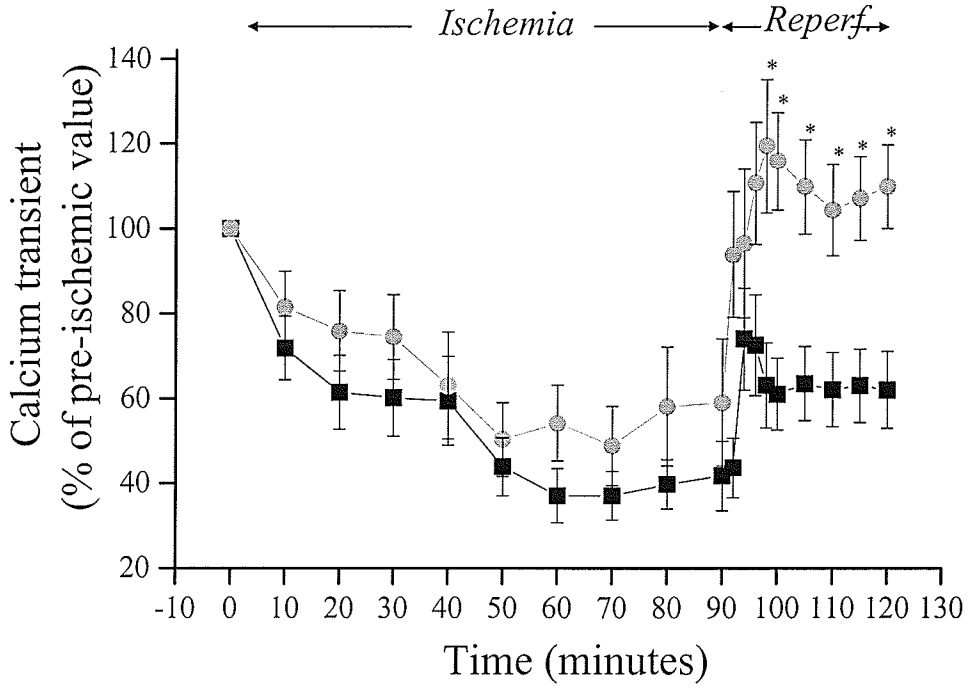

Figure 22. Calcium transients during ischemia and reperfusion as a function of DMA treatment. Drug-untreated cardiomyocytes (■). Cells treated with DMA at reperfusion (●). Values are means ± SEM. of 16 - 20 experiments. * $p < 0.05$ *vs* control (no DMA).

PART II: Down-regulation of the NCX. Effect of NCX depletion in neonatal cardiomyocytes on Ca^{2+} handling and contractility.

Objective: To develop a new methodology to down-regulate the expression of the NCX and to study the effect of this treatment on contractile function of neonatal rat cardiomyocytes.

Hypothesis: Neonatal cardiomyocytes depleted of NCX would not be able to support contractile activity.

Adenoviral vectors that delivered shRNAs with high efficiency into neonatal cardiomyocytes were generated. Figure 12 shows, as an example, one of the plasmid generated for the study and Figure 13 indicates the steps involved in generation of adenovirus vectors for RNA_i. shRNAs were designed to target the sequence of the rat NCX1.1 cDNA. A shRNA scramble sequence was designed, as well, and was used as a control. The Ad-EGFP (recombinant adenovirus coding for EGFP) was made and used to test efficiency of infection. Figure 23 shows that high efficiency of transfection can be achieved at low and high density of cultured neonatal cardiomyocytes using multiplicities of infection 1.5 and 10.

Figure 24A shows representative Western blots and pooled data for NCX protein levels from myocytes infected with adenoviruses encoding shRNA targeting NCX (Ad-NCX-RNAi). Data are shown for different multiplicities of infection (MOI) and different time points after infection. At day 3 post-infection, NCX protein levels measured by Western blot were ~ 60-15 % of that observed in control cells for MOI levels ranging

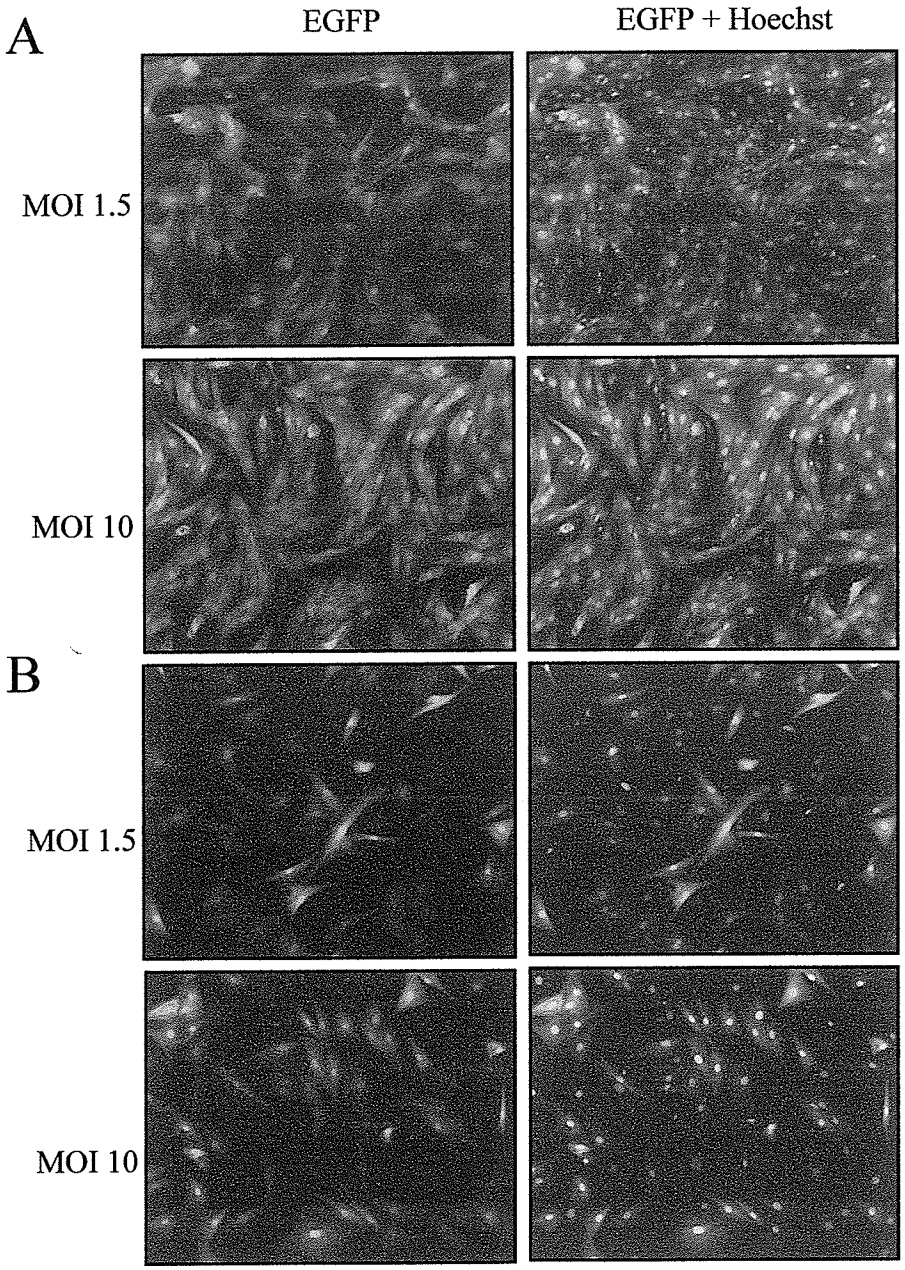

Figure 23. Example of efficiency of transfection achieved with adenovirus vectors. Neonatal cardiomyocytes were infected with Ad-EGFP at MOI 1.5 and MOI 10. Cells were fixed 48 hrs post-infection, stained with Hoechst and observed under fluorescent microscope.A. $0.75x10^6$ and B. $0.2x10^6$ cells plated per 35 mm culture plate

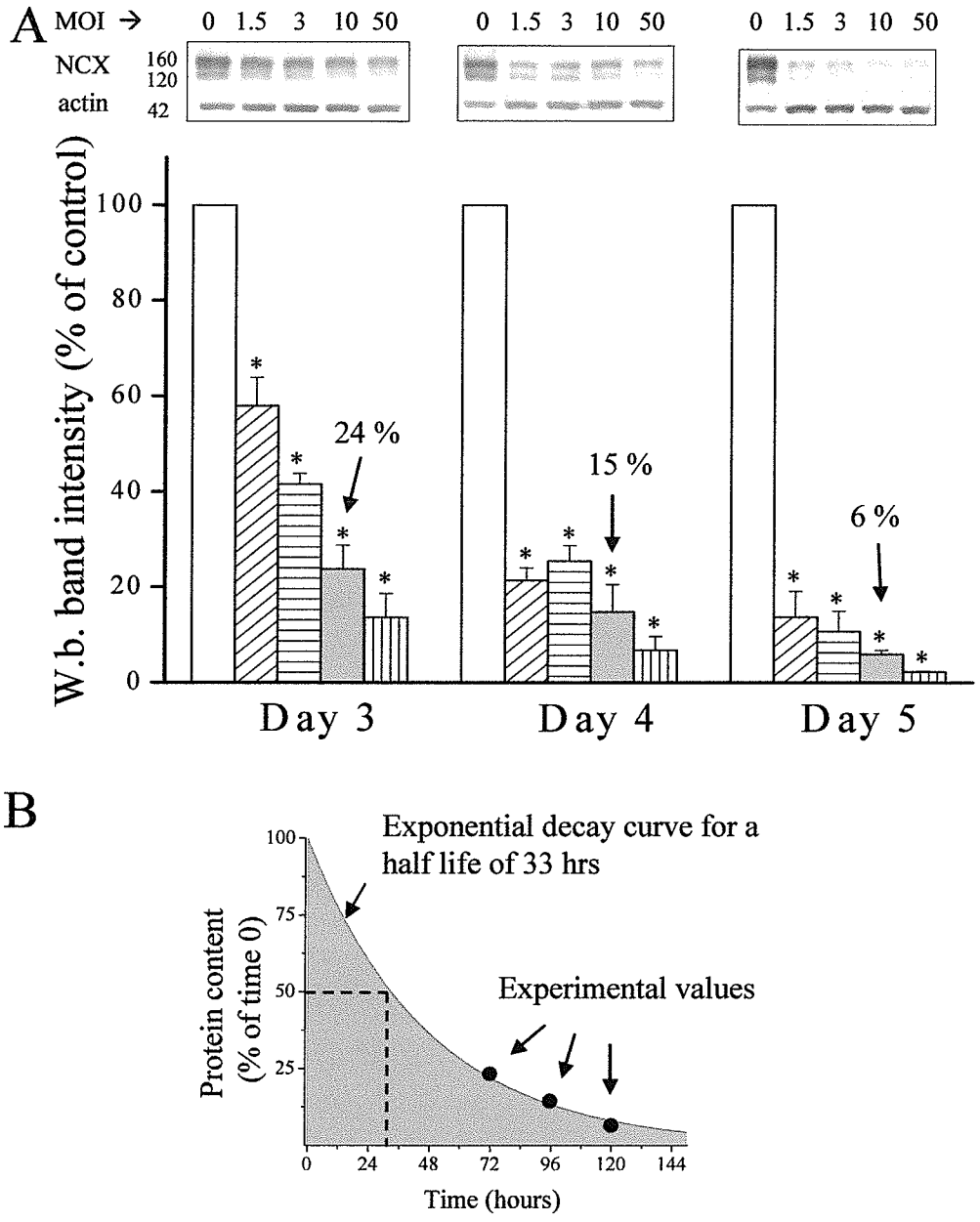

Figure 24. Downregulation of the NCX protein in neonatal cardiomyocytes. A, Western blot analysis of NCX protein. Samples collected at day 3, 4 and 5 post-infection at different MOI (mean ± SEM,* $p < 0.05$ vs control non infected cells). Representative blots are shown on top of the histogram and protein sizes are expressed in kDa. B, Plot of a decay curve for a half life of 33 hours and experimental values obtained in A for MOI 10, day 5.

from 1.5-50. At days 4 and 5, these effects were further augmented with exchanger expression being inhibited up to 97 % at a MOI of 50. Using an Ad-scramble-RNAi, NCX protein expression remained unaltered (91.4 $\pm$ 19.4 % of control; $P > 0.05$ at MOI 10 and day 5). The samples were collected from 3-5 different cell preparations. The efficiency of infection with MOI 10 was ~ 98 %, determined using an adenovirus coding for EGFP. Figure 24B illustrates the decay of 33 hours characteristics of NCX (Slodzinski and Blaustein, 1998) and the protein levels obtained in 24A at MOI 10 and day 3, 4 and 5 (black circles). MOI 10 and day 5 were used for subsequent experiments.

NCX down-regulation in Ad-NCX-RNAi infected cells was corroborated by immunocytochemistry. Figure 25 shows strong NCX staining (arrows) in control (uninfected) cells compared to Ad-NCX-RNAi. We did not observe any differences in NCX staining intensity between uninfected and scrambled RNAi infected cells (not shown).

We also examined the ability of adenovirally delivered siRNA to produce changes in NCX activity, measured by intracellular Na^+ dependent $^{45}Ca^{2+}$ uptake into cardiomyocytes. As shown in Figure 26, NCX activity in Ad-NCX-RNAi cardiomyocytes was 17 % of the activity in control cells.

Neonatal cardiomyocytes plated at confluence form a monolayer of cells that contract spontaneously. This provided us with the opportunity to observe the effects of severe NCX depletion upon spontaneous contractile function. The data was obtained from cells infected with Ad-NCX-RNAi or scrambled control. Spontaneous contractions were observed in Ad-NCX-RNAi cardiomyocytes, although at lower frequencies

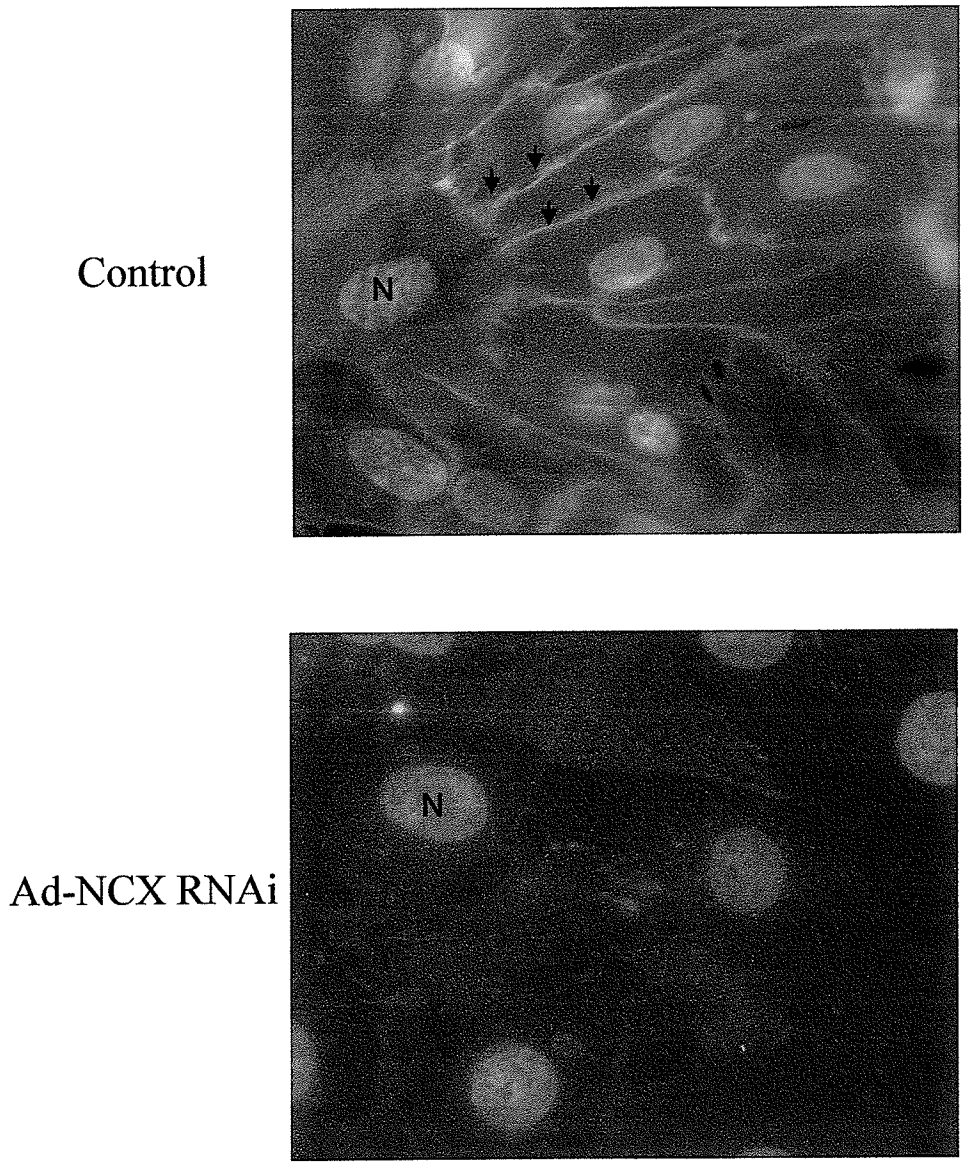

Figure 25. Immunocytochemistry staining of NCX protein in RNAi treated neonatal cardiomyocytes. NCX protein immunostaining (green and arrows) and nuclei staining (blue and N) of control non-infected and Ad-NCX-RNAi neonatal cardiomyocytes at day 5 post-infection with MOI of 10.

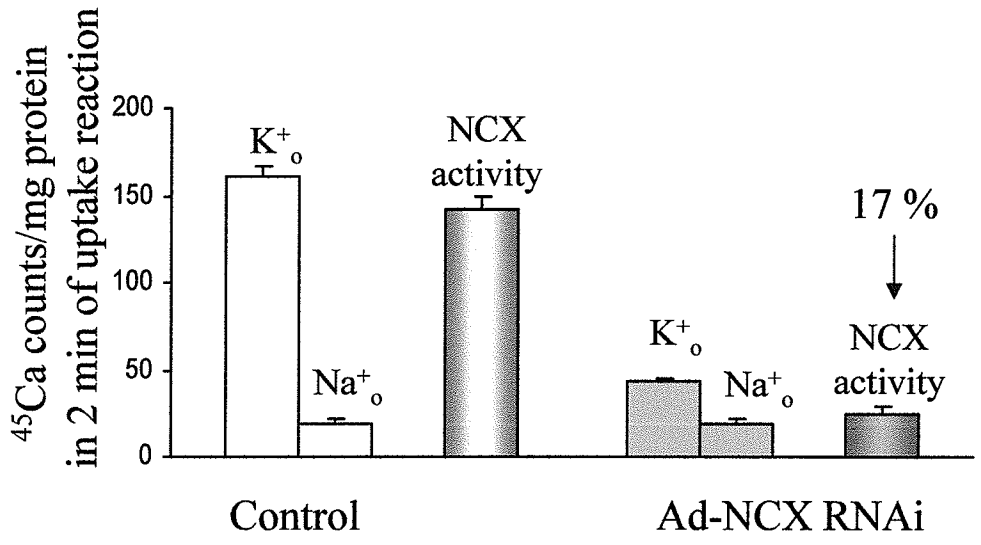

Figure 26. Sodium calcium exchange activity in RNAi treated neonatal cardiomyocytes. Control and Ad-NCX-RNAi cells pre-treated with ouabain were exposed to $^{45}Ca^{2+}$ in the presence of either extracellular K^+ or Na^+. The difference between the uptake in the presence of K^+ to the one in Na^+ represents exchanger activity. Mean ± SEM of 5-9 measurements from two different cell preparations. Cells corresponded to day 5 post-infection and multiplicity of infection 10.

compared to control myocytes (28 ± 11 and 165 ± 34 beats/ minute respectively, $p < 0.05$, n= 4-8). The contractile duration was also longer (0.65 ± 0.11 seconds *vs* 0.37 ± 0.08 seconds in length, respectively). Ad-NCX-RNAi cardiomyocytes were also responsive to electrical stimulation. Ca^{2+} transients of Ad-NCX-RNAi and scrambled adenovirus infected control cells stimulated at 0.5 Hz are shown in Fig 27A. Ad-NCX-RNAi cells exhibited an increased diastolic [Ca^{2+}], no change in peak systolic Ca^{2+}, and a significant decrease in Ca^{2+} transient amplitude (Fig 27A and Table 1). The rates of rise and fall of the Ca^{2+} transient were also significantly slower in Ad-NCX-RNAi cells. Due to the smaller calcium transient, the time to peak transient was also shorter (Table 1).

To determine how NCX activity contributes to the shape of the action potential, we performed action potential measurements in Ad-NCX-RNAi and control scrambled adenovirus infected cells. Data were obtained from cells at 4-5 days post-infection at MOI = 10. Representative tracings are shown in Figure 27B and pooled data appear in Table 1. The action potential duration at 50 % of repolarization (APD_{50}) was significantly shorter (Table 1 and Fig 27B). At 90% of repolarization, there was a tendency to observe shorter APDs in the Ad-NCX-RNAi cells, but this did not achieve statistical significance. The resting membrane potentials were similar between both groups. To study how the cell may adapt to the decrease in NCX, Western blot analyses were used to examine changes in the expression of other Ca^{2+} regulatory proteins and contractile proteins, as shown in Figure 28. In response to infection with Ad-NCX-RNAi, the decrease in NCX protein was accompanied by decreases in the sarcoplasmic-endoplasmic reticulum calcium pump (SERCA2) and myosin. No significant changes in

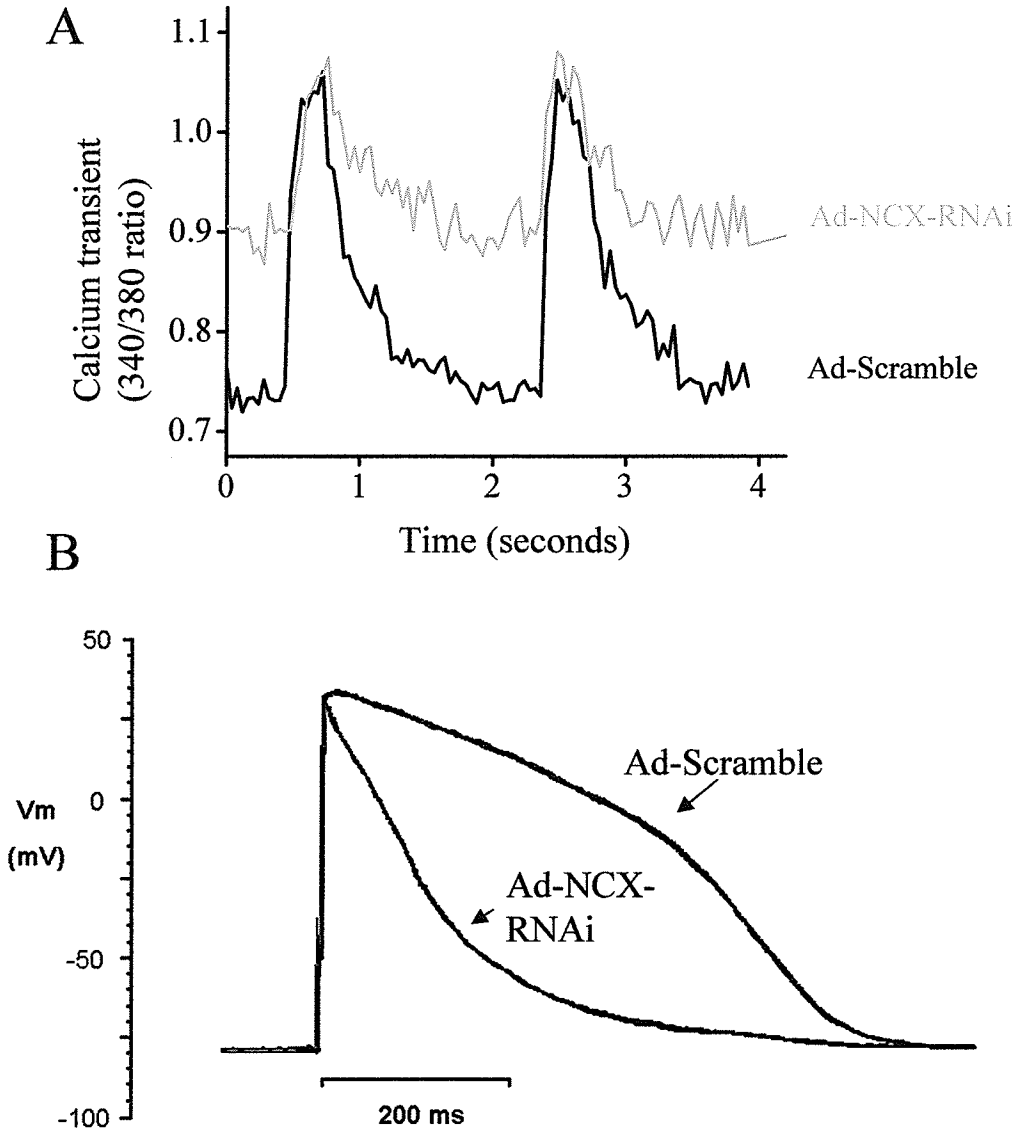

Figure 27. Changes in calcium transients and action potential in NCX down-regulated cardiomyocytes. A. Calcium transients. Representative calcium transients in Fura-2 loaded control Ad-Scramble (black) and Ad-NCX-RNAi (grey) neonatal cardiomyocytes stimulated at 0.5 Hz. The data is expressed as the 340/380 fluorescence ratio. Cells corresponded to day 5 post-infection and multiplicity of infection 10. B. Action potentials. Representative action potentials recorded from control Ad-scramble and Ad-NCX-RNAi neonatal cardiomyocytes at day 5 post-infection and MOI of 10. Cells were stimulated at 0.5 Hz.

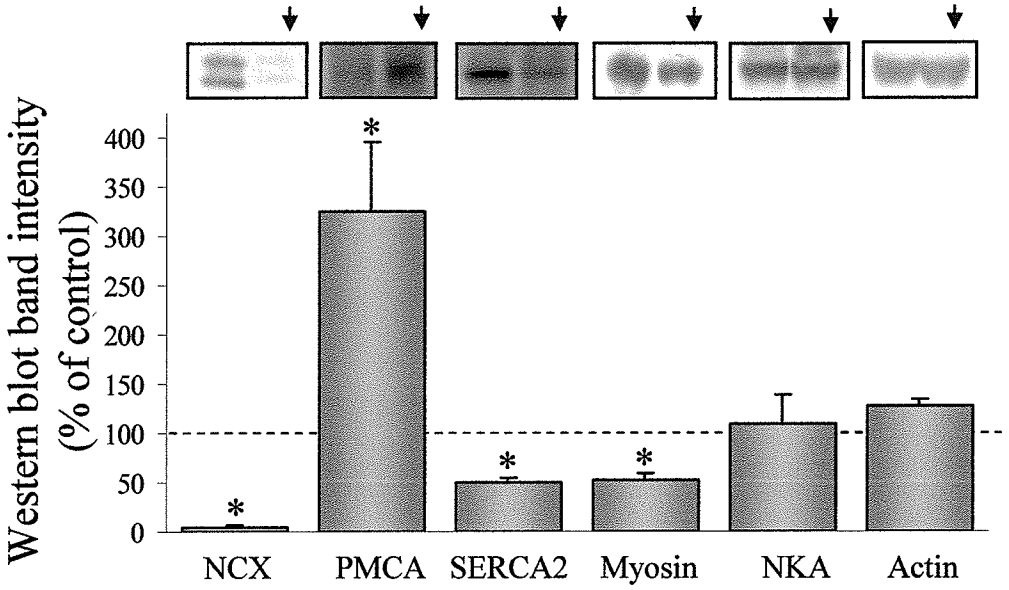

Figure 28. Changes in Na^+-Ca^{2+} exchanger (NCX), plasmalemmal calcium pump (PMCA), sarcoplasmic endoplasmic reticulum calcium pump (SERCA2), myosin, Na^+,K^+-ATPase (NKA) and actin protein analyzed by Western blot. The plotted data were means from 3-5 blots ± SEM (* $p < 0.05$). Representative blots are shown above bars (arrow, Ad-NCX-RNAi).

Table I. Calcium transient and action potential characteristics in RNAi treated neonatal cardiomyocytes.

	Ad-Scramble	Ad-NCX-RNAi
Calcium transients		
Diastolic (Fura-2 $_{340/380}$ ratio)	0.81 ± 0. 01	0.94 ± 0.02 *
Systolic (Fura-2 $_{340/380}$ ratio	1.05 ± 0.01	1.09 ± 0.02
Amplitude	0.25 ± 0.01	0.14 ± 0.01 *
Rate of rise ($Ratio_{340/380}$/sec)	0.95 ± 0.05	0.78 ± 0.05 *
Decay time constant (tau)	0.264 ± 0. 02	0.333 ± 0.02 *
$T_{1/2}$ transient (ms)	619 ± 27	555 ± 67
Time to peak (ms)	263 ± 17	173 ± 19 *
n	15	11
Action potential		
Resting membrane potential (mV)	-74.0 ± 3.1	-72.5 ± 3.8
APD_{50} (ms)	326.9 ± 65.0	52.8 ± 16.0 *
APD_{90} (ms)	560.7 ± 117.3	472.5 ± 60.4
n	4	12

Cells were electrically stimulated at 0.5Hz. Amplitude is the systolic-diastolic difference in fluorescence ratio. $T_{1/2}$ is the time for half decline of Fura-2 fluorescence ratio transient. Rate of rise is the transient amplitude divided by the time to peak. Values are means ± S.E.M. (* $p < 0.05$ *vs* control).

the levels of Na^+-K^+-ATPase and actin expression were observed. Of the studied proteins, the only one that showed an increase in expression in response to NCX depletion was the plasmalemmal calcium pump (PMCA).

The response to a variety of drugs that disturb Ca^{2+} homeostasis was examined in Ad-NCX-RNAi and control scrambled adenovirus infected cells. For example, the response of the cells to caffeine perfusion (10 mM) was examined to determine the functional integrity of the SR. Ca^{2+} transients triggered by the application of caffeine were 126 ± 1 % (Ad-scramble) and 127 ± 2 % (Ad-NCX-RNAi) of their respective transients under un-treated conditions and 0.5 Hz stimulation frequency. This was not significantly different between the two cell populations ($p > 0.05$). However, the time required for the caffeine-induced Ca^{2+} transient to decay was significantly prolonged in the Ad-NCX-RNAi infected cells (9.0 ± 1.0 s) in comparison to control (scrambled) cells (2.6 ± 0.3 seconds). Thapsigargin (1 μM) and ryanodine (10 μM) also affect intracellular Ca^{2+} homeostasis by effectively removing SR function. The Ca^{2+} transient was reduced to 66 ± 5 % and 63 ± 4 % of the transient before exposure to the drugs in cells treated with the Ad-scramble or the Ad-NCX-RNAi, respectively ($p > 0.05$). Finally, cells were exposed to 10 μM nifedipine to block the L-type Ca^{2+} channels. The transient was effectively eliminated in all cells exposed to nifedipine. However, the time to Ca^{2+} transient arrest was significantly prolonged in Ad-scramble infected cells versus those cells treated with Ad-NCX-RNAi (304 ± 76 versus 122 ± 27 seconds, respectively) ($p < 0.05$).

PART III: Over-expression of the cardiac NCX1.1 and expression of the renal NCX1.3 isoforms in neonatal rat cardiomyocytes. Implication of ionic regulation in physiological and pathophysiological conditions.

Objective: To determine if expression of the 1.3 or, over-expression of the 1.1 isoforms of NCX, alters the response of cardiac myocytes to conditions of high Na^+_i and Ca^{2+}_i.

Hypothesis: The NCX1.1 isoform of the sodium-calcium exchanger will cause a larger Ca^{2+} entry upon an increase in Na^+_i and Ca^{2+}_i compared to the NCX1.3.

Adenoviral vectors were generated that code for the expression of the canine NCX1.1 and NCX1.3 proteins. These viruses were used to transduce rat neonatal ventricular cardiomyocytes. As controls, we used for this study Ad-QBI, an adenovirus that codes for β-galactosidase.

Preliminary experiments were performed to determined the best multiplicity of infection (MOI) that could be used with these viruses. We observed that when the cells were plated at confluency, the transfection treatment with Ad-NCX1.1/1.3 was toxic at a MOI of >3. When the cells were plated at lower densities, a MOI of up to 30 could be used. The more confluent the cells were plated, the more likely the cells were to beat spontaneously at high frequency. Therefore, the limitation for cell survival may be related to altered Ca^{2+} handling at higher NCX expression levels with higher beating rates. At the different MOIs and plating densities, Ca^{2+} transients and contractions tended to decrease later on the 2^{nd} day post-infection and most of the cells died on the 3^{rd} day post-infection (data not shown). This did not occur with the Ad-QBI control infected cells indicating

that the observed effects were specific for NCX expression and activity and could be due to extremely high expression of the exchanger. The CMV is a strong promoter and NCX has a long half-life. Therefore, NCX protein may continue to accumulate with time.

Figure 29 shows immunostaining of NCX in control cells and in Ad-NCX1.1 and Ad-NCX1.3 transduced cardiomyocytes. A multiplicity of infection of 1.5 was used and cells were studied 48 hours post-infection. NCX was localized to the membrane of the cells. Stronger staining can be observed in the Ad-NCX1.1 and Ad-NCX1.3 transfected groups. In cells expressing the transgene, NCX staining was also observed within the cells, particularly around the nuclei. This probably represented protein within the SR that was not completely processed. The R3F1 monoclonal antibody recognized both NCX1.1 and NCX1.3.

Western blot analysis (Figure 30A) showed stronger NCX expression in exchanger transduced cardiomyocytes. NCX transgene expression was similar in Ad-NCX1.1 and 1.3 tranduced cells. NCX 1.3 expression was 102 ± 15 % ($p > 0.05$, n=3) compared to NCX1.1 (100 %). We did not quantify this signal with respect to control because transgene protein is of canine origin and the antibody may have a different affinity for rat and canine NCX. Qualitatively similar results were obtained in 3 independent experiments. The fourth line on the gel was from a sample from cells infected with a control adenovirus that expresses β-galactosidase (Ad-QBI).

One possible role of the alternative spliced region of the exchanger could be to direct the NCX protein to a specific location in the cell or to regulate the amount of the protein that is transported to the plasmalemmal membrane. The levels of NCX protein

Control

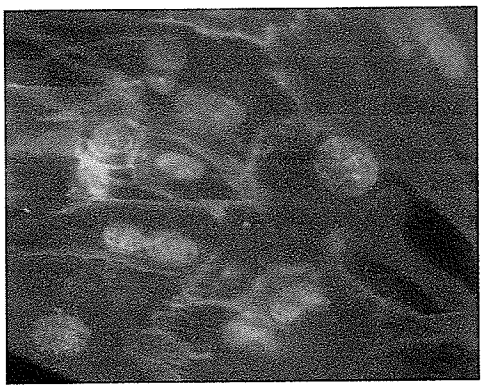

Ad-NCX1.1

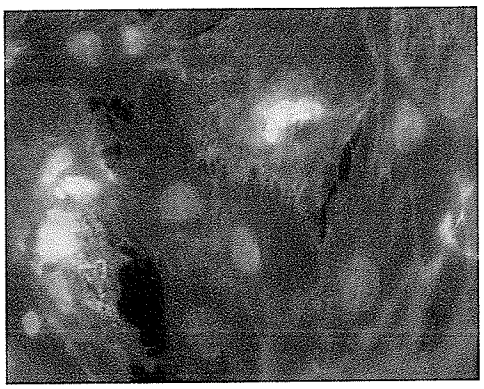

Ad-NCX1.3

Figure 29. Immunostaining of the NCX as a function of the expression of different NCX isoforms in neonatal cardiomyocytes. Superimposed images of NCX (green) and nuclear staining with Hoechst (blue).

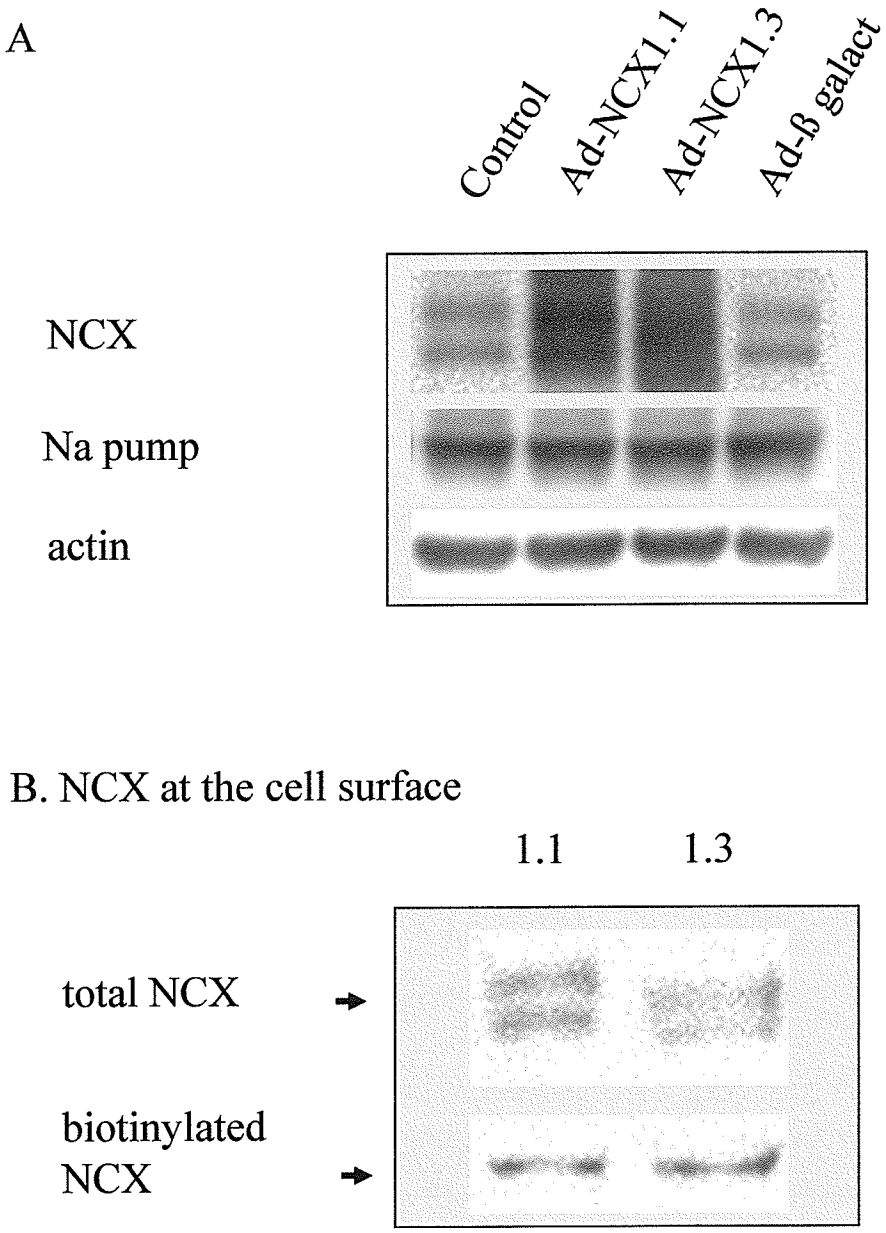

Figure 30. NCX1.1 and NCX1.3 transgene expression in neonatal cardiomyocytes. A. Western blot analysis of sodium calcium exchanger (NCX), Na^+ pump and actin (loading control) from neonatal cardiomyocytes infected at multiplicity of 1.5 with either the NCX 1.1 or 1.3 isoform. B. Biotinylation of surface proteins and IP of NCX to detect NCX at the surface membrane. Top, NCX detected with anti-NCX antibody; bottom, NCX detected with anti-biotin antibody.

expressed at the plasmalemmal membrane (where it is functional) will determine the level of activity of the expressed protein. To verify that similar amounts of NCX1.1 and NCX1.3 were directed to the cell membrane, we proceeded to biotinylate all proteins that were exposed at the extracellular surface of intact cells. Only the NCX molecules that were directed to the membrane could be biotinylated. Next, we immunoprecipitated NCX, separated the proteins by SDS-PAGE and detected the biotinylated NCX using an anti-biotin antibody. Similar levels of biotinylated NCX1.1 and NCX1.3 were detected in Ad-NCX1.1 and Ad-NCX1.3 cells (Figure 30B).

NCX activity was measured in the cells as Na^+ gradient-dependent ^{45}Ca uptake. In the Ad-NCX1.1 and in the Ad-NCX1.3 group, NCX activity was 1.77 ± 0.15 and 1.15 ± 0.01 fold of the activity in control cells ($p < 0.05$ *vs* control). NCX activity was not different in Ad-NCX1.1 and Ad-NCX1.3 transfected cells ($p > 0.05$, n= 4-8) (Figure 31). Infecting the cells with Ad-QBI up to MOI 50 did not affect NCX activity (102 ± 1 % of activity in non-infected cells, $p > 0.05$ *vs* control, n= 4). Because NCX expression levels at the membrane were similar for NCX1.1 and NCX1.3, the activity data indicated that under these experimental conditions, the reverse mode of the NCX isoform 1.3 is less active than the 1.1 isoform. Because this assay measures the reverse mode, it may reflect the intrinsic regulatory characteristics of the isoform. This may explain why similar increases in NCX protein levels between the isoforms resulted in very different increases in activity.

We then performed intracellular Ca^{2+} measurements in the different cellular groups. Ca^{2+}_i was measured with two different techniques. In the first, a cuvette system

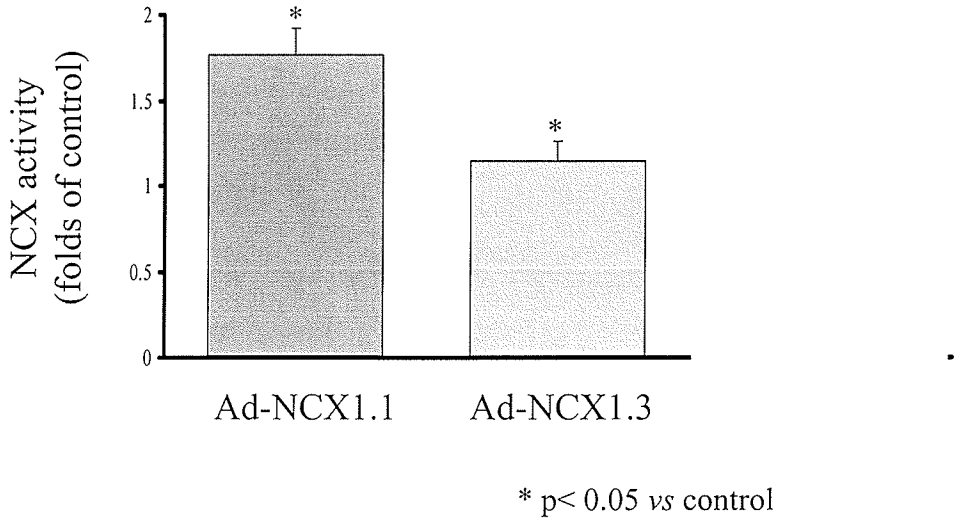

Figure 31. Na-Ca exchange (NCX) activity measured as Na^+_i dependent $^{45}Ca^{2+}$ uptake as a function of the expression of different NCX isoforms in neonatal cardiomyocytes. After ouabain treatment, cells were exposed to a solution containing ^{45}Ca and either K^+_o (to activate NCX activity in the calcium entry mode) or Na^+_o (blank). NCX activity was calculated as the difference in ^{45}Ca uptake/mg protein in K^+_o to Na^+_o and normalized to activity of control cells.

was employed. The advantage of the cuvette system was that it allowed for the study of a large number of cells per experiment (cells plated at confluency on a coverslip). The disadvantage of this methodology was that we could not introduce electrodes for pacing and the cells had to be plated at confluency to obtain enough fluorescent signal to detect reliably. The second methodology that we used to measure Ca^{2+} utilized a microscope stage with cells on a cover slip. This allowed us to visualize any fluorescent changes and it allowed us the opportunity to pace the cells. Cells had to be plated at low density to allow them to follow electrical stimulation. Groups of only 2-3 cells could be studied per experiment.

The effect of manipulating NCX1.1 or 1.3 transgene expression on Ca^{2+} transient characteristics under control conditions was examined. To be able to compare the size of the transients, cells were studied under electrical stimulation (at 0.5 Hz). We observed no changes in resting Ca^{2+} (expressed as Fura-2 fluorescence ratio) with respect to control in either group (Table 2). However, a decrease in systolic Ca^{2+} and Ca^{2+} transient amplitude was observed. The decrease was more pronounced in NCX1.1 than in NCX1.3 expressing cells. Similar effect of NCX1.1 expression was observed in cardiomyocytes from homozygous NCX1.1 transgenic mice and in adenovirally transduced adult rabbit cardiomyocytes (Reuter *et al*, 2004; Schillinger *et al*, 2000).

Other studies have shown that NCX1.1 and NCX1.3 have different responses with respect to Na^{+} and Ca^{2+} regulation (Dyck *et al*, 1999; Ruknudin *et al*, 2000). Therefore, we decided to study the response of cells expressing these isoforms under situations that produce large changes in the intracellular concentration of these ions. For example,

Table II. Characteristics of Ca^{2+} transients in control neonatal cardiomyocytes and in cardiomyocytes transduced with Ad-NCX1.1 or Ad-NCX1.3.

	Control	*Ad-NCX1.1*	*Ad-NCX1.3*
Diastolic Ca^{2+} (Fura-2 340/380 nm ratio)	0. 864 ± 0.009	0.864 ± 0.007	0.867 ± 0.010
Systolic Ca^{2+} (Fura-2 340/380 nm ratio)	0.988 ± 0.009	0.931 ± 0.010 *	0.951 ± 0.010 *
Amplitude (systolic Ca^{2+}– diastolic Ca^{2+})	0.124 ± 0.006	0.066 ± 0.008 *	0.084 ± 0.006 *
N	23	26	28

Cells were paced at 0.5 Hz. Values are expressed as the Fura-2 340/380 fluorescence ratio. * $p < 0.05$ *vs* control. There was no significant difference between Ad-gal and non-infected cardiomyocytes (data not shown).

ouabain toxicity and simulated ischemia are known to induce large changes in the intracellular concentrations of Na^+ and Ca^{2+}.

Ouabain inhibits the Na^+, K^+-ATPase and, therefore, causes an accumulation of Na^+_i. Ischemia is characterized by the accumulation of H^+, through the stimulation of anaerobic metabolism. Protons leave the cell through the Na^+-H^+ exchanger, causing Na^+ accumulation. Lower Na^+, K^+-ATPase activity due to a decrease in ATP content in the cell is thought to contribute to an increase in Na^+_i during the ischemic insult. High Na^+_i, under both pathological situations, causes a secondary increase in Ca^{2+} due to either a decrease in Ca^{2+} removal or an increase in Ca^{2+} entry through the NCX. (Satoh *et al*, 2000).

Figure 32 shows the response of intracellular Ca^{2+} as a function of 10 minutes of treatment with 1 mM ouabain. We chose to work with a concentration of ouabain that would produce almost complete inhibition of the Na^+ pump in order to generate a more pronounced change in $[Na^+]_i$. Rat cardiomyocytes, contain larger proportion of the ouabain insensitive $\alpha 1$ isoform of the Na^+ pump and less of the $\alpha 3$, therefore, higher concentrations are required in comparison to those normally used in other species (Orlowski and Lingrel, 1990; Peng *et al*, 1996). These experiments were performed in the cuvette system. An increase in resting Ca^{2+} was observed in all cells. A gradual increase in resting Ca^{2+} was observed in control and Ad-NCX1.3 cells. However, in Ad-NCX1.1 cells, the change was more pronounced during the first 4 minutes. The change in Fura-2 fluorescence ratio, with respect to the pre-treatment value, was 0.63 ± 0.08 in control cells, 1.98 ± 0.12 in Ad-NCX1.1 ($p < 0.05$ *vs* control) and 0.95 ± 0.12 in Ad-

A

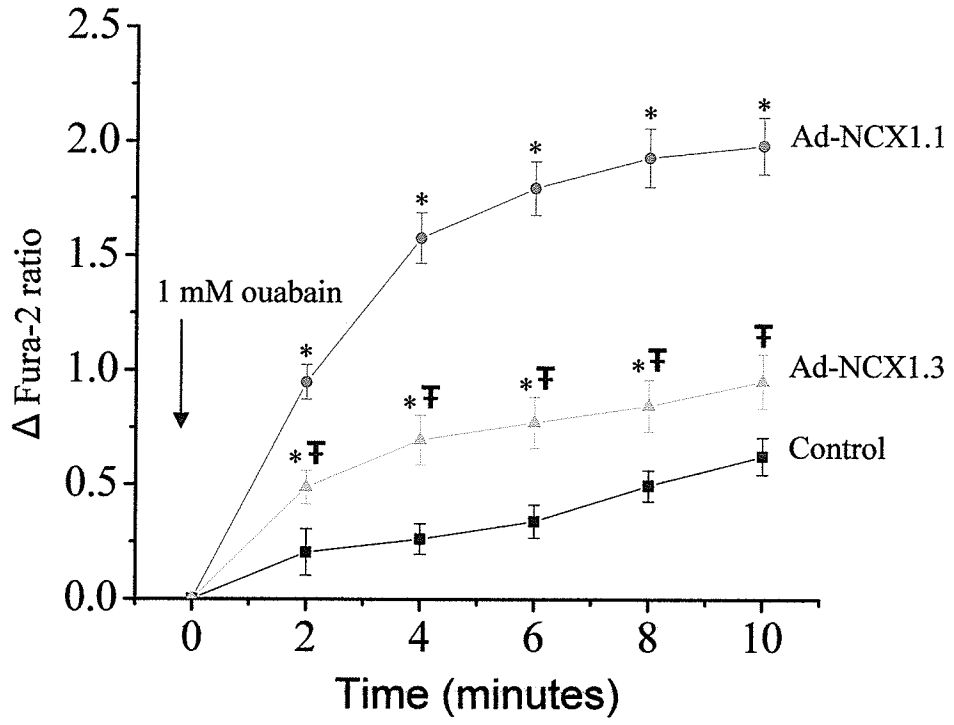

B

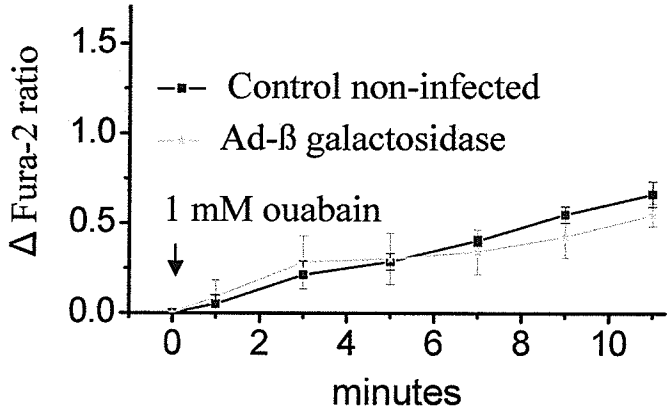

Figure 32. Effect of ouabain treatment on resting Ca^{2+} as a function of the expression of different NCX isoforms in neonatal cardiomyocytes. Values are mean ± SEM. * $p< 0.05$ *vs* control ; Ŧ $p< 0.05$ *vs* Ad-NCX1.1 (n= 11-17).

NCX1.3 ($p < 0.05$ *vs* Ad-NCX1.1) at the end of the 10 minutes of treatment. Although the value at this time point for NCX1.3 was not statistically different from control, there was a tendency for a larger change in resting Ca^{2+} in comparison to control. At all of the previous time points, during treatment, there were statistical differences between the three groups. Figure 32B shows that there were no differences in the response to ouabain between non-infected controls and Ad-QBI infected cells. The difference between control and Ad-NCX1.1 was due to a larger number of the cardiac exchangers. Conversely, the difference between Ad-NCX1.1 and Ad-NCX1.3 expressing cells appears to be due to differences in NCX regulation. Similar qualitative increases in resting Ca^{2+} were observed in cells with or without stimulation.

To test which mode of NCX activity was involved in the increase in Ca^{2+}_i, we used KB-R7943 which is a pharmacological blocker of NCX with higher affinity for the reverse mode (Ca^{2+} influx). Five μM KB-R7943 was present in the buffer solution 10 minutes before and during ouabain application. Figure 33 shows that KB-R7943 significantly attenuated the increase in intracellular Ca^{2+} caused by ouabain treatment in the three groups.

The increase in resting Ca^{2+} during ouabain treatment was accompanied by a decrease in the amplitude of the Ca^{2+} transient. The effects on the Ca^{2+} transient amplitude are shown in Figure 34. The effect was significantly stronger in Ad-NCX1.1 transduced cells and intermediate in Ad-NCX.1.3 expressing cells.

The transduced cells were further challenged with an ischemia mimetic protocol to evaluate the responses of the NCX1.1 and NCX 1.3 isoforms. Figure 35 shows the

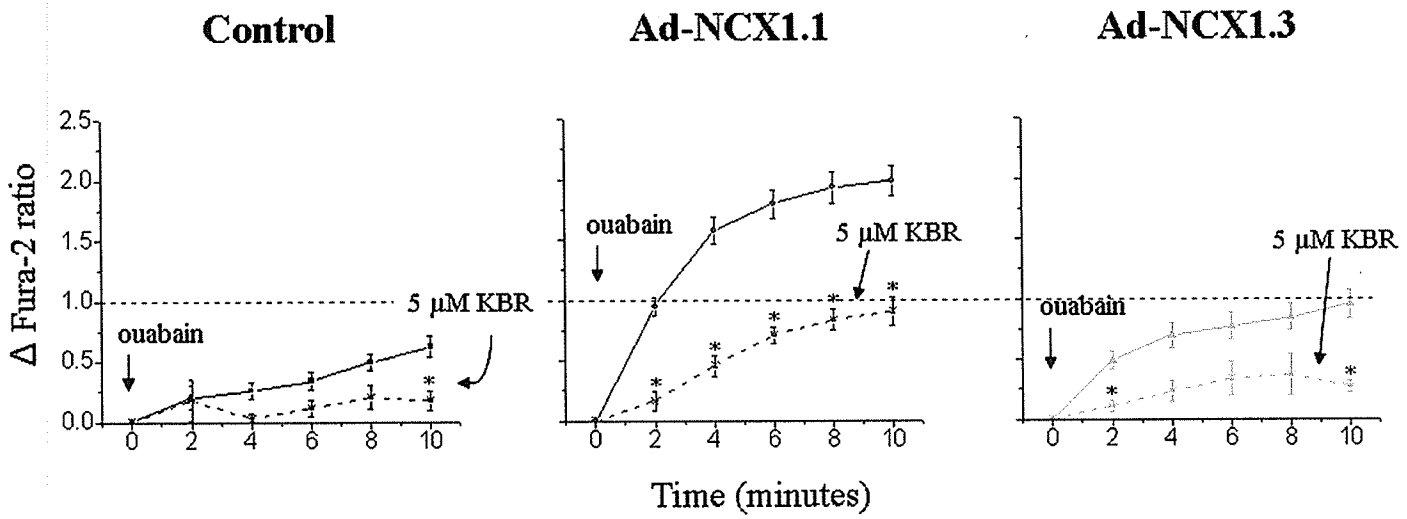

Figure 33. Effect of 5 μM KB-R7943 (KBR) on the ouabain induced increase in resting Ca^{2+} as a function of the expression of different NCX isoforms in neonatal cardiomyocytes. KB-R7943 was present for 5 minutes before and during ouabain application. Solid line, no KB-R7943; dashed line, KB-R7943. Values are mean ± SEM. * $p < 0.05$ *vs* no KB-R7943 for each group (n= 3-17).

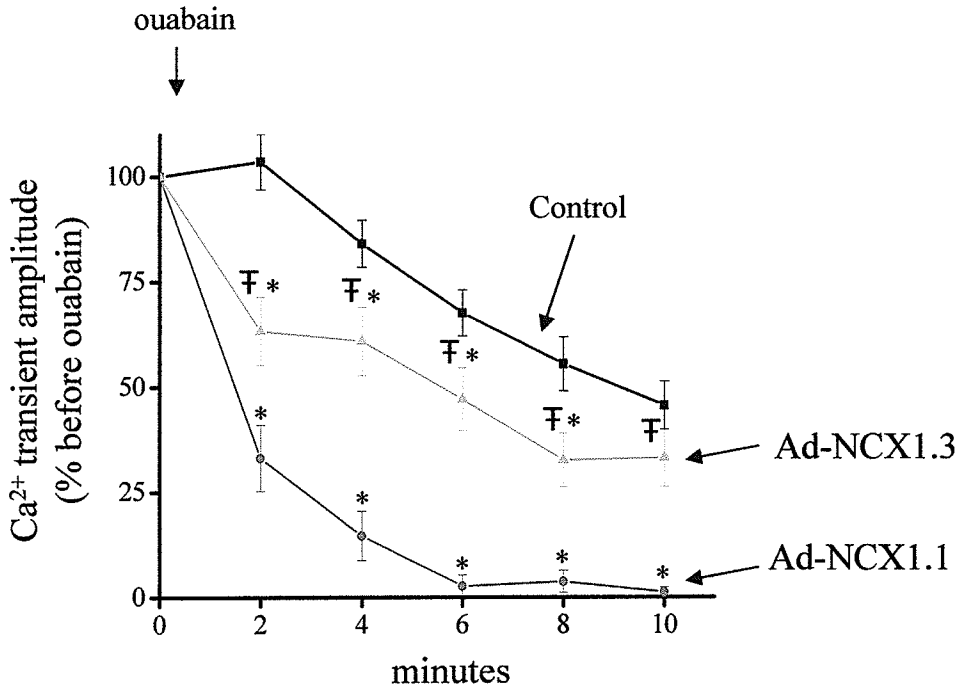

Figure 34. Effect of ouabain treatment on Ca^{2+} transient amplitude as a function of the expression of different NCX isoforms in neonatal cardiomyocytes. Cells were paced at 0.5 Hz throughout the experiment. Values are mean ± SEM. * $p < 0.05$ *vs* control ; Ŧ $p < 0.05$ *vs* Ad-NCX1.1 (n= 23-28). There was no significant difference between Ad-gal and non-infected cells.

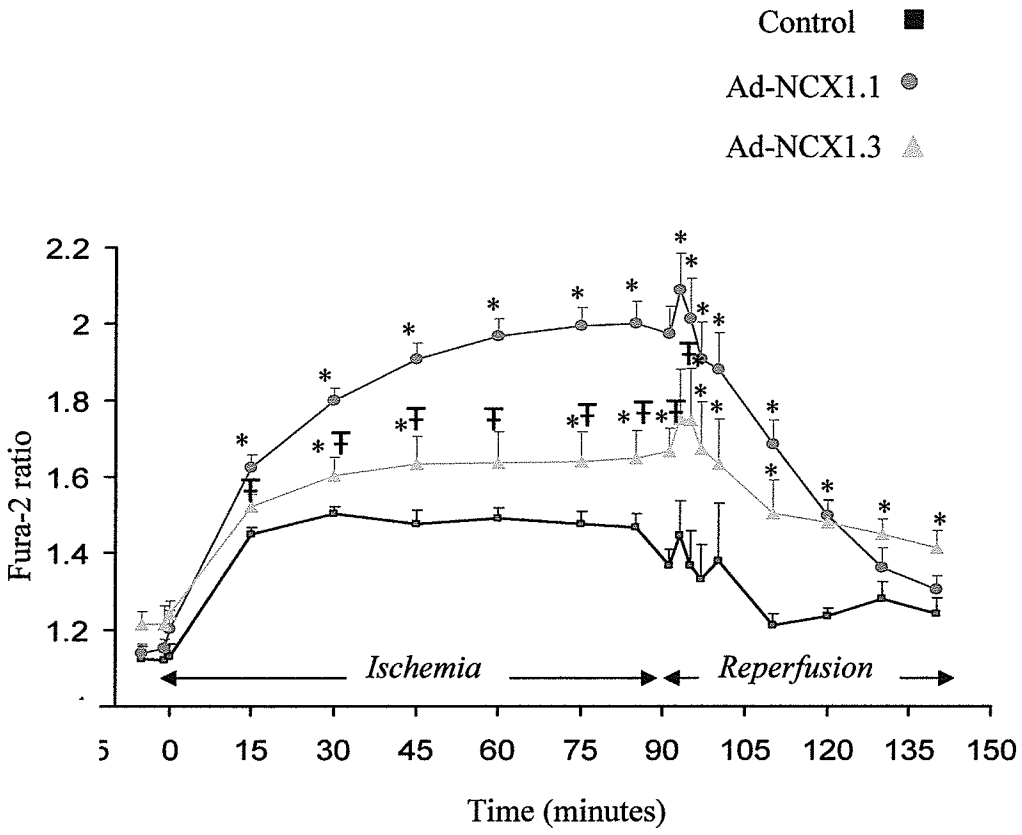

Figure 35. Effect of 90 minutes simulated ischemia and reperfusion on resting Ca^{2+} levels as a function of the expression of different NCX isoforms in neonatal cardiomyocytes. The ischemia mimetic solution contained high [K^+], no glucose and 5 mM sodium cyanide. Values are mean ± SEM. * $p < 0.05$ *vs* control ; Ŧ $p < 0.05$ *vs* Ad-NCX1.1 (n= 23-28). There was no significant difference between Ad-gal and non-infected cells.

changes in Ca^{2+}_i caused by 90 minutes of simulated ischemia and reperfusion in the same three experimental groups. Control cells responded to the ischemic insult with an increase in resting Ca^{2+} during the ischemic period and a slow return to baseline conditions upon reperfusion. The increase in resting Ca^{2+} was more pronounced in cells expressing NCX1.3 in comparison to the response of control cells. At reperfusion there was a further transient increase in Ca^{2+}. The changes in Ca^{2+} were even more pronounced in cells over-expressing NCX1.1. By the end of reperfusion, Ca^{2+}_i decreased in cells over-expressing NCX1.1 to levels similar to control. However, in NCX1.3 cells, Ca^{2+} concentrations remained elevated compared to control.

PART IV: Effect of ischemia-reperfusion on HEK-293 cells expressing NCX1.1 or NCX1.3

Objective: To determine if expression of the 1.1 or 1.3 isoforms of the NCX alter the response of HEK-293 cells to an ischemia mimetic challenge.

Hypothesis: Cells induced to express NCX will be more sensitive to ischemic/reperfusion challenge compared to control HEK-293 cells that do not express NCX. In addition, expression of the NCX1.1 isoform will cause a larger Ca^{2+} entry upon ischemic/reperfusion challenge compared to the NCX1.3.

The role of the NCX 1.1 and NCX 1.3 isoforms in response to simulated ischemia and reperfusion in kidney cells was investigated. HEK-293 cells were chosen as the cell type to study because first, this is a relatively easy cell line to transfect and to maintain in culture, and secondly and more importantly, this cell type does not contain any endogenous NCX protein. Therefore, control non-transfected cells provide important baseline data uncomplicated by background endogenous NCX activity.

Stable transfected clones expressing either NCX1.1 or NCX1.3 were generated. Adenovirus-mediated transfection cannot be used to transduce this cell type because HEK-293 cells support adenovirus replication. All of the cells in a clone typically express the same amount of transgene and different clones express different amounts depending upon where in the genome the gene was introduced. From the several clones that were generated, 1 clone was chosen for each isoform (clones were chosen that had similar expression levels between each other). Quantification of NCX signal by Western blot

analysis showed that NCX1.3 expression was 155 ± 35 % of the expression of NCX1.1 in the corresponding transfected group ($p > 0.05$, $n= 4$). A representative Western blots is shown in Figure 36. NCX1.3 is shown at a slightly lower molecular size than NCX1.1. This is probably because the NCX1.3 contains 36 amino acids less than the NCX1.1. For comparison purposes, a blot is shown that was loaded with equal amounts of total protein sample from HEK-293-NCX1.3 and control neonatal cardiomyocytes. NCX expression is known to be high in neonatal cardiomyocytes. Therefore, exchanger expression per mg of protein was even higher in the NCX clones chosen compared to neonatal cardiomyocytes.

Figure 37 shows NCX immunostaining of control cells (where no NCX signal can be observed), and cells expressing NCX1.1 and NCX1.3. NCX staining for both isoforms was localized to the plasmalemma membrane. Because these are fluorescent microscope photographs and not confocal micrographs, the faint and diffuse signal that was observed within the limits of the cell probably represents NCX molecules located at the plasma membrane that was above or below the plane of focus.

Expression of the NCX influenced the manner by which the cells reacted in culture conditions. For example, differences were observed in the ability of the cells to attach to the culture plate after trypsinization. After 24 hours, control cells were completely attached and spread out on the plate surface. NCX1.1 expressing cells attached and remained rounded for approximately one more day. NCX1.3 expressing cells attached and remained rounded for an even longer period of time (2 days longer than control cells), data is not shown. These observations are consistent with a previous

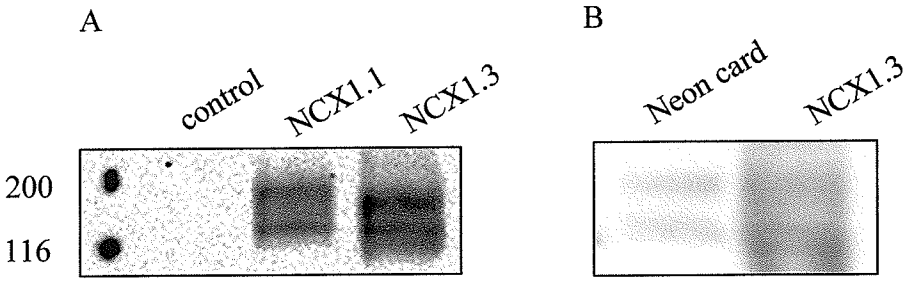

Figure 36. Western blot analysis of NCX expression in HEK 293 cells. A. Control, NCX1.1 and NCX1.3 transfected cells (30 μg total protein) . B. NCX protein in neonatal cardiomyocytes (neon card) and NCX1.3-HEK (30 μg total protein). MW is indicated in kDa.

Control (non transfected)

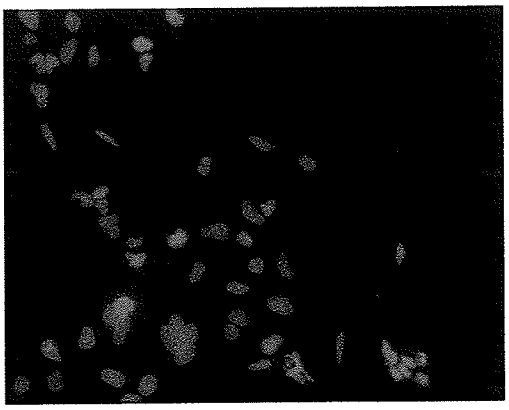

NCX1.1
(stable transfected)

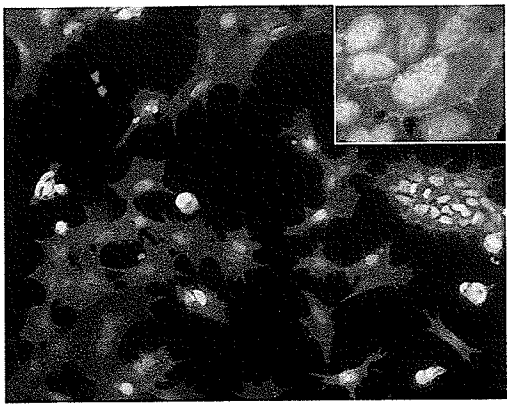

NCX1.3
(stable transfected)

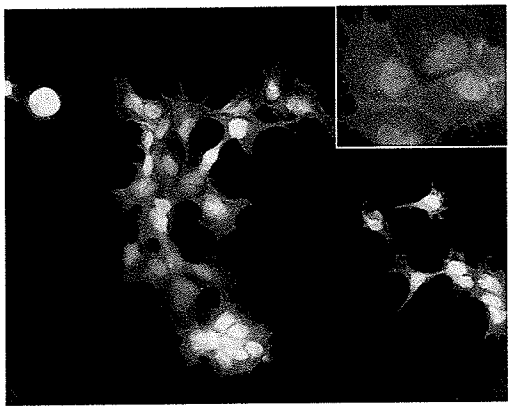

Figure 37. NCX immunostaining of HEK 293 cells in cells as a function of stable transfection of the 1.1 and 1.3 NCX isoforms. Superimposed images of NCX-FITC (green) and nuclear staining with Hoechst (blue). Exposure conditions were identical for the 3 pictures. Inserts: higher magnification.

report that showed that NCX expression altered fibroblasts attachment capacity (Iwamoto *et al*, 1998). In our study, increased expression of either isoform did not affect viability of the cells. Decreased viability was previously oberved by Diaz Horta *et al* (Diaz Horta *et al*, 2002).

NCX activity was measured as the increase in Ca^{2+}_i upon replacement of Na^+_o for Li^+_o in Fura-2 loaded cells. This intervention generates a Na^+ gradient between the inside of the cell and the extracellular space. This gradient drives the exchanger to function in the Ca^{2+} entry mode. Switching solutions had no effect on Ca^{2+}_i in control cells, since these cells had no sodium-calcium exchanger. However, a rapid increase in Ca^{2+}_i was observed in NCX expressing cells (Figure 38). The change in Ca^{2+}_i was significantly larger in cells expressing the NCX1.1 compared to the NCX1.3 isoform (Table 3). During Na^+_o removal, Ca^{2+}_i decayed with a rate that was similar between the groups. After 2 minutes, reintroduction of Na^+_o, reverted the gradient and Ca^{2+}_i decreased rapidly. Because of technical complications involved in the use of cuvettes, it was not possible to collect data that corresponded to the first ~ 20 seconds after the solution change (time needed to re-start aquisition). Therefore, we could only observe data collected at the end of this change. In all the experiments, we observed a similar response. In NCX1.1 expressing cells, Ca^{2+}_i had decreased below resting levels and began to rise again afterwards (a positive slope was observed when we re-started aquisition). In NCX1.3 expressing cells, Ca^{2+}_i decreased towards the pre-treatment level (negative slope) when the scan was re-initiated.

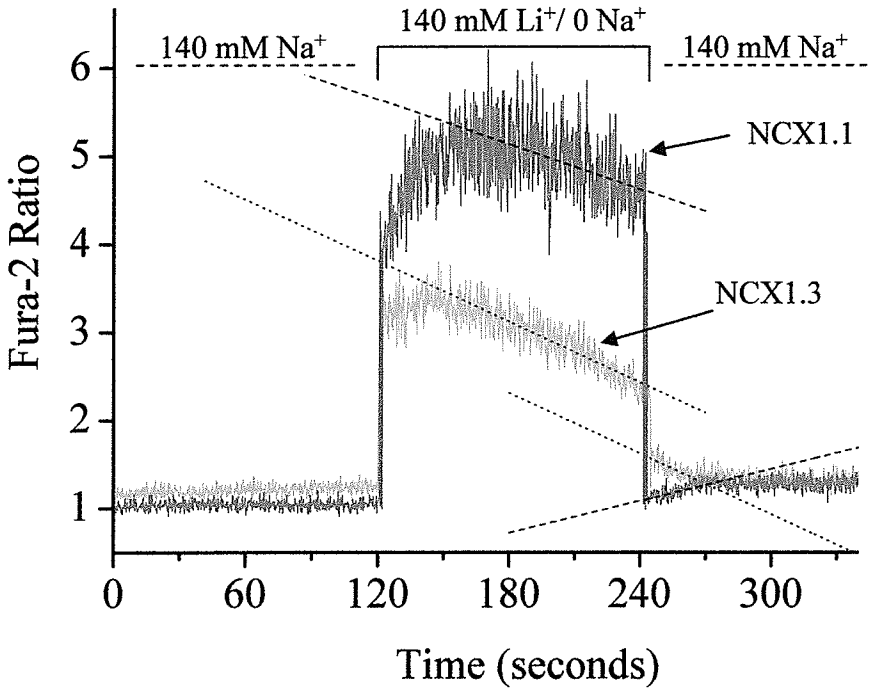

Figure 38. NCX activity in HEK-293 cells expressing NCX1.1 or NCX1.3. Representative experiments showing changes in Ca^{2+}_i upon removal and re-application of Na^+_o in Fura-2 loaded HEK-293 cells expressing NCX1.1 (red) and NCX1.3 (green).

Table III. NCX activity in NCX1.1 and NCX1.3 HEK- 293 cells

	NCX1.1	NCX1.3
Ca^{2+}_i (Fura-2 ratio)	1.10 ± 0.04	1.46 ± 0.26
Change Ca^{2+}_i Upon Na^+_o removal (Fura-2 ratio)	4.05 ± 0.08	1.60 ± 0.24 *
Rate change Ca^{2+}_i During Na^+_o removal (ratio/sec)	- 0.013 ± 0.003	- 0.013 ± 0.002
Rate change Ca^{2+}_i During Na^+_o reapplication (ratio/sec)	0.005 ± 0.0007	- 0.006 ± 0.017 *

Intracellular Ca^{2+} and changes in Ca^{2+}_i upon removal and re-application of Na^+_o in Fura-2 loaded HEK-293 cells expressing NCX1.1 or NCX1.3. Mean data from several experiments. Values are mean ± SEM. * $p < 0.05$ *vs* HEK-293-NCX1.1, n= 4-5. Representative experiments are shown in Figure 38.

Figure 39 shows the changes in Ca^{2+}_i observed during simulated ischemia and reperfusion. Ca^{2+}_i showed a tendency to be higher in the HEK-293-NCX1.3 group before treatment, however, this difference did not reach statistical significance. During ischemia, Ca^{2+}_i rose in all three groups. Ca^{2+}_i was significantly higher during the entire period of ischemia in NCX1.1 expressing cells with respect to control. Ca^{2+}_i showed a tendency to be higher during ischemia in the HEK-293-NCX1.3 cells with respect to control, however, the values did not reach statistical significance. Ca^{2+}_i was significantly higher in HEK-293-NCX1.1 compared to HEK-293-NCX1.3 cells. At reperfusion, all groups showed a further increase in Ca^{2+}_i followed by a decrease as the duration of reperfusion increased. This initial peak was more pronounced in the NCX1.3 group. During almost all of the reperfusion period , Ca^{2+}_i was higher in NCX1.3 expressing cells compared to control. In NCX1.1 expressing cells, Ca^{2+}_i was higher at some time points during early reperfusion and at the end of reperfusion. Resting Ca^{2+}_i during the entire hour of reperfusion was significantly higher than in control cells. In all groups, resting Ca^{2+}_i at the end of reperfusion was higher than it was before ischemia. The difference compared with the pretreatment values was not significant for control cells (0.99 ± 0.03 before *vs* 1.032 ± 0.019 after, $p > 0.05$, $n= 15$), but was significantly different for NCX1.1 (0.98 ± 0.025 before *vs* 1.10 ± 0.016 after, $p < 0.05$, $n= 13$) and NCX1.3 (1.022 ± 0.016 before *vs* 1.14 ± 0.04 after, $p < 0.05$, $n= 12$).

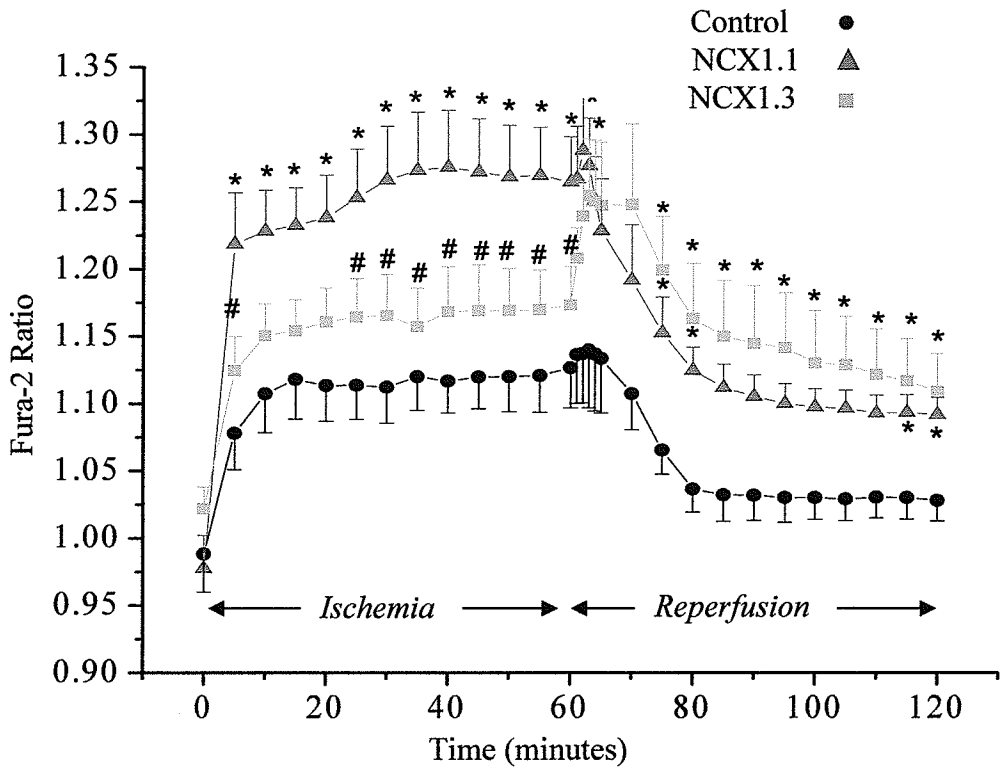

Figure 39. Changes in Ca^{2+}_i during simulated ischemia and reperfusion in HEK-293 cells as a function of stable transfection of the 1.1 and 1.3 isoforms. Control (●), NCX1.1 (▲) and NCX1.3 expressing cells (■). N= 12-15 experiments. Values are mean ± SEM. * $p < 0.05$ *vs* control. # $p < 0.05$ *vs* NCX1.1.

PART V: Use of RNAi to replace the endogenous NCX1.1 with the NCX1.3 isoform

The experiments described in Part III, in which we compared the NCX1.1 (cardiac) and the NCX1.3 (kidney) isoforms expressed in neonatal cardiomyocytes, had the limitation that the 1.3 isoform was expressed on a background of the endogenous 1.1 exchanger. One way to avoid the problem of background NCX expression is to use a cell type that does not express the NCX. The HEK-293 cells are valuable for this reason. However, it is a non-cardiac cell type and other differences in cell function are apparent other than protein expression that may not provide ideal data to be relevant to the cardiac situation. Therefore, another approach to evaluate the role of the NCX1.3 isoform in cardiac cells without the influence of the expression of the background endogenous NCX1.1 isoform was to attempt to inhibit the expression of the background NCX1.1 at the same time as introducing the 1.3 isoform into the cell to be expressed. We designed adenovirally delivered RNAi constructs with the purpose of down-regulating the endogenous protein (1.1) without interfering with the expression of the transgene (1.3).

Previous reports on the use of RNAi had shown that the RNAi system could differentiate sequences with as few as 1 different nucleotide (Ding *et al*, 2003). Rat cardiomyocytes were used for our studies, consequently, our RNAi constructs targeted the rat NCX1.1 sequence. The adenovirus constructs for expression of the NCX1.3 protein were made using the canine cDNA. Therefore, RNAi constructs had to be identical to the rat NCX1.1 sequence and as different as possible from the dog NCX1.3.

One of the RNAi constructs that we made (Ad-RNAi #3) targeted a 29 nucleotide sequence located 142 nucleotides from the start codon of the NCX1.1 (Figures 11 and

40). This sequence is present in NCX1.1 and NCX1.3, however, the rat sequence contains 7 different nucleotides compared with the dog sequence. The sequence corresponding to the N-terminus of this protein is less conserved between species. Regions with more than 7 mismatches could be found close to the start codon. However, it has been recommended to target RNAi to sequences more than 100 nucleotides from this region because proteins that are usually bound to the mRNA translation initiation site limit the access of the siRNA-RISC complex. These considerations, therefore, were taken into account when we devised this construct. However, this strategy did not guarantee its success and two other constructs were made. Another construct (Ad-RNAi # 4) targeted a 29 nucleotide sequence located in exon F. This sequence is only present in NCX1.1 and the corresponding dog sequence has 3 different nucleotides. The last construct (Ad-RNAi #2) targeted a 29 nucleotide sequence located in exon A. This exon is also only present in the NCX1.1 isoform and contains 2 mismatches compared to the dog sequence.

We treated neonatal cardiomyocytes with Ad-RNAi #2, 3 and 4 and NCX1 protein expression levels were determined by Western blot. We found that Ad-RNAi #3 and #4 had a strong silencing effect. However, the silencing effect was modest when Ad-RNAi #2 was used (data not shown). Figure 41 shows on line 2 and 3 the silencing effect of Ad-RNAi #3 and #4 on the endogenous expression of NCX 1.1.

Because the R3F1 antibody recognizes both NCX1.1 and NCX1.3, it is impossible to differentiate the endogenous protein from the transgene in a Western blot. Therefore, we also generated NCX1.1 and NCX1.3 fusion proteins with the Enhanced Green Fluorescent Protein (EGFP). EGFP was located on the C-terminus of NCX. The

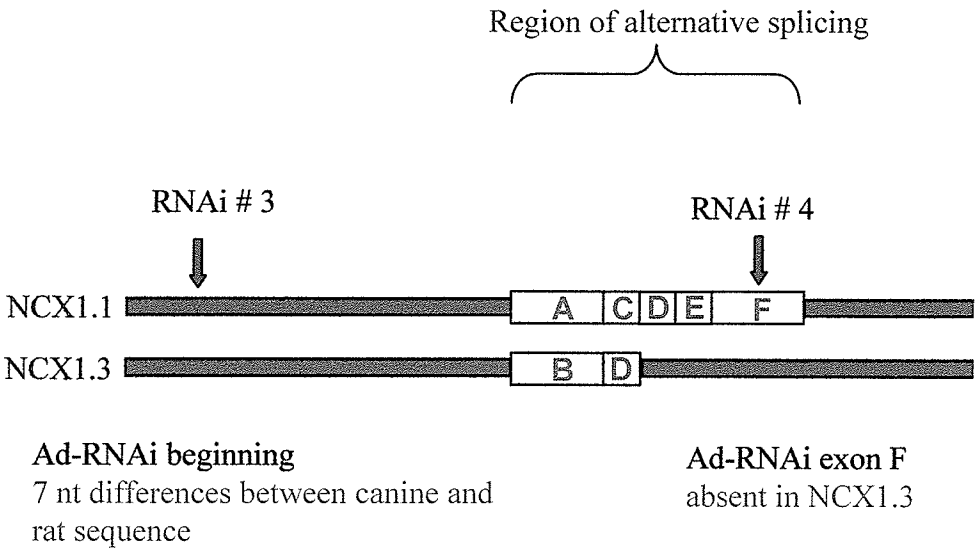

Figure 40. Exons targeted by Ad-RNAi #3 and #4. Diagram of NCX1.1 and 1.3 mRNAs showing exons corresponding to the alternative splice site and sequences targeted by Ad-RNAi #3 (at the beginning of the mRNA) and Ad-RNAi # 4 (at exon F).

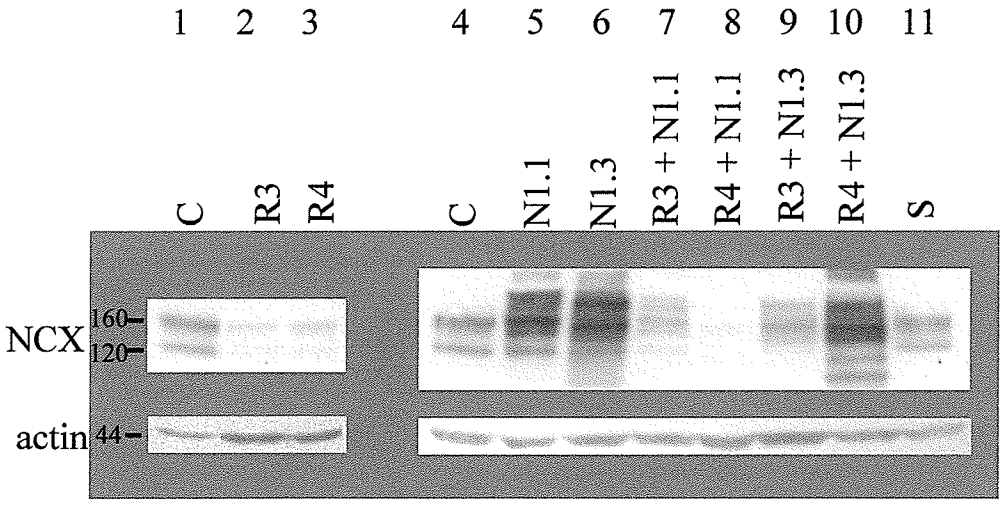

Figure 41. Western blot analysis of the efficacy of isoform replacement.
Line 1: control non-infected cardiomyocytes. Lines 2 and 3: down-regulation of the endogenous cardiac exchanger by RNAi adenovirus constructs R3 and R4. Line 4: C, control non-infected cardiomyocytes. Lines 5 and 6: canine Ad-NCX1.1-EGFP and Ad-NCX1.3-EGFP (fusion proteins) transgene expression in the presence of endogenous rat NCX1.1 expression. Note that the EGFP fusion protein runs at a higher molecular weight on the gel. Lines 7 and 8: Both RNAi constructs (R3 and R4) interfere with the canine NCX1.1 transgene expression. Line 9: R3, which targets a sequence that is present in NCX1.1 and NCX1.3, and has 7 nucleotide mismatches between the endogenous rat and the canine transgene interferes with the expression of NCX1.3 transgene. Line 10: R4 that targets a sequence absent in NCX1.3 does not interfere with Ad-NCX1.3-EGFP transgene expression and therefore can be used to replace the isoforms. Line 11: Ad-RNAi scrambled infected cardiomyocytes.
Abbreviations: C, Control; N1.1, Ad-NCX1.1-EGFP; N1.3,
Ad-NCX1.3-EGFP; 1.3, Ad-NCX1.3; R1, Ad-RNAi beginning;
RF, Ad-RNAi exon F; S, Ad-RNAi Scrambled

fusion protein was functional. Exchanger activity in Ad-NCX1.1 infected neonatal cardiomyocytes was 177 ± 15 % of control, and it was 156 ± 13 % of control in Ad-NCX1.1-EGFP infected myocytes ($p > 0.05$ *vs* Ad-NCX1.1, n= 7-13). EGFP has 240 amino acids and a molecular weight of 27 kDa that caused the NCX fusion protein to resolve at a higher molecular weight on the gels compared to the original protein. Lines 5 and 6 in Figure 41 show strong NCX staining in bands corresponding to NCX1.1-EGFP and NCX1.3-EGFP. The NCX protein in an SDS-PAGE commonly appears as two distinct bands: one at 120 kDa, the calculated molecular weight, and another as a larger band at 160 kDa (the larger size is due to disulfide bond formation) (Philipson *et al*, 1988). The fusion protein corresponding to the smaller band overlapped with the larger band of the native protein.

As was discussed in Part II of this thesis, the NCX protein has a half-life of 33 hours. Therefore, once new protein synthesis is prevented, 5 days are required for the NCX content in the cell to decrease to < 10 % of the original value. We infected neonatal cardiomyocytes with the Ad-RNAi virus and 3 days later the same cells were infected with either Ad-NCX1.1-EGFP or Ad-NCX1.3-EGFP. The cells were studied on the 5^{th} day from the initial infection. Figure 41, shows samples from neonatal cardiomyocytes that were infected with Ad-RNAi #3 and subsequently with Ad-NCX1.1-EGFP (line 7) and Ad-NCX1.3-EGFP (line 9). Unfortunately, the presence of RNAi #3 in the cells significantly interfered not only with the expression of the endogenous NCX1.1, but it interfered with the expression of the the transgenes NCX1.1 and NCX1.3 as well.

Neonatal cardiomyocytes were also infected with Ad-RNAi #4 and subsequently with Ad-NCX1.1-EGFP (line 8) and Ad-NCX1.3-EGFP (line 10). RNAi #4 interfered with the expression of NCX1.1-EGFP. However, this time it allowed the expression of the NCX1.3-EGFP protein. Therefore, we could effectively replace the cardiac NCX1.1 with the renal NCX1.3 isoform using this combination of adenovirus treatments. We also tested the effect of Ad-RNAi#2 on isoform replacement. This construct allowed the replacement of isoforms. However, because it had a more modest silencing effect than that shown for the other constructs, a large quantity of the endogenous NCX could be observed on the blot (not shown). Finally, it was important to insure that any effects that we induced due to the treatment with adenoviruses containing the different NCX constructs were not a result of a non-specific effect of the adenovirus treatment itself. Cells infected with an adenovirus coding for the scrambled sequence of Ad-RNAi#3 had no effect (Figure 41, line 11).

Cells were immunostained against the NCX to demonstrate the expression patterns of the NCX isoforms as a function of the various treatments (Figure 42). NCX staining with FITC is shown in green and Hoechst nuclear staining is shown in blue. Control and NCX silenced neonatal cardiomyocytes are shown in Panels a and b, respectively. As expected, NCX is strongly and preferentially expressed at the cell membrane in control cells and the silencing was successful in repressing the expression of the exchanger in the RNAi treated cells. Panel c depicts cells that were infected with Ad-NCX1.3. Therefore, the signal corresponds to the endogenous NCX1.1 and the transgene NCX1.3. Note the large increase in NCX expression. It is expressed throughout the cell as would be predicted with a cell that is constantly processing NCX and

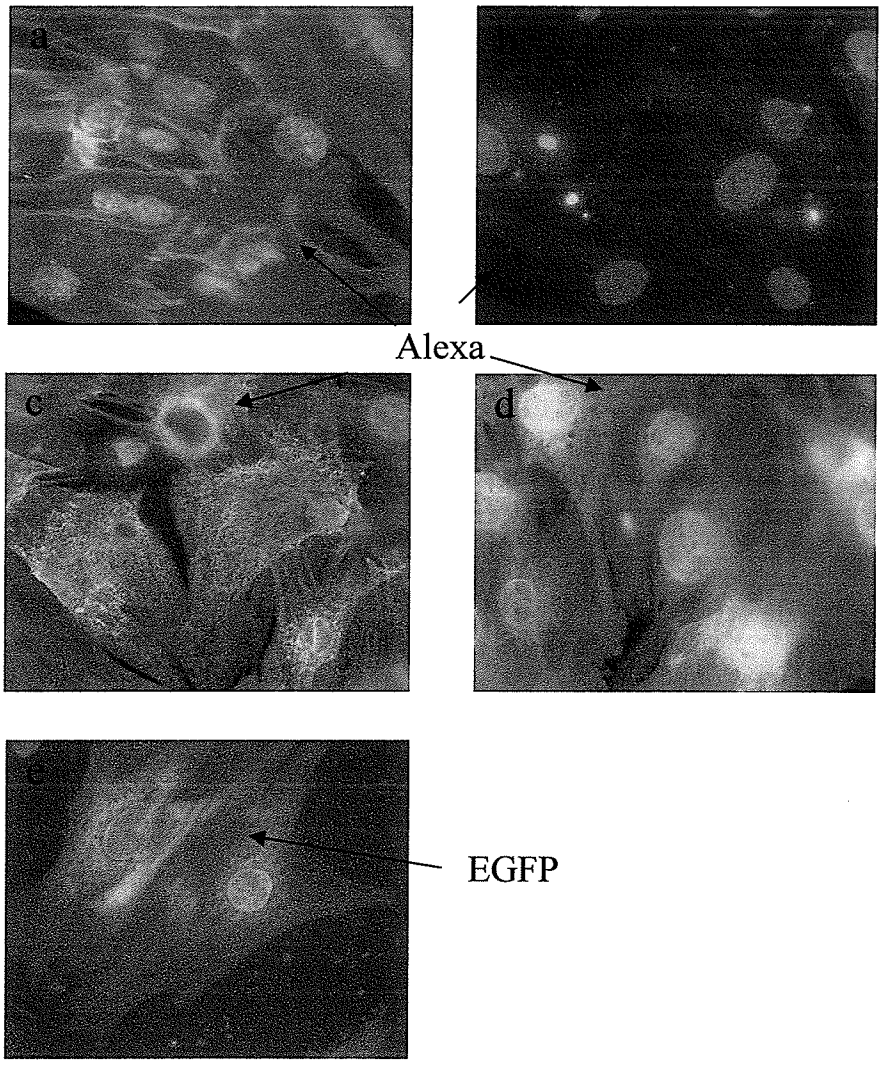

Figure 42. Fluorescence microscopy photographs of NCX expression during isoform replacement. a-d, immunostaining against NCX (green). a, control (endogenous NCX); b, Ad-RNAi# 4 treated (down-regulated NCX); c, Ad-NCX1.3 treated (endogenous NCX + transgene NCX1.3); d, Ad-RNAi# 4 + Ad-NCX1.3 (down-regulated endogenous NCX with NCX1.3 transgene expression); e, EGFP fluorescence of Ad-RNAi# 4 + Ad-NCX1.3-EGFP (down-regulated endogenous NCX (not labeled) with NCX1.3-EGFP transgene expression. Blue: Nuclear hoechst staining.

transporting it throughout the cell. Panel d, shows cells treated first with Ad-RNAi#4 and then with Ad-NCX1.3. Finally, Panel e shows EGFP fluorescence in cells treated first with Ad-RNAi#4 and then with Ad-NCX1.3-EGFP. Panels d and e, therefore, demonstrate the effects of isoform replacement. Cellular distribution patterns in both cases were similar to those found in Panel c where the adenovirus overexpressed the 1.3 in addition to the endogenous 1.1 expression.

These results obtained with the Western blots and the immunostaining allowed us to investigate the functional implications of these interventions on cellular Ca^{2+} homeostasis next. Figure 43 shows diastolic Ca^{2+}_i (expressed as the 340/380 Fura-2 fluorescence ratio) in control, NCX1.3 expressing neonatal cardiomyocytes (with NCX1.1 background), NCX1.1 silenced cells and, NCX1.3 (with NCX1.1 absent or minimally present). We had observed from previous studies (part II) that down-regulation of the NCX resulted in an increase in diastolic Ca^{2+} levels. Consistent with these results, as shown in lane 3 of Figure 43, silencing of the 1.1 isoform resulted in an increase in diastolic $[Ca^{2+}_i]$. Overexpression of the 1.3 isoform did not induce a change in diastolic $[Ca^{2+}_i]$ (lane 2). However, introduction of the NCX1.3 isoform when the 1.1 isoform was silenced reverted the increase in $[Ca^{2+}_i]$ (lane 4). Because of the interference of the RNAi#4 with the expression of the NCX1.1, we were not able to perform the control experiments of re-introducing the NCX1.1 isoform into these cells.

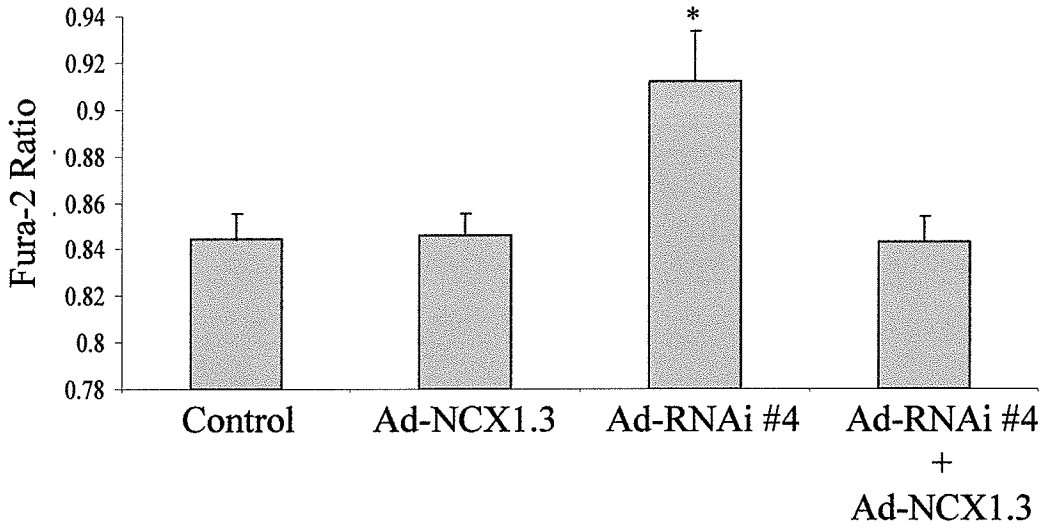

Figure 43. Intracellular Ca^{2+} as a function of NCX expression. Resting Ca^{2+}_i in control neonatal cardiomyocytes (n= 15), or cardiomyocytes that were Ad-NCX1.3 transduced (n= 8), RNAi # 4 treated (down-regulation of NCX1.1)(n= 7), or RNAi #4 treated + Ad-NCX1.3 (NCX1.1 down-regulation and NCX1.3 expression) (n= 3). Values are mean ± SEM. $p < 0.05$ *vs* control.

PART VI: A comparison of adenovirally delivered **E**xchanger **I**nhibitory **P**eptide (XIP) with RNAi and antisense cDNA approach to inhibit NCX expression/activity.

Objective: To determine if adenovirally delivered constructs of XIP can induce expression of XIP and to determine if the XIP can inhibit NCX activity in cardiac myocytes.

Hypothesis: The presence of XIP within the cardiomyocytes will inhibit NCX activity.

XIP is used as a blocker for NCX. It works from the intracellular side of the protein, therefore it has to be either injected into the cells or used in patch clamp experiments. We proposed that constructs coding for this peptide's sequence could be transfected into neonatal cardiomyocytes using adenoviral vectors. The effect of XIP expression with adenovirus methods was compared to two other methods, the use of adenovirally delivered NCX1.1-RNAi and NCX1.1 antisense cDNA.

Figure 44 shows the 20 amino acid sequence of XIP and a diagram of the pshuttle vectors that were constructed for XIP expression. These plasmids were used to make the corresponding adenovirus vectors. The addition of the ATG start codon was required for the expression of the peptide. A Kozak sequence was included with the start codon to assure high levels of expression. The resulting peptide had 21 amino acids. The calculated molecular weight for a 21 amino acid peptide with the sequence of XIP (plus a methionine) is ~ 3.2 kDa. Figure 45 shows a Western blot of HEK-293 cells transfected with the pires2-EGFP-XIP vector (stably transfected). A strong band was observed at the expected molecular weight in the transfected sample whereas no corresponding band was observed in the control HEK cells. A control peptide was also examined in the gel. The

A **Exchanger inhibitory peptide (XIP)**

basic aa

R R L L F Y **K** Y V Y **K R** Y **R** A G **K** Q **R** G hydrophobic aa

B

XIP construct

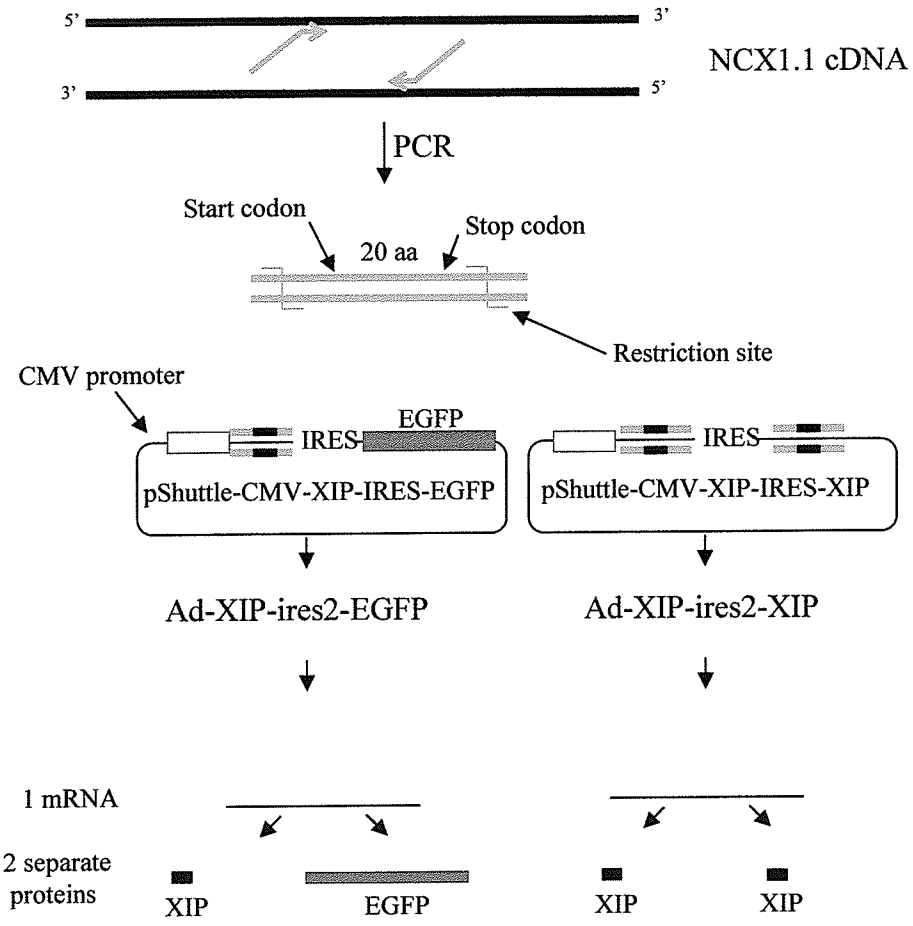

Figure 44. A. XIP (eXchanger Inhibitory Peptide) sequence. B. Procedure and vectors used to express XIP and to generate Ad-XIP.

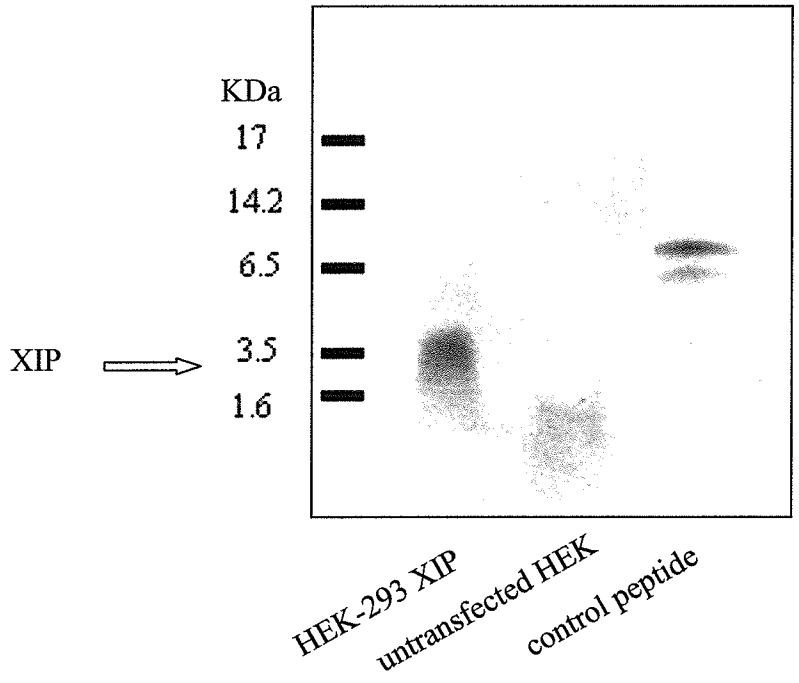

Figure 45. Western blot of XIP expression as a function of transfection. Samples were: HEK-293 transfected with the pShuttle-CMV-XIP-ires2-EGFP, control non infected HEK-293 cells and control peptide.

larger molecular size of the control peptide observed in the blot could be explained by the formation of peptide aggregates. The control peptide was purchased and is not normally used for WB. The XIP sequence was placed upstream of "IRES-EGFP". IRES is an internal ribosome entry site. The promoter drives the transcription of mRNA that is translated into 2 separate proteins (polycystronic mRNA as found in prokaryotes). Once the Ad-XIP-IRES-EGFP was constructed and tested on neonatal cardiomyocytes, however, it was found that an MOI of > 100 was required to decrease NCX activity. At this elevated MOI, Ad-EGFP had similar effects. Furthermore, EGFP fluorescence is within the emission range of Fura-2 and interfered with Ca^{+2}_i measurements. Therefore, the EGFP was removed from the construct and replaced by another XIP sequence. The resulting construct could theoretically stimulate the production of twice the amount of XIP in comparison to the original construct.

An adenovirus coding for rat NCX1.1 in antisense orientation (Ad-AS-NCX1.1) was made. Ad-AS-NCX1.1 was generated introducing the rat NCX1.1 cDNA (a generous gift from Dr. Lytton) in inverted orientation with respect to the promoter in the pShuttle-CMV. A mRNA complementary to the NCX1.1 should be synthesized from this construct upon cell transduction. The binding of the transgene mRNA with the endogenous NCX1.1 mRNA is expected to interfere with protein translation and to cause down-regulation of protein expression. We compared the effect of adenovirus coding for NCX1.1 antisense cDNA (Ad-AS-NCX1.1) and Ad-RNAi on NCX protein levels. Under identical conditions (MOI 10 and 5 days post-infection) NCX content in Ad-RNAi treated neonatal cardiomyocytes decreased 94 ± 1 % respect to control. In Ad-AS-

NCX1.1, NCX content decreased 70 ± 1 % ($p < 0.05$, n = 3-8 *vs* Ad-RNAi) respect to control.

Figure 46 shows NCX activity measured in neonatal cardiomyocytes under the 3 different treatments: Ad-RNAi, Ad-AS-NCX1.1 and Ad-XIP. RNAi was the most effective method to decrease NCX activity. The introduction of antisense cDNA had an intermediate effect and XIP expression was the least effective of the three approaches (activity was 17 ± 1 %; 39 ± 9 % and 83 ± 3 % of the activity in control cells, respectively). Infection with Ad-QBI at an MOI of up to 50 did not affect NCX activity (102 ± 1 %).

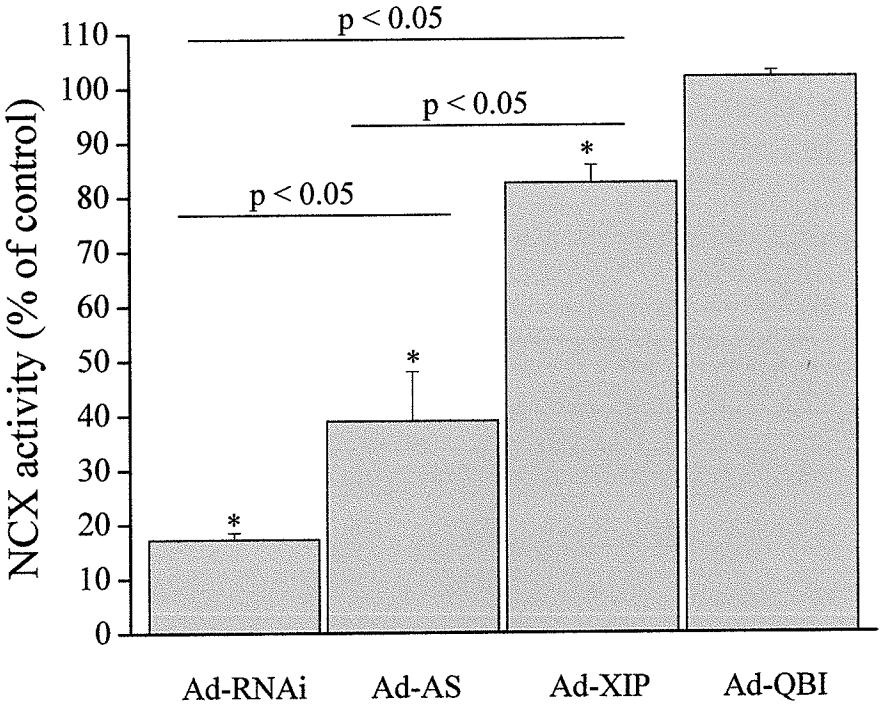

Figure 46. Efficiency of different methods of inhibiting NCX activity. NCX activity was measured as the Na^+ gradient induced $^{45}Ca^{2+}$ uptake in neonatal cardiomyocytes. Down-regulation of NCX's activity was induced by treatment of neonatal cardiomyocytes with: RNAi (Ad-RNAi at MOI 10); antisense cDNA (Ad-AS at MOI 10) or XIP (Ad-XIP at MOI 50). Ad-QBI (MOI 50) was used as the control for adenovirus infection. (N= 3-10). Values are mean ± SEM. * $p < 0.05$ *vs* non-infected neonatal cardiomyocytes.

DISCUSSION

PART I

The Na^+-H^+ exchanger has been proposed to participate in the ischemia-reperfusion injury by activating a cascade of events that leads to cellular dysfunction, damage and necrosis (Avkiran, 1999; Pierce and Czubryt, 1995; Steenbergen *et al*, 1990). Inhibition of the exchanger is expected to protect the cells and increase cell survival. Whether the Na^+-H^+ exchanger is active during reperfusion and whether its inhibition solely during reperfusion is beneficial remains controversial (Avkiram, 2003). Previous work indicates that the time it took DMA to cross the vascular wall to inhibit Na^+-H^+ exchange at the cardiomyocyte maybe a critical limitation to these experiments(Maddaford and Pierce, 1997). In this study we obviated the diffusion limitation by using a model of single cells.

One way to study the activity of the Na^+-H^+ antiporter is by measuring pH_i variation in the absence and presence of a blocker of this transporter. To eliminate the activity of the other alkalinizing mechanism present in the cells, the Na^+/HCO_3^- cotransporter, experiments were performed in HCO_3^- free solution. Although this represents a non-physiological experimental setting, it allows us to identify the contribution and activity of the Na^+-H^+ exchanger to intracellular pH regulation during ischemia and reperfusion. Our results demonstrate that the exchanger is highly active at the beginning of reperfusion. This would be expected when perfusion with a physiologic pH solution generates a large proton gradient between the inside and outside of the cell. When DMA was present in the ischemic perfusate, the pH_i during ischemia was

significantly lower than in the absence of the drug. This suggests that the exchanger is active during ischemia as well. The activity of the exchanger at this time, however, must be limited since the Na^+-H^+ exchanger is subject to inhibition by extracellular acidosis (Vaughan-Jones and Wu, 1990; Wallert and Frohlich, 1989). Previous studies had proposed that the exchanger was inactive during ischemia (Docherty *et al*, 1997; Murphy *et al*, 1991) but the ischemic period was of 20-30 minutes. In the present study, 60 minutes of ischemia were required before a difference in intracellular pH was detectable. It would appear that the Na^+-H^+ exchanger is only mildly active during ischemia, and thus becomes detectable only during ischemia of a relatively long duration, or perhaps, during severe ischemic insult. pH_i remained below pre-ischemic values at the end of reperfusion, even in the absence of DMA. The HCO_3^- dependent systems may be necessary for the complete recovery of pH_i after acidosis.

The changes in contractile activity of cells during ischemia were in apparent opposition to the $[Ca^{2+}]_i$ measured. Resting cell length (Figure 17) increased during ischemia (indicative of relaxation) despite an increase in diastolic $[Ca^{2+}]$ (Figure 21). This is likely due to the cellular acidosis (Figure 20). This was also true for active cell shortening. Intracellular pH decreased at the beginning of ischemia and active cell shortening was inhibited with a similar time course. In intact heart tissue, it has been shown that a reduction in force development occurs during acidosis without a decrease in the Ca^{2+} transients [208]. Similarly, in our study, Ca^{2+} transients could be recorded during ischemia, even though contractile activity was not detectable. The rapid fall in active cell shortening may be explained by a decrease in myofilament sensitivity to calcium under acidic pH (Fabiato and Fabiato, 1978; Solaro *et al*, 1989).

DMA administered at the beginning of reperfusion in the present study has a strong protective effect on the cardiomyocytes. There was an increase in cell survival and preservation of resting cell length (hypercontracture was prevented). The mechanism for cardioprotection may involve an improvement in Ca^{2+} homeostasis within the myocardial cell through normalized Ca^{2+} transients, and ultimately better contractile activity. Our data show that there is a significantly better recovery of Ca^{2+} transients, and this correlates with the better recovery of contractile activity. This post-ischemic improvement in recovery of the contractile activity after DMA treatment is consistent with tissue work (Hendrikx *et al*, 1994; Karmazyn, 1988; Maddaford and Pierce, 1997; Meng *et al*, 1991; Meng and Pierce, 1990; Tani and Neely, 1989).

Another possible cardioprotection mechanism may involve an inhibition by DMA of the rise in basal $[Ca^{2+}]$ during reperfusion. The results in Figure 21 are likely underestimations of the effects of ischemia and the effects of DMA. It is important to identify two factors that may have influenced the data. One limitation of our data is that up to 40% of the drug-untreated cells did not survive the insult (Figure 16). The Ca^{2+} data presented in Figures 21 and 22, therefore, were obtained from a select population of cells that did survive the ischemic challenge. Data were not collected from cells that did not survive because they usually detached from the coverslip. The severe increases in basal Ca^{2+} that one would expect after ischemia or during reperfusion (Meng *et al*, 1991) were not observed in the present study. This was likely because either the cells detached completely and moved off the screen, or they balled up so severely that the motion artifact made the signal unreliable. Only in the surviving, active cells was a reliable Ca^{2+} signal obtained. Thus, these data must be acknowledged as selective and any changes that

we detected were a significant underestimation of the actual disturbances that occurred. This also has implications for the differences that we observed in other parameters studied in the two experimental groups. Again, because the survival rates were significantly better in the post-ischemic DMA-treated group, the differences from the other experimental groups in contractile activity and $[Ca^{2+}]$ are likely greater than actually represented in this study. A second and potentially important limitation is that the cells were not contracting against a resistance (i.e. attached at one end to a micropipette). As identified elsewhere (Pierce *et al*, 1993), this stress may influence the recovery of contractile activity and may have dampened the extent of rise in $[Ca^{2+}]_i$ under pathological conditions.

Even though the Na^+-H^+ exchanger was shown to be active during ischemia, no significant cardioprotection, in regard to cell survival, was obtained by the inhibition of the exchanger at this time. However, this procedure did improve the contractile recovery of the myocytes at reperfusion and prevented further passive shortening of the cells. Thus, Na^+-H^+ exchange activity during ischemia contributes little to injury in the present conditions. In view of results obtained in tissue perfusion experiments, it was surprising that administration of DMA throughout ischemia and early reperfusion did not help cell survival. It is possible that exposing the cells to 20 μM DMA during the long ischemic perfusion (90 minutes) could have had a cytotoxic effect (Pierce *et al*, 1993). However, when isolated cardiomyocytes were perfused with a control non-ischemic solution containing 20 μM DMA for 93 minutes followed by 27 minutes of perfusion without DMA, cell survival was not different than cells perfused for the same time without the drug (data not shown). Thus, extended exposure of the cells to the DMA itself did not

damage the cells. Alternatively, it is possible that the lower intracellular pH present during ischemia may have exacerbated the damage caused by the ischemic insult, masking any beneficial effect that inhibition of the exchanger had against reperfusion injury. The use of a bicarbonate free buffer and DMA would inhibit the most important pH buffering systems within the cardiomyocyte (Fliegel and Frohlich, 1993) to induce a severe acidic challenge to the cell. Severe intracellular acidity has been shown to influence recovery of the cells (Maddaford *et al*, 1999).

The use of HCO_3^- free buffer may have enhanced the activity of the Na^+-H^+ exchange system, and therefore over-estimated its involvement in ischemia-reperfusion injury. However, Leem *et al* have shown that at pH_i lower than 6.9, the main H^+ extrusion mechanism is the Na^+-H^+ exchange system (Leem *et al*, 1999). Furthermore, results from clinical trials and experimental studies show that Na^+-H^+ exchange blockers, even in the presence of HCO_3^-, have strong cardioprotective effect (Bolli, 2003; Chaitman, 2003; Meng and Pierce, 1990; Mosca and Cingolani, 2000).

In summary, our results demonstrate that inhibition of the exchanger solely at the beginning of reperfusion has a strong cardioprotective effect. Our results, therefore, suggest that the exchanger is primarily active during reperfusion and this activity is an important contributory factor in cell injury. This work, then strengthens existing data using perfused tissue preparations (Maddaford and Pierce, 1997) or neonatal cardiomyocytes (Bond *et al*, 1993) and supports the use of Na^+-H^+ exchange inhibition as a potent therapeutic agent to prevent ischemia-reperfusion damage.

PART II

In view of the limited access to selective pharmacological inhibitors for the NCX, molecular biology techniques may provide us with alternative approaches to decrease the expression and activity of this important Ca^{2+} regulatory protein. The NCX global knock-out mouse proved to be lethal during development and ventricular-specific knock-out mice models ablated the NCX1 gene in only 80 - 90 % of the cells. Whereas these two models provided valuable data regarding the activity of the NCX (Henderson *et al*, 2004; Koushik *et al*, 2001; Reuter *et al*, 2003), unsolved questions regarding the exchanger's function still remain. A new genetic tool to target NCX will yield important data to help us define the role of the NCX in physiological conditions and in pathological challenges as well.

RNAi was developed in the last decade as a very powerful technique for gene silencing (Bass, 2001). It has several advantages compared to genetic knock-outs. The development of knock-out animals is a time consuming and expensive process and therefore, inaccessible to many research laboratories. Furthermore, gene knock-out is not feasible in all species. For example, it is very difficult to produce knock-out models in the rat because rat embryonic stem cells cannot be maintained in culture (the recombination step that removes the gene of interest is performed in embryonic stem cells that are then injected into the embryo at the blastula stage to generate a chimera). RNAi, in contrast to the animal knock-out models, is relatively inexpensive, and can be applied to any species. The only requirement to insure that the technique is successful is to know the precise cDNA sequence of the protein to be targeted. In addition, because it is easier to generate

a transgenic than a knock-out animal, RNAi can be used to generate transgenic animals with a silenced gene product (Kunath *et al*, 2003).

We decided to test this new technique to down-regulate the cardiac NCX. Cardiomyocytes are difficult to transfect. To achieve high efficiency of transfection and down-regulate the cardiac NCX, we combined the use of RNAi with the use of adenovirus transfection vectors. We designed and generated adenovirus vectors that code for short hairpins of RNA (Figures 12 and 13). The human U6 promoter drives the transcription of a short-hairpin RNA (29 base pairs long RNA duplex) that is subsequently processed within the cell into siRNA (19-22 base pairs long) that causes gene specific silencing (Paddison *et al*, 2002).

Using this approach, we found that NCX protein expression and activity can be markedly decreased. Our data clearly demonstrates that NCX plays an important, though not essential, role in cardiac excitation-contraction coupling. We found that the spontaneous beating rates were inhibited by ~61 % and twitch duration was markedly prolonged in Ad-NCX-RNAi treated neonatal cardiomyocytes. Similar changes were also observed in the Ca^{2+} transient where inhibiting NCX expression resulted in significantly slower rates of rise and decline of the Ca^{2+} transient. Presumably, the reduced rate of rise for the Ca^{2+} transient may reflect a contribution of reverse Na^{+}-Ca^{2+} exchange to this process. However, the substantial elevation in diastolic Ca^{2+} levels would also impair L-type Ca^{2+} channel function and SR Ca^{2+} triggering, which may serve a greater role in this phenotype (Keating and Sanguinetti, 2001). The reduced rates of relaxation are consistent with the anticipated consequences of depressed Na^{+}-Ca^{2+} exchange as a prominent Ca^{2+} efflux pathway. These characteristics for the Ca^{2+} transient in the Ad-

NCX-RNAi cells resemble those observed in de-tubulated cardiomyocytes where ~80 % of NCX is thought to be removed (Brette *et al*, 2004). De-tubulated cells exhibit a similarly depressed, elongated Ca^{2+} transient as that observed in this study. Moreover, the decrease in myosin expression in Ad-NCX-RNAi treated cells may also have contributed to an attenuated contractile activity, although this was obviously not sufficient to prevent contraction. Other investigators have found alterations in the contractile apparatus in embryonic preparations when the NCX was genetically deleted (Koushik *et al*, 2001).

The Ca^{2+} transient was primarily influenced by changes in diastolic rather than systolic $[Ca^{2+}]$ after disruption of NCX expression. The increased diastolic $[Ca^{2+}]$ likely explains the shortened APD_{50} exhibited by the Ad-NCX-RNAi cells. Increased diastolic $[Ca^{2+}]$ promotes Ca^{2+}-induced inactivation of L-type Ca^{2+} channels (Keating and Sanguinetti, 2001) with shortened APD and depressed Ca^{2+} transients as anticipated consequences. The APD would also be directly affected by NCX activity. With a 3 Na^{+}:1 Ca^{2+} transport ratio, Ca^{2+} extrusion through NCX results in an inward, depolarizing current over a wide range of membrane potentials, which would prolong the action potential duration (Litwin and Bridge, 1997). Therefore, decreasing NCX activity would be anticipated to reduce action potential duration directly, as we observed. Shortening of the APD with NCX depletion was not entirely unexpected. NCX overexpression in cardiomyocytes has resulted in a lengthening of the APD (Yao *et al*, 1998). Pharmacological inhibition of the NCX activity has resulted in a shortening of the APD (Armoundas *et al*, 2003; Spencer and Sham, 2003). Computer modelling programs have also predicted that NCX silencing will shorten the APD (Puglisi and Bers, 2001).

The mechanistic interpretation for the changes in the Ca^{2+} transient is complicated by the concomitant reduction in SERCA expression. However, it is more likely that the alterations observed were due to the decrease in NCX expression rather than the SERCA changes for two important reasons. First, although SERCA expression was inhibited, a large amount of protein (~50 %) still remained. In contrast, NCX expression was inhibited ~10x more than SERCA expression and very little protein remained. The remaining SERCA protein was fully functional, as estimated by the results obtained after caffeine, thapsigargin and ryanodine application. Secondly, we have used a neonatal cardiomyocyte in the present study. Even under control conditions, the SR is not fully developed and is a minor contributor to E-C coupling (Antman and Braunwald, 1997; Bassani and Bassani, 2002; Escobar *et al*, 2004; Wibo *et al*, 1991). When SR function was fully removed by the application of thapsigargin and ryanodine in the present study, this resulted in only a ~30 % decrease in the Ca^{2+} transient in control cells. This is consistent with data in the literature for neonatal cardiomyocytes and in contrast to the adult cardiomyocyte (Escobar *et al*, 2004; Wibo *et al*, 1991). We may argue that if a fully functional SR only contributes about 30 % to the Ca^{2+} transient, it is reasonable to expect that the remaining SERCA expression (50 %) may have depressed the transient by only ~15 %. We may conclude that although the decrease in SERCA expression undoubtedly contributed to the depression in the Ca^{2+} transient, the silencing of NCX expression was the primary factor responsible for the changes in the Ca^{2+} transient.

The data in the present study refutes the hypothesis that NCX is essential for cardiac contractile activity. Similar conclusions have recently appeared from a study examining ventricular specific conditional knock-out mice of NCX1.1 (Henderson *et al*,

2004). In our study, cells continued to beat spontaneously (albeit less frequently) and responded to electrical stimulation despite a severe depletion of NCX. This is rather surprising considering that trans-sarcolemmal Ca^{2+} movements are proposed to be even more important to excitation-contraction coupling in neonatal compared to adult myocardial cells (Artman, 1992; Bassani and Bassani, 2002; Escobar *et al*, 2004; Wibo *et al*, 1991). In our study, there appear to be two primary adaptive mechanisms in the neonatal cells that may have supported contraction despite NCX depletion. First, the only other important transsarcolemmal Ca^{2+} efflux pathway is the sarcolemmal Ca^{2+} pump. Significant and specific up-regulation of its expression argues persuasively for an adaptive role. Secondly, as discussed, the rise in diastolic $[Ca^{2+}]$ would inactivate the L-type Ca^{2+} channel (Keating and Sanguinetti, 2001) and induce less influx that would consequently require less Ca^{2+} efflux from the cell in order to maintain $[Ca^{2+}]_i$. These data challenge the prevailing opinion that Ca^{2+} movements through the sarcolemmal Ca^{2+} pump contribute very little to cytoplasmic $[Ca^{2+}]$ and cardiac function (Carafoli, 1985), at least under the conditions of our study. Here, it appears that this protein can transport relatively large amounts of Ca^{2+} and its activity can compensate when other important sarcolemmal Ca^{2+} transporters are absent from the cell. Our data suggest that under extreme conditions when NCX activity is severely depressed, the sarcolemmal Ca^{2+} pump can readily up-regulate its activity. It will be of interest in future investigations to focus upon this adaptive potential of the sarcolemmal pump when the NCX is depressed during pathological challenges.

The long half-life of the NCX requires that, to achieve significant protein silencing, cells have to be maintained in culture for at least 5 days. This is not a limitation

for neonatal cardiomyocytes models. However, it may make the use of RNAi targeting of NCX more difficult in adult cardiomyocytes. Some studies show that in the absence of serum and in the presence of supplements, adult ventricular myocytes can maintain their contractile phenotype (Volz *et al*, 1991). Culture of adult ventricular myocytes under electrical stimulation may also prevent changes in phenotype (Zhang *et al*, 2001).

It will be very valuable to analyze the use of RNAi targeting of NCX in adult ventricular myocytes with respect to E-C coupling. However, because the adult rat heart depends less on transsarcolemmal Ca^{2+} fluxes, we may expect to find milder effects on Ca^{2+} homeostasis in NCX depleted rat adult cardiomyocytes compared to the ones we observed in rat neonatal cardiomyocytes. The changes in Ca^{2+} handling with development may explain the different results obtained in our study and the study by Henderson *et al* (Henderson *et al*, 2004), where no changes in resting Ca^{2+} or amplitude of Ca^{2+} transient were observed. Conversely, if we were to deplete NCX in cardiomyocytes from species that depend more on NCX for cardiac relaxation (eg rabbit, human and guinea pig), we may observe more severe changes in Ca^{2+} handling.

In conclusion, our data demonstrate that RNAi can be used successfully to severely interfere with the expression of NCX in cardiomyocytes. The data support an important but not a critical role for NCX in excitation-contraction coupling in the heart. Cardiomyocytes maintain contractile function despite NCX depletion and RNA interference may be a valuable tool to analyze the function of other cardiac proteins.

PART III

The Ca^{2+} overload observed during ischemia-reperfusion or glycoside toxicity could be due to either a decrease in NCX-mediated Ca^{2+} efflux or an increase in NCX-mediated Ca^{2+} influx. To address this question we compared neonatal cardiomyocytes with normal levels of NCX expression with NCX overexpressing cells.

The observation that cells with higher expression levels of NCX1.1 showed a larger increase in Ca^{2+} compared to control cells would suggest that increased activity of the reverse mode might be involved. We would expect that Na^{+}_{i} increases in a similar way in both control and Ad-NCX1.1 cells. We observed no differences in Na^{+}, K^{+}-ATPase expression levels between the three groups (Figure 30). It is reasonable to assume that a decrease in the activity of a greater number of NCX molecules would not be able to cause a larger accumulation of $[Ca^{2+}]_{i}$. It is more likely that it would either cause no change in Ca^{2+} or a small decrease. However, a larger number of NCX molecules working in the reverse mode (to induce Ca^{2+} influx) could effectively cause a rise in Ca^{2+}_{i}. The involvement of the reverse mode (Ca^{2+} entry) was corroborated using KB-R7943 which inhibits this mode with higher affinity. We conclude that the reverse mode of NCX activity was involved in the increase in Ca^{+2}_{i} during ouabain treatment. A study by Satoh *et al*, showed that an increased activity of the reverse mode of NCX was involved in calcium overload in adult ventricular myocytes and that decreased activity of the forward mode was involved in a strophanthidin-induced ionotropic response.

Our results from NCX1.1 overexpressing cells also support the idea that reverse NCX activity contributes to Ca^{2+}_i overload during ischemia-reperfusion injury. Increasing the expression of NCX in cardiomyocytes resulted in greater Ca^{2+}_i overload. These data are consistent with the general hypothesis advanced over the last 15 years that intracellular H^+ accumulation during ischemia stimulates the Na^+-H^+ exchanger to remove intracellular H^+ in exchange for extracellular Na^+. The elevated $[Na^+]$ will stimulate NCX activity to promote Ca^{2+}_i overload (Tani and Neely, 1989). These data are consistent with results shown in cardiac NCX transgenic mice that were shown to be more susceptible to ischemia-reperfusion injury (Cross *et al*, 1995). In this study, after 30 minutes of ischemia, $[Ca^{2+}]_i$ in myocytes from transgenic mice was 1.5 fold higher than it was in cells from wild type mice. Drugs that selectively inhibit NCX have also produced a cardioprotective action during ischemic insult that is again consistent with the hypothesis that NCX activity is critical to ischemic-reperfusion injury to the heart (Yoshiyama *et al*, 2004).

The observation that increased NCX expression alters the response to ischemia-reperfusion is also important to understand the way that the NCX functions in pathological states like hypertrophy and heart failure. It has been suggested that NCX activity may participate in the pathology associated with cardiac hypertrophy (Kent *et al*, 1993) and heart failure (Flesch *et al*, 1996; Hobai and O'Rourke, 2000; Pogwizd *et al*, 1999; Studer *et al*, 1994). It is possible that the elevated NCX activity in these disease states may contribute to a disruption of intracellular Ca^{2+} homeostasis and altered contractile function. Targeting the NCX in the future with drug interventions or gene therapy may prove to be particularly rewarding.

In this study, we also compared the response to ouabain treatment and ischemia reperfusion of cells expressing high levels of two isoforms product of the NCX1 gene. The NCX1.1 and NCX1.3 proteins are identical except for the variable region located in the large intracellular loop (Figure 1 and 2). This region is composed, in NCX1.1 of 76 amino acids corresponding to exons ACDEF and, in NCX1.3 of 40 amino acids corresponding to exons BD. We found that both isoforms can be effectively expressed in neonatal cardiomyocytes and that equal quantities of both isoforms are targeted to the membrane. It is unlikely, therefore, that this variable region of the protein has any effect on signaling the amount of protein that is expressed at the sarcolemma, as is the case for the isoform 3 of the Na^+-H^+ exchanger (D'Souza *et al*, 1998; Kurashima *et al*, 1998).

Previous studies have demonstrated that the NCX 1.1 and NCX 1.3 isoforms have pronounced differences in their ionic regulation characteristics (Dyck *et al*, 1999; Hryshko, 2002). Using the giant patch clamp technique in membranes from Xenopus oocytes expressing the NCX1 isoforms, it was shown that the NCX1.3 is under extensive I_1 inactivation, and that increases in Na^+_i and/or Ca^{2+}_i are not able to cause a significant increase in steady state current. The NCX1.1 and the NCX1.4 behave in a different way. They show I_1, however, even if the degree of I_1 increases with increasing $Na^+_{i,}$, the steady state current is able to increase and, elevations in $[Ca^{2+}]_i$ can alleviate I_1. Figure 6 compares the regulatory properties of NCX1.4 (which responds in a similar way in these sort of experiments to NCX1.1) and NCX1.3, this figure was obtained from Dyck *et al.* (Dyck *et al*, 1999).

Since NCX outward current corresponds to the Ca^{2+} entry mode, we hypothesized that NCX1.1 would allow more Ca^{2+} to enter the cell than the NCX1.3 isoform,

particularly under situations where we might expect $[Na^+]_i$, and $[Ca^{2+}]_i$ to be elevated, as occurs during ischemia or complete inhibition of the Na^+ pump by ouabain. As $[Na^+]_i$, and $[Ca^{2+}]_i$ increase, I_1 would decrease in the 1.1 form, and more Ca^{2+} would enter the cell. This would also further alleviate I_1 to cause more Ca^{2+} entry, resulting in a positive feed-back. On the contrary, the 1.3 isoform would remain strongly inactivated under these same conditions. The activity of these isoforms was previously studied using electrophysiological methods on excised patches and never in intact cardiomyocytes (Dyck *et al*, 1999; Ruknudin *et al*, 2000). Our data, therefore, should provide additional information that may be more physiologically relevant. Our results agree with our hypothesis and demonstrated that ouabain treatment and ischemia can cause a larger increase in $Ca^{2+}{}_i$ in cells overexpressing the NCX1.1 isoform compared to the 1.3 isoform. Therefore, these data would support the hypothesis that the 1.1 isoform allows more Ca^{2+} to enter the cells. The different response to ionic regulation appears to play important roles in the sensitivity of the cell to both types of insult. Furthermore, our results, agree with the idea that ionic regulation occurs within physiological levels of $[Ca^{2+}]_i$. Together with results from Maxwell *et al* (Maxwell *et al*, 1999) and Weber *et al* (Weber *et al*, 2001), support the Ca^{2+} affinity of the regulatory site to be in the micromolar range (Levitsky *et al*, 1994) instead of the nanomolar range (Fang *et al*, 1998).

Little is known regarding the physiological role of the different isoforms. Tissues with different Ca^{2+} requirements express different NCX1 isoforms. Furthermore, excitable tissues contain exon A, whereas non excitable tissues contain exon B isoforms, suggesting that there may be a physiological significance for these differences. It is

possible to speculate that the cardiac isoform (NCX1.1) is activated by increases in Ca^{2+}_i and this permits the cell to adapt to situations where more Ca^{2+} enters the cell (eg. under adrenergic stimulation). It may also prevent excessive removal of Ca^{2+} from the cell, since the exchanger would inactivate at very low $[Ca^{2+}]_i$. However, our results show that even if the regulatory properties evolved to allow the cell to cope with different Ca^{2+} demands, the same regulatory properties may be detrimental in extreme conditions of elevated $[Na^+]_i$, and $[Ca^{2+}]_i$.

The observation that NCX1.3 activity does not cause as severe Ca^{2+} overload as the NCX1.1 form, can be attributed to its increased sensitivity to I_1 inactivation. The most potent NCX inhibitor available today, SEA0400, functions by stabilizing the I_1 state of the exchanger (Bouchard *et al*, 2004; Lee *et al*, 2004). This drug was shown to protect the heart against ischemia-reperfusion injury (Yoshiyama *et al*, 2004). Therefore, we may possibly compare the NCX1.3 protein with a NCX1.1 exchanger after SEA treatment. Our findings that the NCX1.3 leads to less severe Ca^{2+} overload support this idea. It would be interesting to know if the Ca^{2+} efflux role of the NCX 1.3 protein during ischemia remains active as in NCX1.1 after treatment with SEA (to be able to promote Ca^{2+} efflux).

It is important to identify the limitations of this work. One limitation of our study was that the method we had available in our laboratory to measure NCX activity, measures the reverse mode, which is under the regulatory effect we describe in the study (we are measuring inactivated 1.3 Ca^{2+} uptake). It would be interesting to record the activity of both isoforms using electrophysiological techniques. Measurements of outward current in patches from these cells before and following chymotrypsin treatment

(to remove regulation) would corroborate that the differences we observe in our experiments are due to the regulatory properties of the protein. Measurements of inward current would be valuable as well, since this mode is less affected by I_1. Another limitation of the study is that the NCX1.3 isoform was expressed on a background of endogenous NCX1.1 exchanger. Transgenic mice expressing a deletion mutant lacking ionic regulation showed that the transgene phenotype predominated in the cell (Maxwell *et al*, 1999). It is possible, therefore, that our transduced isoform may have predominated as well. However, patch clamp studies would be necessary to quantitate the contribution of the 1.3 transgene.

Another limitation of the study is that we did not measure $[Na^+]_i$. This would provide very valuable data and will have to be done in the future. Results from other studies showed that Na^+ influx in rat cardiomyocyts (under Na^+ pump inhibition) causes an increase of 1.7 mM/minute at rest and 2.2 mM/minute when the cells are stimulated at 1 Hz (Despa *et al*, 2002). In Langendorff-perfused rat hearts, nuclear magnetic resonance measurements showed that during ischemia $[Na^+]_i$ rises to approximately 28 mM and $[Ca^{2+}]_i$ to approximately 3 μM.(Murphy *et al*, 1991).

PART IV

Our previous experiments examined the effects of expressing the NCX1.3 isoform over the existing endogenous NCX1.1 isoform in neonatal cardiomyocytes. In the next series of experiments, the response to ischemia of cells expressing pure populations of

NCX1.1 or NCX1.3 isoforms of the exchanger was compared. For this purpose, we expressed both isoforms in HEK-293 cells that do not express endogenous NCX. It was also important to determine if the results obtained with neonatal cardiomyocytes were cell specific, or if NCX expression could lead to Ca^{2+} overload even in cells without the high metabolic requirements of cardiomyocytes. We were also able to study untransfected HEK-293 cells to determine exactly how much of the effect observed was due to NCX.

In this study, we observed that simulated ischemia caused an increase in $Ca^{2+}{}_i$ in control cells. Because HEK-293 cells do not express endogenous NCX, Ca^{2+} must have entered the cytoplasm through other pathways. HEK cells express endogenous Ca^{2+} channels. Trp Ca^{2+} channels are store-operated Ca^{2+} channels found in HEK-293 cells (Wu *et al*, 2000). It is not clear from our data if Ca^{2+} channels were involved in the entry of Ca^{2+} from the extracellular space in control HEK-293 cells.

The elevation in intracellular Ca^{2+} may also have originated from impaired Ca^{2+} extrusion through the plasmalemmal membrane. The plasmalemmal calcium pump may not have been sufficiently active to remove enough Ca^{2+} from the cell during the ischemic insult. The decreased metabolic state of the cells may have limited Ca^{2+} removal via this pathway because PMCA activity is ATP dependent.

Intracellular storage sources may also have been responsible for the increase in $Ca^{2+}{}_i$. These intracellular storage sites include the ER or mitochondria. In non-excitable cells, Ca^{2+} signaling through the ER is initiated through PLC mechanisms. Receptor/PLC coupled production of IP_3 can induce Ca^{2+} release from the ER that will increase intracellular $[Ca^{2+}]$. In addition, emptying of the ER also activates the entry of Ca^{2+} from

the extracellular space via capacitative Ca^{2+} entry through store operated Ca^{2+} channels located at the plasma membrane (Putney, 1986). PLA_2 production is also increased in ischemia [234]. Activation of PLA2 can cause the release of arachidonic acid that in turn can activate the PLC-IP3 pathway and ER Ca^{2+} strores. Ca^{2+} may also be released from mithochondria through the opening of the mithochondrial transition pore during ischemia (Bernardi, 1999). It would be interesting in the future to identify the sources for the increase in Ca^{2+}_i during ischemia in the control HEK-293 cells but at this point in time, we do not have the data to address this issue.

The increase in Ca^{2+}_i during ischemia was more than 2 fold larger in cells expressing NCX1.1 compared to control cells. This difference can be directly attributed to the expression of the NCX1.1 transporter. The increase in Ca^{2+}_i in NCX1.3 expressing cells was slightly larger compared to control but it did not reach statistical significance. This result supports our hypothesis that the NCX1.3 isoform allows less Ca^{2+} to enter the cell than the NCX1.1 isoform. The results are also very similar to the ischemia results obtained in neonatal cardiomyocytes suggesting that the background expression of NCX1.1 in the neonatal cardiomyocytes did not influence the results significantly.

NCX1.3 cells showed a large peak of Ca^{2+}_i at reperfusion. We would have expected NCX1.1 expressing cells to show a similar or more pronounced peak at reperfusion, however a smaller peak was observed. It is possible that the peak was not due to reverse NCX activity but to Ca^{2+} release from an intracellular store. NCX1.1 at reperfusion may rapidly reverse its direction of transport and contribute to Ca^{2+}_i removal, therefore, decreasing the peak. Ca^{2+}_i remained elevated after one hour of reperfusion. This was surprising, because we would have expected that the exchanger would facilitate

Ca^{2+} removal from the cells. It seems that one hour is not enough for the NCX and the PMCA to remove the Ca^{2+} that entered the cytoplasm during ischemia.

We conclude that during ischemia the NCX causes a rise in Ca^{2+} in HEK-293 cells. Therefore, the effect of NCX expression on the sensitivity of the cell to ischemic insult is independent of the cell type in which the NCX is expressed. We also demonstrated that the NCX1.1 isoform allows more Ca^{2+} to enter the cell compared to the NCX1.3 isoform. This too was consistent with the neonatal cardiomyocytes data.

PART V

To be able to study pure populations of the alternative isoforms of the exchanger within cardiac cells, it is necessary to first remove the endogenous NCX1.1 protein from the cells. This can be done using RNAi as it was shown in Part II of this thesis. In this section of the study we show that, if appropriate target sequences are chosen, the endogenous protein can be removed and the transgene protein can be expressed.

RNAi is thought to be a very specific mechanism for gene silencing. It has been used to target mutants of proteins that contain a single point mutation compared to the wild type (Ding *et al*, 2003). However, when we chose a sequence that contained 7 mismatches between the endogenous and the transgene nucleotide sequence, the RNAi interfered with the expression of the transgene. Alternatively, because the NCX1.3 sequence does not contain some of the exons present in the NCX1.1 sequence, we could direct the RNAi against these sequences instead. In this case, we could efficiently replace

the isoforms. Therefore, at least for these specific sequences, RNAi was unable to distinguish between sequences with 22 out of 29 homologous nucleotides but it could successfully function when all of the nucleotides were different. As a result of this limitation, we were not able to re-introduce the cardiac NCX1.1 into the cells. This would have been the ideal control for our experiments.

Because the antibody used in our study recognizes both the cardiac and the renal isoform, it was difficult to differentiate between the endogenous protein and the transgene. This problem was partially addressed by tagging the transgene with EGFP. This now allowed us to identify the new protein that was introduced in the cells by the transgene. However, the problem remained that we could not determine the amount of endogenous protein remaining in the cells in the transfected samples (because the antibody would still recognize the endogenous protein and also that expressed by the transgene). Recently, Thomas *et al.* developed a new antibody to an epitope of the exchanger that is present in exon F of the NCX1.1 (Thomas *et al*, 2003). This antibody could be used in the future to verify the complete replacement of the isoforms. The new antibody could be used to detect NCX1.1 and anti-EGFP to detect the tagged NCX1.3.

A large number of mutants and chimeras of the exchanger have been generated and expressed in *Xenopus* oocytes or in cell lines (Bouchard *et al*, 2004; Pan *et al*, 2000; Shuba *et al*, 1998). The approach we described here will be very useful to study those mutants in cardiac cells. Factors that modulate the activity of the exchanger and that are cell type specific could be then recognized. In case the transgene (eg the mutant) is very similar in sequence to the endogenous protein, one approach that could be used would be to target the RNAi to a 29 nucleotide long sequence known to be unimportant for NCX

activity (deletion of this sequence should not affect exchange activity). The mutant and a wild type protein should then be generated where the RNAi targeting sequence is missing. The wild type missing the 29 nucleotide sequence could be used as the control. An epitope (eg, HIS tag) could be added to the mutant and the control to be able to follow transgene expression with antibodies.

In conclusion, using adenovirally delivered RNAi and transgene expression we were able to replace the endogenous cardiac isoform by the renal isoform. At the function level, this was corroborated by the observation that the transgene could revert the changes in $[Ca^{2+}]_i$ caused by NCX depletion. The protocol here described will allow the study of pure populations of different NCX1 isoforms or NCX mutants using cardiac cell models.

PART VI

In addition to adenovirally delivered RNAi (discussed in Part II), we developed another novel method to block the activity of the exchanger. We designed adenovirus vectors to transduce the eXchanger Inhibitory Peptide (XIP) with high efficiency into cardiomyocytes. The XIP inhibits the exchanger only if it is applied from the cytoplasmic side of the sarcolemmal membrane. This has limited the use of XIP in cellular experiments because it is difficult to introduce the peptide into a living cell. Only through dialysis or injection could XIP be introduced into the cells. XIP has been used frequently in electrophysiological experiments with excised patches or in isolated membrane preparations to inhibit NCX activity (Kuruma *et al*, 1998; Ottolia *et al*, 2001).

Our results demonstrate that the introduction of XIP into the neonatal cardiomyocytes did not result in a large inhibition of NCX activity. The other methods were far more potent. The RNAi method was the most successful. This may not be too surprising. The approach to design an adenovirus vectors to transduce XIP into cardiomyocytes to inhibit NCX activity was not an easy proposal. To date, few reports exist in the literature about constructs coding for short peptides (Querfurth *et al*, 2001). In addition, even if the approach was effective and the peptide was synthesized within the cells and it blocked NCX activity, the efficiency for blocking NCX function was likely to be significantly lower compared to the other approaches tested. The most effective method to inhibit NCX activity was Ad-RNAi.

The antisense approach was used to inhibit NCX expression as well. Antisense NCX1.1 cDNA was less effective in silencing the NCX than RNAi. Antisense NCX1.1 cDNA was previously used to downregulate NCX expression in adult ventricular myocytes (Tadros *et al*, 2002). After 6 days, NCX expression was 66 % of control. This result was similar to the values obtained in our study with neonatal cardiomyocytes (70 % decrease after 5 days). These results were not as potent as those obtained with Ad-RNAi (94 % inhibition). We did not analyze the specificity of the antisense approach. However, it is possible that the transgene mRNA could form a duplex of RNA through base pairing with the endogenous NCX mRNA. It is known that RNA duplexes longer than 30 nucleotides can activate non-specific pathways that lead to the inhibition of all protein synthesis and apoptosis (Minks *et al*, 1979; Paddison and Hannon, 2003). In preliminary studies in our laboratory, we tested the feasibility of antisense cDNA to downregulate NCX expression. Our construct was made using dog cDNA (rat cDNA was

not available for us at this point in time). Therefore, to test the ability of the antisense sequence to knock-down protein synthesis (in rat cells), we co-transfected neonatal rat ventricular cardiomyocytes with Ad-NCX1.1 (sense from dog) and Ad-AS-NCX1.1 (antisense from dog), with the idea that the transfected antisense would prevent the expression of the transfected sense protein. It was anticipated that we would be able to detect this effect by WB. We observed that either adenovirus could be used on their own to infect myocytes. The antisense had no effect on the endogenous NCX expression. And the Ad-NCX1.1 caused over-expression of NCX1.1. However, when as low as MOI of 1 of each virus were combined, all of the cells died within 24 hours. This was a clear indication of a toxic effect. In this case, both sense and antisense messages were transcribed from a strong promoter (CMV). It is possible that when the sense is the endogenous sequence, a low number of sense mRNAs are available for base pairing with the antisense and, therefore, the non-specific effects are not as severe. This aspect should be analyzed before antisense cDNA is used for experiments.

In conclusion, adenovirally delivered RNAi seems to be the most effective and efficient method available today to knock-down sodium-calcium exchange. Antisense oligonucleotides and naked siRNA are difficult to transfect into cardiomyocytes (discussed in the introduction). Antisense cDNA might also have non-specific effects. Inducing XIP expression in the cell did not achieve much inhibition of the NCX. In addition, XIP has an additional limitation: it may interfere with calmodulin signaling pathways and block PMCA expression (Enyedi and Penniston, 1993). Adenovirally delivered RNAi appears to be the method of choice to effectively silence NCX expression and function in neonatal cardiomyocytes today.

BIBLIOGRAPHY

1991. The Sicilian gambit. A new approach to the classification of antiarrhythmic drugs based on their actions on arrhythmogenic mechanisms. Task Force of the Working Group on Arrhythmias of the European Society of Cardiology. *Circulation* 84 (4):1831-1851.

Adachi-Akahane S, Lu L, Li Z, Frank JS, Philipson KD, Morad M. 1997. Calcium signaling in transgenic mice overexpressing cardiac Na^+-Ca^{2+} exchanger. *J Gen Physiol* 109 (6):717-729.

Agata N, Tanaka H, Shigenobu K. 1993. Possible action of cyclopiazonic acid on myocardial sarcoplasmic reticulum: inotropic effects on neonatal and adult rat heart. *Br J Pharmacol* 108 (3):571-572.

Amran MS, Homma N, Hashimoto K. 2004. Effects of sodium-calcium exchange inhibitors, KB-R7943 and SEA0400, on aconitine-induced arrhythmias in guinea pigs in vivo, in vitro and computer simulation studies. *J Pharmacol Exp Ther.*

Antman EM, Braunwald E. 1997. Acute myocardial infarction. In: Braunwald E, editor. Heart disease. 5 ed: W B Saunders. p 1184-1288.

Armoundas AA, Hobai IA, Tomaselli GF, Winslow RL, O'Rourke B. 2003. Role of sodium-calcium exchanger in modulating the action potential of ventricular myocytes from normal and failing hearts. *Circ Res* 93 (1):46-53.

Artman M. 1992. Sarcolemmal Na^+-Ca^{2+} exchange activity and exchanger immunoreactivity in developing rabbit hearts. *Am J Physiol* 263 (5 Pt 2):H1506-1513.

Avkiram M. 2003. Basic Biology and Pharmacology of the Cardiac Sarcolemmal Sodium/Hydrogen Exchanger. *J Card Surg* 18:3-12.

Avkiran M. 1999. Rational basis for use of sodium-hydrogen exchange inhibitors in myocardial ischemia. *Am J Cardiol* 83:10G-18G.

Barnes KV, Cheng G, Dawson MM, Menick DR. 1997. Cloning of cardiac, kidney, and brain promoters of the feline ncx1 gene. *J Biol Chem* 272 (17):11510-11517.

Barry WH, Bridge JH. 1993. Intracellular calcium homeostasis in cardiac myocytes. *Circulation* 87 (6):1806-1815.

Bass B. 2001. The short answer. *Nature* 411:428-429.

Bassani RA, Bassani JW. 2002. Contribution of Ca^{2+} transporters to relaxation in intact ventricular myocytes from developing rats. *Am J Physiol Heart Circ Physiol* 282 (6):H2406-2413.

Bernardi P. 1999. Mitochondrial Transport of Cations: Channels, Exchangers, and Permeability Transition. *Physiol Rev* 79 (4):1127-1155.

Berne R, Levy M. 1998. Physiology. Fourth ed: Mosby. 1131 p.

Bers DM. 1991. Species differences and the role of sodium-calcium exchange in cardiac muscle relaxation. *Ann N Y Acad Sci* 639:375-385.

Bers DM. 2000. Calcium fluxes involved in control of cardiac myocyte contraction. *Circ Res* 87 (4):275-281.

Bers DM. 2001. Excitation-Contraction Coupling and Cardiac Contractile Force. Second ed: Kluwer Academic Publishers.

Bers DM. 2002. Cardiac Na/Ca Exchange Function in Rabbit, Mouse and Man: What's the Difference? *J Mol Cell Cardiol* 34:369-373.

Bers DM, Barry WH, Despa S. 2003. Intracellular Na^+ regulation in cardiac myocytes. *Cardiovasc Res* 57 (4):897-912.

Bers DM, Christensen DM, Nguyen TX. 1988. Can Ca entry via Na-Ca exchange directly activate cardiac muscle contraction? *J Mol Cell Cardiol* 20 (5):405-414.

Blaustein MP, Lederer WJ. 1999. Sodium/calcium exchange: its physiological implications. *Physiol Rev* 79 (3):763-854.

Boerth SR, Zimmer DB, Artman M. 1994. Steady-state mRNA levels of the sarcolemmal Na^+-Ca^{2+} exchanger peak near birth in developing rabbit and rat hearts. *Circ Res* 74 (2):354-359.

Bolli R. 2003. The role of sodium-hydrogen ion exchange in patients undergoing coronary artery bypass grafting. *J Card Surg* 18 Suppl 1:21-26.

Bond JM, Chacon E, Herman B, Lemasters JJ. 1993. Intracellular pH and Ca^{2+} homeostasis in the pH paradox of reperfusion injury to neonatal rat cardiac myocytes. *Am J Physiol* 265 (Cell Physiol. 34):C129-C137.

Bouchard R, Clark R, Giles W. 1993. Role of sodium-calcium exchange in activation of contraction in rat ventricle. *J Physiol* 472:391-413.

Bouchard R, Omelchenko A, Le HD, Choptiany P, Matsuda T, Baba A, Takahashi K, Nicoll DA, Philipson KD, Hnatowich M, Hryshko LV. 2004. Effects of SEA0400 on mutant NCX1.1 Na^+-Ca^{2+} exchangers with altered ionic regulation. *Mol Pharmacol* 65 (3):802-810.

Bourdeau JE, Taylor AN, Iacopino AM. 1993. Immunocytochemical localization of sodium-calcium exchanger in canine nephron. *J Am Soc Nephrol* 4 (1):105-110.

Braunwald E, Kloner RA. 1985. Myocardial reperfusion: a double-edged sword? *J Clin Invest* 11:1713-1719.

Brette F, Rodriguez P, Komukai K, Colyer J, Orchard CH. 2004. beta-adrenergic stimulation restores the Ca transient of ventricular myocytes lacking t-tubules. *J Mol Cell Cardiol* 36 (2):265-275.

Bridge JH, Spitzer KW, Ershler PR. 1988. Relaxation of isolated ventricular cardiomyocytes by a voltage-dependent process. *Science* 241 (4867):823-825.

Carafoli E. 1985. The homeostasis of calcium in heart cells. *J Mol Cell Cardiol* 17 (3):203-212.

Chaitman BR. 2003. A review of the GUARDIAN trial results: clinical implications and the significance of elevated perioperative CK-MB on 6-month survival. *J Card Surg* 18 Suppl 1:13-20.

Cho CH, Kim SS, Jeong MJ, Lee CO, Shin HS. 2000. The Na^+ -Ca^{2+} exchanger is essential for embryonic heart development in mice. *Mol Cells* 10 (6):712-722.

Cho CH, Lee SY, Shin HS, Philipson KD, Lee CO. 2003. Partial rescue of the Na^+-Ca^{2+} exchanger (NCX1) knock-out mouse by transgenic expression of NCX1. *Exp Mol Med* 35 (2):125-135.

Cohen N, Lederer W. 1988. Changes in the calcium current of rat heart ventricular myocytes during development. *J Physiol* 406:115-146.

Crespo LM, Grantham CJ, Cannell MB. 1990. Kinetics, stoichiometry and role of the Na-Ca exchange mechanism in isolated cardiac myocytes. *Nature* 345 (6276):618-621.

Cross HR, Clarke K, Opie LH, Radda GK. 1995. Is lactate-induced myocardial ischaemic injury mediated by decreased pH or increased intracellular lactate? *J Mol Cell Cardiol* 27 (7):1369-1381.

Cross HR, Lu L, Steenbergen C, Philipson KD, Murphy E. 1998. Overexpression of the cardiac Na^+/Ca^{2+} exchanger increases susceptibility to ischemia/reperfusion injury in male, but not female, transgenic mice. *Circ Res* 83 (12):1215-1223.

Denli A, Hannon G. 2003. RNAi: an ever-growing puzzle. *Trends Bioch Sci* 28 (4):196-201.

Despa S, Islam MA, Pogwizd SM, Bers DM. 2002. Intracellular $[Na^+]$ and Na^+ pump rate in rat and rabbit ventricular myocytes. *J Physiol* 539 (Pt 1):133-143.

Diaz Horta O, Herchuelz A, Van Eylen F. 2002. Na/Ca Exchanger Overexpression Induces Endoplasmic Reticulum-Related Apoptosis and Caspase-12 Release. *Ann N Y Acad Sci* 976:487.

Ding H, Schwarz DS, Keene A, Affar el B, Fenton L, Xia X, Shi Y, Zamore PD, Xu Z. 2003. Selective silencing by RNAi of a dominant allele that causes amyotrophic lateral sclerosis. *Aging Cell* 2 (4):209-217.

Doble BW, Chen Y, Bosc DG, Litchfield DW, Kardami E. 1996. Fibroblast growth factor-2 decreases metabolic coupling and stimulates phosphorylation as well as masking of connexin43 epitopes in cardiac myocytes. *Circ Res* 79 (4):647-658.

Docherty JC, Yang L, Pierce GN, Deslauriers R. 1997. Na^+-H^+ exchange inhibition at reperfusion is cardioprotective during myocardial ischemia-reperfusion; 31P NMR studies. *Mol Cell Biochem* 176 (1-2):257-264.

Doering AE, Nicoll DA, Lu Y, Lu L, Weiss JN, Philipson KD. 1998. Topology of a functionally important region of the cardiac Na^+/Ca^{2+} exchanger. *J Biol Chem* 273 (2):778-783.

D'Souza S, Garcia-Cabado A, Yu F, Teter K, Lukacs G, Skorecki K, Moore HP, Orlowski J, Grinstein S. 1998. The epithelial sodium-hydrogen antiporter Na^+/H^+ exchanger 3 accumulates and is functional in recycling endosomes. *J Biol Chem* 273 (4):2035-2043.

Dunn J, Elias CL, Le HD, Omelchenko A, Hryshko LV, Lytton J. 2002. The molecular determinants of ionic regulatory differences between brain and kidney Na^+/Ca^{2+} exchanger (NCX1) isoforms. *J Biol Chem* 277 (37):33957-33962.

Durkin JT, Ahrens DC, Pan YC, Reeves JP. 1991. Purification and amino-terminal sequence of the bovine cardiac sodium-calcium exchanger: evidence for the presence of a signal sequence. *Arch Biochem Biophys* 290 (2):369-375.

duToit E, Poie L. 1993. Role for the Na^+/H^+ exchanger in reperfusion stunning in the isolated perfused rat heart. *J Cardiovasc Pharmacol* 22 (6):877-883.

Dyck C, Omelchenko A, Elias CL, Quednau BD, Philipson KD, Hnatowich M, Hryshko LV. 1999. Ionic regulatory properties of brain and kidney splice variants of the NCX1 Na^+-Ca^{2+} exchanger. *J Gen Physiol* 114 (5):701-711.

Egger M, Ruknudin A, Niggli E, Lederer WJ, Schulze DH. 1999. Ni^{2+} transport by the human Na^+/Ca^{2+} exchanger expressed in Sf9 cells. *Am J Physiol* 276 (5 Pt 1):C1184-1192.

Ehara T, Matsuoka S, Noma A. 1989. Measurement of reversal potential of Na^+-Ca^{2+} exchange current in single guinea-pig ventricular cells. *J Physiol* 410:227-249.

Eigel BN, Hadley RW. 2001. Antisense inhibition of Na^+/Ca^{2+} exchange during anoxia/reoxygenation in ventricular myocytes. *Am J Physiol Heart Circ Physiol* 281 (5):H2184-2190.

Elbashir SM, Harborth J, Lendeckel W, Yalcin A, Weber K, Tuschl T. 2001. Duplexes of 21-nucleotide RNAs mediate RNA interference in cultured mammalian cells. *Nature* 411 (6836):494-498.

Elias CL, Lukas A, Shurraw S, Scott J, Omelchenko A, Gross GJ, Hnatowich M, Hryshko LV. 2001. Inhibition of Na^+/Ca^{2+} exchange by KB-R7943: transport mode selectivity and antiarrhythmic consequences. *Am J Physiol Heart Circ Physiol* 281 (3):H1334-1345.

Eng S, Maddaford TG, Kardami E, Pierce GN. 1998. Protection against myocardial ischemic/reperfusion injury by inhibitors of two separate pathways of Na^+ entry. *J Mol Cell Cardiol* 30:829-835.

Enyedi A, Penniston JT. 1993. Autoinhibitory domains of various Ca^{2+} transporters cross-react. *J Biol Chem* 268 (23):17120-17125.

Er F, Larbig R, Ludwig A, Biel M, Hofmann F, Beuckelmann DJ, Hoppe UC. 2003. Dominant-negative suppression of HCN channels markedly reduces the native pacemaker current I_f and undermines spontaneous beating of neonatal cardiomyocytes. *Circulation* 107 (3):485-489.

Escobar A, Ribeiro-Costa R, Villalba-Galea C, Zoghbi M, Perez C, Mejia-Alvarez R. 2004. Developmental changes of intracellular Ca^{2+} transients in beating rat hearts. *Am J Physiol* 286 (3):H971-H978.

Fabiato A. 1982. Calcium release in skinned cardiac cells: variations with species, tissues, and development. *Fed Proc* 41 (7):2238-2244.

Fabiato A. 1985. Time and calcium dependence of activation and inactivation of calcium-induced release of calcium from the sarcoplasmic reticulum of a skinned canine cardiac Purkinje cell. *J Gen Physiol* 85 (2):247-289.

Fabiato A, Fabiato F. 1978. Effects of the pH on the myofilaments and the sarcoplasmic reticulum of skinned cells from cardiac and skeletal muscle. *J Physiol (Lond)* 276:233-255.

Fang Y, Condrescu M, Reeves JP. 1998. Regulation of Na^+/Ca^{2+} exchange activity by cytosolic Ca^{2+} in transfected Chinese hamster ovary cells. *Am J Physiol* 275 (1 Pt 1):C50-55.

Fire A, Albertson D, Harrison S, Moerman D. 1991. Production of antisense RNA leads to effective and specific inhibition of gene expression in *C. elegans* muscle. *Development* 113:503-514.

Fire A, Xu S, Montgomery MK, Kostas SA, Driver SE, Mello CC. 1998. Potent and specific genetic interference by double-stranded RNA in Caenorhabditis elegans. *Nature* 391 (6669):806-811.

Fiset P, Soussi Gounni A. 2001. Antisense oligonucleotides: problems with use and solutions. *Rev Biol Biotech* 1 (2):27-33.

Flesch M, Schwinger RH, Schiffer F, Frank K, Sudkamp M, Kuhn-Regnier F, Arnold G, Bohm M. 1996. Evidence for functional relevance of an enhanced expression of the Na^+-Ca^{2+} exchanger in failing human myocardium. *Circulation* 94 (5):992-1002.

Fliegel L, Frohlich O. 1993. The Na^+/H^+ exchanger: an update on structure, regulation and cardiac physiology. *Biochem J* 296:273-285.

Forman MB, Virmani R, Puett DW. 1990. Mechanisms and therapy of myocardial reperfusion injury. *Circulation* 81 (suppl IV):IV69-IV78.

Frank JS, Mottino G, Reid D, Molday RS, Philipson KD. 1992. Distribution of the Na^+-Ca^{2+} exchange protein in mammalian cardiac myocytes: an immunofluorescence and immunocolloidal gold-labeling study. *J Cell Biol* 117 (2):337-345.

Fujioka Y, Hiroe K, Matsuoka S. 2000a. Regulation kinetics of Na^+-Ca^{2+} exchange current in guinea-pig ventricular myocytes. *J Physiol* 529 Pt 3:611-623.

Fujioka Y, Komeda M, Matsuoka S. 2000b. Stoichiometry of Na^+-Ca^{2+} exchange in inside-out patches excised from guinea-pig ventricular myocytes. *J Physiol* 523 Pt 2:339-351.

Goll D, Thomson V, Li H, Wei W, Cong J. 2003. The Calpain System. *Physiol Rev* 83:731-801.

Gomez AM, Schwaller B, Porzig H, Vassort G, Niggli E, Egger M. 2002. Increased exchange current but normal Ca^{2+} transport via Na^+-Ca^{2+} exchange during cardiac hypertrophy after myocardial infarction. *Circ Res* 91 (4):323-330.

Grantham CJ, Cannell MB. 1996. Ca^{2+} influx during the cardiac action potential in guinea pig ventricular myocytes. *Circ Res* 79 (2):194-200.

Gumina RJ, Gross GJ. 1999. If ischemic preconditioning is the gold standard, has a platinum standard of cardioprotection arrived? Comparison with NHE inhibition. *Journal of Thrombosis and Thrombolysis* 8:39-44.

Hampton T, Wang J, DeAngelis J, Amende I, Philipson KD, Morgan JP. 2000. Enhanced gene expression of Na^+/Ca^{2+} exchanger attenuates ischemic and hypoxic contractile dysfuction. *Am J Physiol* 279:H2846-2854.

Hannon GJ. 2002. RNA interference. *Nature* 418:244-251.

Hasenfuss G. 1998. Alterations of calcium-regulatory proteins in heart failure. *Cardiovasc Res* 37 (2):279-289.

Hasenfuss G, Schillinger W, Lehnart SE, Preuss M, Pieske B, Maier LS, Prestle J, Minami K, Just H. 1999. Relationship between Na^+-Ca^{2+}-exchanger protein levels and diastolic function of failing human myocardium. *Circulation* 99 (5):641-648.

Hearse DJ, Bolli R. 1992. Reperfusion induced injury: manifestations, mechanisms, and clinical relevance. *Cardiovasc Res* 26:101-108.

Henderson SA, Goldhaber JI, So JM, Han T, Motter C, Ngo A, Chantawansri C, Ritter MR, Friedlander M, Nicoll DA, Frank JS, Jordan MC, Roos KP, Ross RS, Philipson KD. 2004. Functional Adult Myocardium in the Absence of Na^+-Ca^{2+} Exchange: Cardiac-Specific Knockout of NCX1. *Circ Res* 95 (6):604-611.

Hendrikx M, Mubagwa K, Verdonck F. 1994. New Na^+-H^+ exchange inhibitor HOE 694 improves postischemic function and high-energy phosphate resynthesis and reduces Ca^{2+} overload in isolated perfused rabbit heart. *Circulation* 89:2787-2798.

Heyliger CE, Takeo S, Dhalla NS. 1985. Alterations in sarcolemmal Na^+-Ca^{2+} exchange and ATP-dependent Ca^{2+}-binding in hypertrophied heart. *Can J Cardiol* 1 (5):328-339.

Hilgemann DW. 1989. Giant excised cardiac sarcolemmal membrane patches: sodium and sodium-calcium exchange currents. *Pflugers Arch* 415 (2):247-249.

Hilgemann DW. 1990. Regulation and deregulation of cardiac Na^+-Ca^{2+} exchange in giant excised sarcolemmal membrane patches. *Nature* 344 (6263):242-245.

Hilgemann DW, Collins A, Matsuoka S. 1992a. Steady-state and dynamic properties of cardiac sodium-calcium exchange. Secondary modulation by cytoplasmic calcium and ATP. *J Gen Physiol* 100 (6):933-961.

Hilgemann DW, Matsuoka S, Nagel GA, Collins A. 1992b. Steady-state and dynamic properties of cardiac sodium-calcium exchange. Sodium-dependent inactivation. *J Gen Physiol* 100 (6):905-932.

Hobai IA, O'Rourke B. 2000. Enhanced Ca^{2+}-activated Na^+-Ca^{2+} exchange activity in canine pacing-induced heart failure. *Circ Res* 87 (8):690-698.

Hoya A, Venosa RA. 1995. Characteristics of Na^+-Ca^{2+} exchange in frog skeletal muscle. *J Physiol* 486 (Pt 3):615-627.

Hryshko LV. 2002. Tissue-specific modes of Na/Ca exchanger regulation. *Ann N Y Acad Sci* 976:166-175.

Hryshko LV, Nicoll DA, Weiss JN, Philipson KD. 1993. Biosynthesis and initial processing of the cardiac sarcolemmal Na^+-Ca^{2+} exchanger. *Biochim Biophys Acta* 1151 (1):35-42.

Hurtado C, Pierce GN. 2000. Inhibition of Na^+/H^+ exchange at the beginning of reperfusion is cardioprotective in isolated, beating adult cardiomyocytes. *J Mol Cell Cardiol* 32 (10):1897-1907.

Iwamoto T, Kita S, Uehara A, Imanaga I, Matsuda T, Baba A, Katsuragi T. 2004. Molecular determinants of Na^+/Ca^{2+} exchange (NCX1) inhibition by SEA0400. *J Biol Chem* 279 (9):7544-7553.

Iwamoto T, Kita S, Uehara A, Inoue Y, Taniguchi Y, Imanaga I, Shigekawa M. 2001. Structural domains influencing sensitivity to isothiourea derivative inhibitor KB-R7943 in cardiac Na^+/Ca^{2+} exchanger. *Mol Pharmacol* 59 (3):524-531.

Iwamoto T, Shigekawa M. 1998. Differential inhibition of Na^+/Ca^{2+} exchanger isoforms by divalent cations and isothiourea derivative. *Am J Physiol* 275 (2 Pt 1):C423-430.

Iwamoto T, Uehara A, Imanaga I, Shigekawa M. 2000. The Na^+/Ca^{2+} exchanger NCX1 has oppositely oriented reentrant loop domains that contain conserved aspartic acids whose mutation alters its apparent Ca^{2+} affinity. *J Biol Chem* 275 (49):38571-38580.

Iwamoto T, Wakabayashi S, Imagawa T, Shigekawa M. 1998. Na^+/Ca^{2+} exchanger overexpression impairs calcium signaling in fibroblasts: inhibition of the $[Ca^{2+}]$ increase at the cell periphery and retardation of cell adhesion. *Eur J Cell Biol* 76 (3):228-236.

Iwamoto T, Watano T, Shigekawa M. 1996. A novel isothiourea derivative selectively inhibits the reverse mode of Na^+/Ca^{2+} exchange in cells expressing NCX1. *J Biol Chem* 271 (37):22391-22397.

Jongsma HJ, Tsjernina L, de Bruijne J. 1983. The establishment of regular beating in populations of pacemaker heart cells. A study with tissue-cultured rat heart cells. *J Mol Cell Cardiol* 15 (2):123-133.

Jorgensen R. 1990. Altered gene expression in plants due to trans interactions between homologous genes. *Trends Biotechnol* 8:340-344.

Kang TM, Hilgemann DW. 2004. Multiple transport modes of the cardiac Na^+/Ca^{2+} exchanger. *Nature* 427:544-548.

Karmazyn M. 1988. Amiloride enhances postischemic ventricular recovery: possible role of Na^+/H^+ exchange. *Am J Physiol* 255:H608-H615.

Karwatowska-Prokopczuk E, Nordberg JA, Li HL, Engler RL, Gottlieb RA. 1998. Effect of vacuolar proton ATPase on pH^i, Ca^{2+}, and apoptosis in neonatal cardiomyocytes during metabolic inhibition/recovery. *Circ Res* 82 (11):1139-1144.

Keating MT, Sanguinetti MC. 2001. Molecular and cellular mechanisms of cardiac arrhythmias. *Cell* 104 (4):569-580.

Kent RL, Rozich JD, McCollam PL, McDermott DE, Thacker UF, Menick DR, McDermott PJ, Cooper Gt. 1993. Rapid expression of the Na^+-Ca^{2+} exchanger in response to cardiac pressure overload. *Am J Physiol* 265 (3 Pt 2):H1024-1029.

Khandoudi N, Laville M, Bril A. 1997. Protective effect of the sodium/hydrogen exchange inhibitors during global low-flow ischemia. *J Cardiovas Pharmacol* 28:540-546.

Kieval RS, Bloch RJ, Lindenmayer GE, Ambesi A, Lederer WJ. 1992. Immunofluorescence localization of the Na-Ca exchanger in heart cells. *Am J Physiol* 263 (2 Pt 1):C545-550.

Kimura J, Miyamae S, Noma A. 1987. Identification of sodium-calcium exchange current in single ventricular cells of guinea-pig. *J Physiol* 384:199-222.

Klein HH, Pich S, Bohle RM, Lindert-Heimberg S, Nebendahl K. 2000. Na^+/H^+ exchange inhibitor cariporide attenuates cell injury predominantly during

ischemia and not at onset of reperfusion in porcine hearts with low residual blood flow. *Circulation* 102 (16):1977-1982.

Kofuji P, Lederer WJ, Schulze DH. 1994. Mutually exclusive and cassette exons underlie alternatively spliced isoforms of the Na/Ca exchanger. *J Biol Chem* 269 (7):5145-5149.

Koushik SV, Bundy J, Conway SJ. 1999. Sodium-calcium exchanger is initially expressed in a heart-restricted pattern within the early mouse embryo. *Mech Dev* 88 (1):119-122.

Koushik SV, Wang J, Rogers R, Moskophidis D, Lambert NA, Creazzo TL, Conway SJ. 2001. Targeted inactivation of the sodium-calcium exchanger (Ncx1) results in the lack of a heartbeat and abnormal myofibrillar organization. *Faseb J* 15 (7):1209-1211.

Kunath T, Gish G, Lickert H, Jones N, Pawson T, Rossant J. 2003. Transgenic RNA interference in ES cell-derived embryos recapitulates a genetic null phenotype. *Nature Biotech* 21:559-561.

Kurashima K, Szabo EZ, Lukacs G, Orlowski J, Grinstein S. 1998. Endosomal recycling of the Na+/H+ exchanger NHE3 isoform is regulated by the phosphatidylinositol 3-kinase pathway. *J Biol Chem* 273 (33):20828-20836.

Kuro T, Kobayashi Y, Takaoka M, Matsumura Y. 1999. Protective effect of KB-R7943, a novel Na^{+}/Ca^{2+} exchange inhibitor, on ischemic acute renal failure in rats. *Jpn J Pharmacol* 81 (2):247-251.

Kuruma A, Hiraoka M, Kawano S. 1998. Activation of Ca2+-sensitive Cl- current by reverse mode Na^+/Ca^{2+} exchange in rabbit ventricular myocytes. *Pflugers Arch* 436 (6):976-983.

Ladilov Y, Haffner S, Balser-Schafer C, Maxeiner H, Piper HM. 1999. Cardioprotective effects of KB-R7943: a novel inhibitor of the reverse mode of Na^+/Ca^{2+} exchanger. *Am J Physiol* 276 (6 Pt 2):H1868-1876.

Langer GA, Brady A, Tan S, Serena S. 1975. Correlation of the Glycoside Response, the Force Staircase, and the Action Potential Configuration in the Neonatal Rat Heart. *Circ Res* 36:744-752.

Lazdunski M, Frelin C, Vigne P. 1985. The sodium/hydrogen exchange system in cardiac cells: Its biochemical and pharmacological properties and its role in regulating internal concentrations of sodium and internal pH. *J Mol Cell Cardiol* 17:1029-1042.

Leblanc N, Hume JR. 1990. Sodium current-induced release of calcium from cardiac sarcoplasmic reticulum. *Science* 248 (4953):372-376.

Lee C, Visen N, Dhalla NS, Le HD, Isaac M, Choptiany P, Gross G, Omelchenko A, Matsuda T, Baba A, Takahashi K, Hnatowich M, Hryshko LV. 2004. Inhibitory Profile of SEA0400 Assessed on the Cardiac Na^+-Ca^{2+} Exchanger, NCX1.1. *J Pharmacol Exp Ther.*

Lee SL, Yu AS, Lytton J. 1994. Tissue-specific expression of Na^+-Ca^{2+} exchanger isoforms. *J Biol Chem* 269 (21):14849-14852.

Leem CH, Lagadic-Gossmann D, Vaughan-Jones RD. 1999. Characterization of intracellular pH regulation in the guinea-pig ventricular myocyte. *J Physiol* 517 (Pt 1):159-180.

Levesque PC, Leblanc N, Hume JR. 1994. Release of calcium from guinea pig cardiac sarcoplasmic reticulum induced by sodium-calcium exchange. *Cardiovasc Res* 28 (3):370-378.

Levitsky DO, Nicoll DA, Philipson KD. 1994. Identification of the high affinity Ca^{2+}-binding domain of the cardiac Na^{+}-Ca^{2+} exchanger. *J Biol Chem* 269 (36):22847-22852.

Li Z, Matsuoka S, Hryshko LV, Nicoll DA, Bersohn MM, Burke EP, Lifton RP, Philipson KD. 1994. Cloning of the NCX2 isoform of the plasma membrane Na^{+}-Ca^{2+} exchanger. *J Biol Chem* 269 (26):17434-17439.

Li Z, Nicoll DA, Collins A, Hilgemann DW, Filoteo AG, Penniston JT, Weiss JN, Tomich JM, Philipson KD. 1991. Identification of a peptide inhibitor of the cardiac sarcolemmal Na^{+}-Ca^{2+} exchanger. *J Biol Chem* 266 (2):1014-1020.

Linz W, Albus U, Crause P, Jung W, Weichert A, Scholkens B, Scholz W. 1998. Dose-dependent reduction of myocardial infarct mass in rabbits by the NHE-1 inhibitor cariporide (HOE 642). *Clin Exp Hypertens* 20:733-749.

Lipp P, Schwaller B, Niggli E. 1995. Specific inhibition of Na-Ca exchange function by antisense oligodeoxynucleotides. *FEBS Lett* 364 (2):198-202.

Litwin SE, Bridge JH. 1997. Enhanced Na^{+}-Ca^{2+} exchange in the infarcted heart. Implications for excitation-contraction coupling. *Circ Res* 81 (6):1083-1093.

Litwin SE, Li J, Bridge JH. 1998. Na-Ca exchange and the trigger for sarcoplasmic reticulum Ca release: studies in adult rabbit ventricular myocytes. *Biophys J* 75 (1):359-371.

Lohmann J, Endl I, Bosch T. 1999. Silencing of developmental genes in *Hydra*. *Dev Biol* 214:211-214.

Lompre A, Lambert F, Lakatta E, Schwartz K. 1991. Expression of sarcoplasmic reticulum Ca^{2+}-ATPase and calsequestrin genes in rat heart during ontogenic development and aging. *Circ Res* 69 (5):1380-1388.

Maddaford TG, Hurtado C, Sobrattee S, Czubryt MP, Pierce GN. 1999. A model of low-flow ischemia and reperfusion in single, beating adult cardiomyocytes. *Am J Physiol* 277 (Heart Circ. Physiol. 46):H788-H798.

Maddaford TG, Pierce GN. 1997. Myocardial dysfunction is associated with activation of Na^+/H^+ exchange immediately during reperfusion. *Am J Physiol* 273 (5 Pt 2):H2232-2239.

Makino N, Dhruvarajan R, Elimban V, Beamish RE, Dhalla NS. 1985. Alterations of sarcolemmal Na^+-Ca^{2+} exchange in catecholamine-induced cardiomyopathy. *Can J Cardiol* 1 (3):225-232.

Marban E, Koretsune K, Corretti M, Chacko VP, Kusuoka H. 1989. Calcium and its role in myocardial cell injury during ischemia and reperfusion. *Circulation* 80 (suppl. IV):IV17-IV22.

Massaeli H, Pierce GN. 1997. Methods for measuring sodium-hydrogen exchange in the heart. In: Mc-Neill JH, editor. Biochemical Techniques in the Heart. Boca Raton, FL.

Matsuda T, Arakawa N, Takuma K, Kishida Y, Kawasaki Y, Sakaue M, Takahashi K, Takahashi T, Suzuki T, Ota T, Hamano-Takahashi A, Onishi M, Tanaka Y, Kameo K, Baba A. 2001. SEA0400, a novel and selective inhibitor of the Na^+-Ca^{2+} exchanger, attenuates reperfusion injury in the in vitro and in vivo cerebral ischemic models. *J Pharmacol Exp Ther* 298 (1):249-256.

Matsuoka S, Nicoll DA, He Z, Philipson KD. 1997. Regulation of cardiac Na^+-Ca^{2+} exchanger by the endogenous XIP region. *J Gen Physiol* 109 (2):273-286.

Matsuoka S, Nicoll DA, Hryshko LV, Levitsky DO, Weiss JN, Philipson KD. 1995. Regulation of the cardiac Na^+-Ca^{2+} exchanger by Ca^{2+}. Mutational analysis of the Ca^{2+}-binding domain. *J Gen Physiol* 105 (3):403-420.

Matsuoka S, Nicoll DA, Reilly RF, Hilgemann DW, Philipson KD. 1993. Initial localization of regulatory regions of the cardiac sarcolemmal Na^+-Ca^{2+} exchanger. *Proc Natl Acad Sci U S A* 90 (9):3870-3874.

Maxwell K, Scott J, Omelchenko A, Lukas A, Lu L, Lu Y, Hnatowich M, Philipson KD, Hryshko LV. 1999. Functional role of ionic regulation of Na^+/Ca^{2+} exchange assessed in transgenic mouse hearts. *Am J Physiol* 277 (6 Pt 2):H2212-2221.

Meng H-P, Lonsberry BB, Pierce GN. 1991. Influence of perfusate pH on the postischemic recovery of cardiac contractile function: involvement of sodium-hydrgen exchange. *J Pharm Exp Ther* 258 (3):772-777.

Meng HP, Maddaford TG, Pierce GN. 1993. Effect of amiloride and selected analogues on postischemic recovery of cardiac contractile function. *Am J Physiol* 264 (6 Pt 2):H1831-1835.

Meng H-P, Pierce GN. 1990. Protective effects of 5-(N,N-dimethyl) amiloride on ischemia-reperfusion injury in hearts. *Am J Physiol* 258 (Heart Circ Physiol 27):H1615-H1619.

Menick DR, Barnes KV, Thacker UF, Dawson MM, McDermott DE, Rozich JD, Kent RL, Cooper Gt. 1996. The exchanger and cardiac hypertrophy. *Ann N Y Acad Sci* 779:489-501.

Minks M, West D, Benvin S, Baglioni C. 1979. Structural requirements of double-stranded RNA for the activation of 2',5'-oligo(A)polymerase and protein kinase of interferon-treated HeLa cells. *J Biol Chem* 254:10180-10183.

Miura T, Ogawa T, Suzuki K, Goto M, Shimamoto K. 1997. Infarct size limitation by a new Na^+-H^+ exchange inhibitor, Hoe 642: difference from preconditioning in the role of protein kinase C. *J Am Coll Cardiol* 29 (3):693-701.

Moorman A, Vermeulen J, Koban M, Schwartz K, Lamers W, Boheler K. 1995. Patterns of expression of sarcoplasmic reticulum Ca^{2+}-ATPase and phospholamban mRNAs during rat heart development. *Circ Res* 76 (4):616-625.

Mosca SM, Cingolani HE. 2000. Comparison of the protective effects of ischemic preconditioning and the Na^+/H^+ exchanger blockade. *Naunyn Schmiedebergs Arch Pharmacol* 362 (1):7-13.

Murphy E, Perlman M, London RE, Steenbergen C. 1991. Amiloride delays the ischemia-induced rise in cytosolic free calcium. *Circ Res* 68:1250-1258.

Nabauer M, Morad M. 1992. Modulation of contraction by intracellular Na^+ via Na^+-Ca2+ exchange in single shark (Squalus acanthias) ventricular myocytes. *J Physiol* 457:627-637.

Nakanishi T, Seguchi M, Takao A. 1988. Development of the myocardial contractile system. *Experientia* 44 (11-12):936-944.

Ngo H, Tschudi C, Gull K, Ullu E. 1998. Double-stranded RNA induces mRNA degradation in *Trypanosoma brucei*. *Proc Natl Acad Sci U S A* 95:14687-14692.

Nicholas SB, Philipson KD. 1999. Cardiac expression of the Na^+/Ca^{2+} exchanger NCX1 is GATA factor dependent. *Am J Physiol* 277 (1 Pt 2):H324-330.

Nicoll DA, Hryshko LV, Matsuoka S, Frank JS, Philipson KD. 1996a. Mutation of amino acid residues in the putative transmembrane segments of the cardiac sarcolemmal Na^+-Ca^{2+} exchanger. *J Biol Chem* 271 (23):13385-13391.

Nicoll DA, Longoni S, Philipson KD. 1990. Molecular cloning and functional expression of the cardiac sarcolemmal Na^+-Ca^{2+} exchanger. *Science* 250 (4980):562-565.

Nicoll DA, Ottolia M, Lu L, Lu Y, Philipson KD. 1999. A new topological model of the cardiac sarcolemmal Na+-Ca2+ exchanger. *J Biol Chem* 274 (2):910-917.

Nicoll DA, Quednau BD, Qui Z, Xia YR, Lusis AJ, Philipson KD. 1996b. Cloning of a third mammalian Na^+-Ca^{2+} exchanger, NCX3. *J Biol Chem* 271 (40):24914-24921.

O'Brien T, Lee K, Chien K. 1993. Positional specification of ventricular myosin light chain 2 expression in the primitive murine heart tube. *Proc Natl Acad Sci U S A* 90:5157-5161.

Omelchenko A, Bouchard R, Le HD, Choptiany P, Visen N, Hnatowich M, Hryshko LV. 2003. Inhibition of canine (NCX1.1) and Drosophila (CALX1.1) Na^+-Ca^{2+} exchangers by 7-chloro-3,5-dihydro-5-phenyl-1H-4,1-benzothiazepine-2-one (CGP-37157). *J Pharmacol Exp Ther* 306 (3):1050-1057.

Opie LH. The Heart. Third ed: Lippincott-Raven. 637 p.

Orlowski J, Lingrel JB. 1990. Thyroid and glucocorticoid hormones regulate the expression of multiple Na,K-ATPase genes in cultured neonatal rat cardiac myocytes. *J Biol Chem* 265 (6):3462-3470.

Ottolia M, John S, Qiu Z, Philipson KD. 2001. Split Na^+-Ca^{2+} exchangers. Implications for function and expression. *J Biol Chem* 276 (22):19603-19609.

Ottolia M, Philipson KD, John S. 2004. Conformational changes of the Ca^{2+} regulatory site of the Na^+-Ca^{2+} exchanger detected by FRET. *Biophys J* 87 (2):899-906.

Paddison PJ, Caudy AA, Bernstein E, Hannon GJ, Conklin DS. 2002. Short hairpin RNAs (shRNAs) induce sequence-specific silencing in mammalian cells. *Genes Dev* 16 (8):948-958.

Paddison PJ, Hannon GJ. 2003. siRNAs and shRNAs: skeleton keys to the human genome. *Curr Opin Mol Ther* 5 (3):217-224.

Pal-Bhadra M, Bhadra U, Birchler J. 1997. Cosuppression in *Drosophila*: gene silencing of *Alcohol dehydrogenase* by *white-Adh* transgenes is *Polycomb* dependent. *Cell* 90:479-490.

Pan Y, Iwamoto T, Uehara A, Nakamura TY, Imanaga I, Shigekawa M. 2000. Physiological functions of the regulatory domains of the cardiac Na^+/Ca^{2+} exchanger NCX1. *Am J Physiol Cell Physiol* 279 (2):C393-402.

Papp Z, van der Velden J, Stienen GJ. 2000. Calpain-I induced alterations in the cytoskeletal structure and impaired mechanical properties of single myocytes of rat heart. *Cardiovasc Res* 45 (4):981-993.

Peng M, Huang L, Xie Z, Huang WH, Askari A. 1996. Partial inhibition of Na^+/K^+-ATPase by ouabain induces the Ca^{2+}-dependent expressions of early-response genes in cardiac myocytes. *J Biol Chem* 271 (17):10372-10378.

Perez NG, Marban E, Cingolani HE. 1999. Preservation of myofilament calcium responsiveness underlies protection against myocardial stunning by ischemic preconditioning. *Cardiovasc Res* 42 (3):636-643.

Philipson KD, Longoni S, Ward R. 1988. Purification of the cardiac Na^+-Ca^{2+} exchange protein. *Biochim Biophys Acta* 945 (2):298-306.

Philipson KD, Nicoll DA, Ottolia M, Quednau BD, Reuter H, John S, Qiu Z. 2002. The Na^+/Ca^{2+} exchange molecule: an overview. *Ann N Y Acad Sci* 976:1-10.

Pierce GN, Cole WC, Liu K, Massaeli H, Maddaford TG, Chen YJ, Pherson CDM, Jain S, Sontag D. 1993. Modulation of cardiac performance by amiloride and several selected derivatives of amiloride. *J Pharm Exp Ther* 265 (3):1280-1291.

Pierce GN, Czubryt MP. 1995. The contribution of ionic imbalance to ischemia/reperfusion-induced injury. *J Mol Cell Cardiol* 27 (1):53-63.

Piper HM, Meuter K, Schafer C. 2003. Cellular mechanisms of ischemia-reperfusion injury. *Ann Thorac Surg* 75 (2):S644-648.

Pogwizd SM, Qi M, Yuan W, Samarel AM, Bers DM. 1999. Upregulation of Na^+/Ca^{2+} exchanger expression and function in an arrhythmogenic rabbit model of heart failure. *Circ Res* 85 (11):1009-1019.

Puglisi JL, Bers DM. 2001. LabHEART: an interactive computer model of rabbit ventricular myocyte ion channels and Ca transport. *Am J Physiol Cell Physiol* 281 (6):C2049-2060.

Putney JW, Jr. 1986. A model for receptor-regulated calcium entry. *Cell Calcium* 7 (1):1-12.

Quednau BD, Nicoll DA, Philipson KD. 1997. Tissue specificity and alternative splicing of the Na^+/Ca^{2+} exchanger isoforms NCX1, NCX2, and NCX3 in rat. *Am J Physiol* 272 (4 Pt 1):C1250-1261.

Querfurth H, Suhara T, Rosen K, McPhie D, Fujio Y, Tejada G, Neve R, Adelman L, Walsh K. 2001. Beta Amyloid Peptide Expression Is Sufficient for Myotubule Death: Implications for Human Inclusion Body Myopathy. *Mol Cell Neurosc* 17:793-810.

Ranu HK, Terracciano CM, Davia K, Bernobich E, Chaudhri B, Robinson SE, Bin Kang Z, Hajjar RJ, MacLeod KT, Harding SE. 2002. Effects of Na^+/Ca^{2+}-exchanger overexpression on excitation-contraction coupling in adult rabbit ventricular myocytes. *J Mol Cell Cardiol* 34 (4):389-400.

Reed TD, Babu GJ, Ji Y, Zilberman A, Ver Heyen M, Wuytack F, Periasamy M. 2000. The expression of SR calcium transport ATPase and the Na^+/Ca^{2+}Exchanger are antithetically regulated during mouse cardiac development and in Hypo/hyperthyroidism. *J Mol Cell Cardiol* 32 (3):453-464.

Reilly RF, Lattanzi D. 1996. Identification of a novel alternatively spliced isoform of the Na^+-Ca^{2+} exchanger (NACA8) in heart. *Ann N Y Acad Sci* 779:129-131.

Reilly RF, Shugrue CA, Lattanzi D, Biemesderfer D. 1993. Immunolocalization of the Na^+/Ca^{2+} exchanger in rabbit kidney. *Am J Physiol* 265 (2 Pt 2):F327-332.

Reuter H, Han T, Motter C, Philipson KD, Goldhaber JI. 2004. Mice overexpressing the cardiac sodium-calcium exchanger: defects in excitation-contraction coupling. *J Physiol* 554 (Pt 3):779-789.

Reuter H, Henderson SA, Han T, Matsuda T, Baba A, Ross RS, Goldhaber JI, Philipson KD. 2002a. Knockout mice for pharmacological screening: testing the specificity of Na^+-Ca^{2+} exchange inhibitors. *Circ Res* 91 (2):90-92.

Reuter H, Henderson SA, Han T, Mottino GA, Frank JS, Ross RS, Goldhaber JI, Philipson KD. 2003. Cardiac excitation-contraction coupling in the absence of Na^+- Ca^{2+} exchange. *Cell Calcium* 34 (1):19-26.

Reuter H, Henderson SA, Han T, Ross RS, Goldhaber JI, Philipson KD. 2002b. The Na^+-Ca^{2+} exchanger is essential for the action of cardiac glycosides. *Circ Res* 90 (3):305-308.

Rohmann S, Weygandt H, Mink K. 1995. Preischaemic as well as postischaemic application of a Na^+/H^+exchange inhibitor reduces infarct size in pigs. *Cardiovasc Res* 35:80-89.

Romano N, Macino G. 1992. Quelling: transient inactivation of gene expression in *Neurospora crassa* by transformation with homologous sequences. *Mol Microbiol* 6:3343-3353.

Ruknudin A, He S, Lederer WJ, Schulze DH. 2000. Functional differences between cardiac and renal isoforms of the rat Na^+-Ca^{2+} exchanger NCX1 expressed in Xenopus oocytes. *J Physiol* 529 Pt 3:599-610.

Satoh H, Ginsburg KS, Qing K, Terada H, Hayashi H, Bers DM. 2000. KB-R7943 block of Ca^{2+} influx via Na^+/Ca^{2+} exchange does not alter twitches or glycoside inotropy

but prevents Ca^{2+} overload in rat ventricular myocytes. *Circulation* 101 (12):1441-1446.

Schagger H, von Jagow G. 1987. Tricine-sodium dodecyl sulfate-polyacrylamide gel electrophoresis for the separation of proteins in the range from 1 to 100 kDa. *Anal Biochem* 166 (2):368-379.

Scheller T, Kraev A, Skinner S, Carafoli E. 1998. Cloning of the multipartite promoter of the sodium-calcium exchanger gene NCX1 and characterization of its activity in vascular smooth muscle cells. *J Biol Chem* 273 (13):7643-7649.

Schillinger W, Janssen PM, Emami S, Henderson SA, Ross RS, Teucher N, Zeitz O, Philipson KD, Prestle J, Hasenfuss G. 2000. Impaired contractile performance of cultured rabbit ventricular myocytes after adenoviral gene transfer of Na^{+}-Ca^{2+} exchanger. *Circ Res* 87 (7):581-587.

Scholz W, Albus U, Counillon L, Gogelein H, Lang HJ, Linz W, Weichert A, Scholkens BA. 1995. Protective effects of HOE642, a selective sodium-hydrogen exchange subtype 1 inhibitor, on cardiac ischaemia and reperfusion. *Cardiovasc Res* 29 (2):260-268.

Seki S, Nagashima M, Yamada Y, Tsutsuura M, Kobayashi T, Namiki A, Tohse N. 2003. Fetal and postnatal development of Ca^{2+} transients and Ca^{2+} sparks in rat cardiomyocytes. *Cardiovasc Res* 58 (3):535-548.

Shuba YM, Iwata T, Naidenov VG, Oz M, Sandberg K, Kraev A, Carafoli E, Morad M. 1998. A novel molecular determinant for cAMP-dependent regulation of the frog heart Na^{+}-Ca^{2+} exchanger. *J Biol Chem* 273 (30):18819-18825.

Siegl PK, Cragoe EJ, Jr., Trumble MJ, Kaczorowski GJ. 1984. Inhibition of Na^+/Ca^{2+} exchange in membrane vesicle and papillary muscle preparations from guinea pig heart by analogs of amiloride. *Proc Natl Acad Sci U S A* 81 (10):3238-3242.

Sipido KR, Maes M, Van de Werf F. 1997. Low efficiency of Ca^{2+} entry through the Na^+-Ca^{2+} exchanger as trigger for Ca^{2+} release from the sarcoplasmic reticulum. A comparison between L-type Ca^{2+} current and reverse-mode Na^+-Ca^{2+} exchange. *Circ Res* 81 (6):1034-1044.

Slodzinski MK, Blaustein MP. 1998. Na^+/Ca^{2+} exchange in neonatal rat heart cells: antisense inhibition and protein half-life. *Am J Physiol* 275 (2 Pt 1):C459-467.

Slodzinski MK, Juhaszova M, Blaustein MP. 1995. Antisense inhibition of Na^+/Ca^{2+} exchange in primary cultured arterial myocytes. *Am J Physiol* 269 (5 Pt 1):C1340-1345.

Solaro JR, El-Saleh SC, Kentish JC. 1989. Ca^{2+}, pH and the regulation of cardiac myofilament force and ATPase activity. *Molecular and Cellular Biochemistry* 89:163-167.

Spencer CI, Sham JS. 2003. Effects of Na^+/Ca2+ exchange induced by SR Ca^{2+} release on action potentials and afterdepolarizations in guinea pig ventricular myocytes. *Am J Physiol Heart Circ Physiol* 285 (6):H2552-2562.

Steenbergen C, Murphy E, Watts HA, London RE. 1990. Correlation between cytosolic free calcium, contracture, ATP, and irreversible ischemic injury in perfused rat heart. *Circ Res* 66:135-146.

Studer R, Reinecke H, Bilger J, Eschenhagen T, Bohm M, Hasenfuss G, Just H, Holtz J, Drexler H. 1994. Gene expression of the cardiac Na^+-Ca^{2+} exchanger in end-stage human heart failure. *Circ Res* 75 (3):443-453.

Sugishita M, Su Z, Li F, Philipson KD, Barry WH. 2001. Gender Influences $[Ca^{2+}]_i$ During Metabolic Inhibition in Myocytes Overexpressing the Na^+-Ca^{2+} Exchanger. *Circulation* 104:2101-2106.

Tadros GM, Zhang XQ, Song J, Carl LL, Rothblum LI, Tian Q, Dunn J, Lytton J, Cheung JY. 2002. Effects of Na^+/Ca^{2+} exchanger downregulation on contractility and $[Ca^{2+}]_i$ transients in adult rat myocytes. *Am J Physiol Heart Circ Physiol* 283 (4):H1616-1626.

Takahashi K, Azuma M, Huschenbett J, Michaelis ML, Azuma J. 1999. Effects of antisense oligonucleotides to the cardiac Na^+/Ca^{2+} exchanger on calcium dynamics in cultured cardiac myocytes. *Biochem Biophys Res Commun* 260 (1):117-121.

Takahashi K, Takahashi T, Suzuki T, Onishi M, Tanaka Y, Hamano-Takahashi A, Ota T, Kameo K, Matsuda T, Baba A. 2003. Protective effects of SEA0400, a novel and selective inhibitor of the Na^+/Ca^{2+} exchanger, on myocardial ischemia-reperfusion injuries. *Eur J Pharmacol* 458 (1-2):155-162.

Tanaka H, Shigenobu K. 1989. Effect of ryanodine on neonatal and adult rat heart: developmental increase in sarcoplasmic reticulum function. *J Mol Cell Cardiol* 21 (12):1305-1313.

Tani M, Neely JR. 1989. Role of intracellular Na^+ in Ca^{2+} overload and depressed recovery of ventricular function of reperfused ischemic rat hearts. Possible involvement of H^+-Na^+ and Na^+-Ca^{2+} exchange. *Circ Res* 65 (4):1045-1056.

Terracciano CM, Souza AI, Philipson KD, MacLeod KT. 1998. Na^+-Ca^{2+} exchange and sarcoplasmic reticular Ca^{2+} regulation in ventricular myocytes from transgenic mice overexpressing the Na^+-Ca^{2+} exchanger. *J Physiol* 512 (Pt 3):651-667.

Thomas MJ, Sjaastad I, Andersen K, Helm PJ, Wasserstrom JA, Sejersted OM, Ottersen OP. 2003. Localization and function of the Na^+/Ca^{2+}-exchanger in normal and detubulated rat cardiomyocytes. *J Mol Cell Cardiol* 35 (11):1325-1337.

Tsuji T, Ohga Y, Yoshikawa Y, Sakata S, Abe T, Tabayashi N, Kobayashi S, Kohzuki H, Yoshida KI, Suga H, Kitamura S, Taniguchi S, Takaki M. 2001. Rat cardiac contractile dysfunction induced by Ca^{2+} overload: possible link to the proteolysis of alpha-fodrin. *Am J Physiol Heart Circ Physiol* 281 (3):H1286-1294.

Vaughan-Jones R, Wu M. 1990. Extracellular H^+ inactivation of Na^+-H^+ exchange in the sheep cardiac Purkinje fibre. *J Physiol* 428:441-466.

Vemuri R, Longoni S, Philipson KD. 1989. Ouabain treatment of cardiac cells induces enhanced Na^+-Ca^{2+} exchange activity. *Am J Physiol* 256 (6 Pt 1):C1273-1276.

Vetter R, Studer R, Reinecke H, Kolar F, Ostadalova I, Drexler H. 1995. Reciprocal changes in the postnatal expression of the sarcolemmal Na^+-Ca^{2+}-exchanger and SERCA2 in rat heart. *J Mol Cell Cardiol* 27 (8):1689-1701.

Volz A, Piper HM, Siegmund B, Schwartz P. 1991. Longevity of adult ventricular rat heart muscle cells in serum-free primary culture. *J Mol Cell Cardiol* 23 (2):161-173.

Vornanen M. 1984. Activation of contractility and sarcolemmal Ca^{2+}-ATPase by Ca^{2+} during postnatal development of the rat heart. *Comp Biochem Physiol A* 78 (4):691-695.

Vornanen M. 1996. Contribution of sarcolemmal calcium current to total cellular calcium in postnatally developing rat heart. *Cardiovasc Res* 32 (2):400-410.

Wagner JA, Weisman HF, Snowman AM, Reynolds IJ, Weisfeldt ML, Snyder SH. 1989. Alterations in calcium antagonist receptors and sodium-calcium exchange in cardiomyopathic hamster tissues. *Circ Res* 65 (1):205-214.

Wakimoto K, Kobayashi K, Kuro OM, Yao A, Iwamoto T, Yanaka N, Kita S, Nishida A, Azuma S, Toyoda Y, Omori K, Imahie H, Oka T, Kudoh S, Kohmoto O, Yazaki Y, Shigekawa M, Imai Y, Nabeshima Y, Komuro I. 2000. Targeted disruption of Na^{+}/Ca^{2+} exchanger gene leads to cardiomyocyte apoptosis and defects in heartbeat. *J Biol Chem* 275 (47):36991-36998.

Wallert M, Frohlich O. 1989. Na^{+}-H^{+} exchange in isolated myocytes from adult rat heart. *Am J Physiol* 257:C207-C213.

Watanabe Y, Kimura J. 2000. Inhibitory effect of amiodarone on Na^{+}/Ca^{2+} exchange current in guinea-pig cardiac myocytes. *Br J Pharmacol* 131 (1):80-84.

Watano T, Kimura J, Morita T, Nakanishi H. 1996. A novel antagonist, No. 7943, of the Na^{+}/Ca^{2+} exchange current in guinea-pig cardiac ventricular cells. *Br J Pharmacol* 119 (3):555-563.

Weber CR, Ginsburg KS, Philipson KD, Shannon TR, Bers DM. 2001. Allosteric regulation of Na/Ca exchange current by cytosolic Ca in intact cardiac myocytes. *J Gen Physiol* 117 (2):119-131.

White KE, Gesek FA, Friedman PA. 1996. Structural and functional analysis of Na^+/Ca^{2+} exchange in distal convoluted tubule cells. *Am J Physiol* 271 (3 Pt 2):F560-570.

Wibo M, Bravo G, Godfraind T. 1991. Postnatal maturation of excitation-contraction coupling in rat ventricle in relation to the subcellular localization and surface density of 1,4-dihydropyridine and ryanodine receptors. *Circ Res* 68 (3):662-673.

Wier WG. 1990. Cytoplasmic $[Ca^{2+}]$ in mammalian ventricle: dynamic control by cellular processes. *Annu Rev Physiol* 52:467-485.

Wu X, Babnigg G, Villereal ML. 2000. Functional significance of human trp1 and trp3 in store-operated Ca^{2+} entry in HEK-293 cells. *Am J Physiol Cell Physiol* 278 (3):C526-536.

Xiao XH, Allen DG. 2000. Activity of the Na^+/H^+ exchanger is critical to reperfusion damage and preconditioning in the isolated rat heart. *Cardiovasc Res* 48 (2):244-253.

Xu X, Best P. 1992. Postnatal changes in T-type calcium current density in rat atrial myocytes. *J Physiol* 454:657-672.

Yang HT, Tweedie D, Wang S, Guia A, Vinogradova T, Bogdanov K, Allen PD, Stern MD, Lakatta EG, Boheler KR. 2002. The ryanodine receptor modulates the spontaneous beating rate of cardiomyocytes during development. *Proc Natl Acad Sci U S A* 99 (14):9225-9230.

Yao A, Su Z, Nonaka A, Zubair I, Lu L, Philipson KD, Bridge JH, Barry WH. 1998. Effects of overexpression of the Na^+-Ca^{2+} exchanger on $[Ca^{2+}]i$ transients in murine ventricular myocytes. *Circ Res* 82 (6):657-665.

Yoshida K, Inui M, Harada K, Saido TC, Sorimachi Y, Ishihara T, Kawashima S, Sobue K. 1995. Reperfusion of rat heart after brief ischemia induces proteolysis of calspectin (nonerythroid spectrin or fodrin) by calpain. *Circ Res* 77 (3):603-610.

Yoshiyama M, Nakamura Y, Omura T, Hayashi T, Takagi Y, Hasegawa T, Nishioka H, Takeuchi K, Iwao H, Yoshikawa J. 2004. Cardioprotective effect of SEA0400, a selective inhibitor of the Na^+/Ca^{2+} exchanger, on myocardial ischemia-reperfusion injury in rats. *J Pharmacol Sci* 95 (2):196-202.

Yu AS, Hebert SC, Lee SL, Brenner BM, Lytton J. 1992. Identification and localization of renal Na^+-Ca^{2+} exchanger by polymerase chain reaction. *Am J Physiol* 263 (4 Pt 2):F680-685.

Zhang XQ, Song J, Rothblum LI, Lun M, Wang X, Ding F, Dunn J, Lytton J, McDermott PJ, Cheung JY. 2001. Overexpression of Na^+/Ca^{2+} exchanger alters contractility and SR Ca^{2+} content in adult rat myocytes. *Am J Physiol Heart Circ Physiol* 281 (5):H2079-2088.